UNIVERSIDAD COMPLUTENSE DE MADRID

FACULTAD DE CIENCIAS QUÍMICAS

Departamento de Bioquímica y Biología Molecular I

TESIS DOCTORAL

Transcriptional profile of human anti-inflamatory macrophages under homeostatic, activating and pathological conditions

Perfil transcripcional de macrófagos antiinflamatorios humanos en condiciones de homeostasis, activación y patológicas

MEMORIA PARA OPTAR AL GRADO DE DOCTOR

PRESENTADA POR

Víctor Delgado Cuevas

Directores

María Marta Escribese Alonso
Ángel Luís Corbí López

Madrid, 2017

Universidad Complutense de Madrid
Facultad de Ciencias Químicas
Dpto. de Bioquímica y Biología Molecular I

TRANSCRIPTIONAL PROFILE OF HUMAN ANTI-INFLAMMATORY MACROPHAGES UNDER HOMEOSTATIC, ACTIVATING AND PATHOLOGICAL CONDITIONS

Perfil transcripcional de macrófagos antiinflamatorios humanos en condiciones de homeostasis, activación y patológicas.

Víctor Delgado Cuevas

Tesis Doctoral
Madrid 2016

Universidad Complutense de Madrid
Facultad de Ciencias Químicas
Dpto. de Bioquímica y Biología Molecular I

TRANSCRIPTIONAL PROFILE OF HUMAN ANTI-INFLAMMATORY MACROPHAGES UNDER HOMEOSTATIC, ACTIVATING AND PATHOLOGICAL CONDITIONS

Perfil transcripcional de macrófagos antiinflamatorios humanos en condiciones de homeostasis, activación y patológicas.

Este trabajo ha sido realizado por Víctor Delgado Cuevas para optar al grado de Doctor en el Centro de Investigaciones Biológicas de Madrid (CSIC), bajo la dirección de la Dra. María Marta Escribese Alonso y el Dr. Ángel Luís Corbí López

Fdo. Dra. María Marta Escribese Alonso

Fdo. Dr. Ángel Luís Corbí López

Gracias a los que me enseñan, me pagan, me ayudan, me prestan, me acompañan, me soportan, me quieren, me dan de comer, me invitan a beber y me llevan a bailar. Esto no ha hecho más que empezar.

INDEX

ABBREVIATIONS

AHR: aryl hydrocarbon receptor

ARNT: aryl hydrocarbon receptor nuclear translocator

bHLH-PAS: basic helix-loop-helix-PER-ARNT-SIM

BMP: bone morphogenic protein

CCL: C-C motif chemokine ligand

CCR: C-C chemokyne receptor

CD: cluster of differentiation

ChIP-seq: chromatin immunoprecipitation sequencing

ChIP: chromatin immunoprecipitation assay

CLEC: C-type lectin

CRE: cAMP-responsive element

CREB: cAMP response element binding protein

CSF1R: colony-stimulating factor 1 receptor

CXCL: C-X-C motif ligand

DAMP: damage-associated molecular pattern

DMSO: dimethyl sulfoxide

EGF: epidermal growth factor

ELISA: enzyme-linked immunosorbent assay

Enrichr: interactive and collaborative HTML5 gene list enrichment tool

ERK: extracellular signal-regulated kinase

FDR: false discovery rate

FOS: Fos proto-oncogene, AP-1 transcription factor subunit

GATA6: GATA binding protein 6

GM-CSF: granulocyte macrophage-colony stimulating factor

GM-MØ: GM-CSF-polarized macrophage

GSEA: gene set enrichment analysis

GSK3: glycogen synthase kinase 3

HIF: hypoxia-inducible factor

HMGB1: high mobility group box 1 protein

HTR: 5-hydroxytryptamine receptor

IFN: interferon

IL: interleukin

IL-34-MØ: IL-34-polarized macrophage

IRAK: interleukin-1 receptor-associated kinase

IRF: interferon-regulatory transcription factor

JNK: JUN N-terminal kinase

LPS: lipopolysaccharide

LRR: leucine-rich repeat

LXR: liver X receptor

M-CSF: macrophage-colony stimulating factor

M-MØ: M-CSF-polarized macrophage

MAF: v-Maf avian musculoaponeurotic fibrosarcoma oncogene homolog

MAL: MYD88-adapter like

MAPK: mitogen-activated protein kinase

MARE: Maf-recognition element

MCTO: multicentric carpotarsal osteolysis

MEK: MAPK/ERK kinase

MHC: major histocompatibility complex

MITF: melanogenesis associated transcription factor

MMP: matrix metalloproteinase

MONA: multicentric osteolysis, nodulosis and arthropathy

MYD88: myeloid differentiation primary response 88

NFATc1: nuclear factor of activated T cell 1

NFκB: nuclear factor-kappa B

NPAS4: neuronal PAS domain protein 4

NRL: neural retina leucine zipper protein

p38: p38 mitogen activated protein kinase

PAM3CSK4: N-palmitoyl-S-[2,3-bis (palmitoyloxy)-(2RS)-propyl]-[R]-cysteinyl-[S]-seryl-[S]-lysyl-[S]-lysyl-[S]-lysyl-[S]-lysine

PAMP: pathogen-associated molecular pattern

PBMC: peripheral blood mononuclear cells

PDGF: platelet-derived growth factor

pMAFB: MAFB pCDNA3.1(+) expression vector

PPAR: peroxisome proliferator activated receptor

PRR: pattern recognition receptor

qRT-PCR: quantitative real-time polymerase chain reaction

RANKL: receptor activator of nuclear factor-kappaB ligand

RPMI: Roswell Park Memorial Institute medium

SARM: sterile alpha and TIR motif-containing protein

SIM: single-minded family bHLH transcription factor 1

siRNA: small interfering RNA

SLC40A1: solute carrier family 40 member 1

SOCS: suppressor of cytokine signaling

SPIC: Spi-C transcription factor

STAT: signal transducer and activator of transcription

TCDD: 2,3,7,8-tetrachlorodibenzo-p-dioxin

TGF: transforming growth factor

TIR: Toll/interleukin-1 receptor

TLR: toll-like receptor

TNF: tumor necrosis factor

TRAF: TNF receptor-associated factor

TRAM: TRIF-related adaptor molecule

TRAP: tartrate-resistant acid phosphatase

TRE: 12-O-tetradecanoyl phorbol 13-acetate (TPA)-responsive element

TRIF: TIR domain-containing adaptor protein inducing interferon beta

VEGF: vascular endothelial growth factor

WT: wild type

ZXDC: ZXD family zinc finger C protein

ABSTRACT

Macrophages are cells of the innate immune system that exhibit a huge phenotypic and functional heterogeneity, what gives macrophages the ability to sense and respond accurately to the needs of their microenvironment. Thus, macrophage differentiation and functions are dependent on the integration of cues provided by their ontogeny, surrounding tissue, microbiota, metabolism and pathogens. In line with their functional plasticity, macrophages are able to both initiate and resolve inflammation. Besides, macrophages have essential roles in development, homeostasis and inflammation and, consequently, deregulation of macrophage functions leads to the onset and maintenance of numerous chronic inflammatory pathologies. Therefore, determination of the molecular basis of the macrophage functional heterogeneity should pave the way for the development of tissue-specific anti-inflammatory therapies.

Macrophage activation relies on the recognition of pathogen- and danger-associated molecular patterns from exogenous and endogenous factors by a variety of receptors, like TLRs. Depending on the nature of previous cues received by macrophages, the response to activating stimuli may be pro- or anti-inflammatory. The former is characteristic of macrophages exposed to GM-CSF or IFNγ and results in the production of TNF-α, IL-12, IL-6 and IL-23. The latter is specific for macrophages exposed to M-CSF, IL-4 or glucocorticoids and leads to the secretion of IL-10. Unlike the macrophage pro-inflammatory response, which has been extensively studied, scarce knowledge is currently available on the activation of anti-inflammatory macrophages, especially in humans. To address this issue, we have thoroughly analyzed the transcriptome of TLR-activated, human M-CSF-polarized anti-inflammatory macrophages (M-MØ). Microarray analysis of M-MØ after a short exposure to LPS revealed the existence of a gene set that includes chemokines (e.g., CCL19), signaling molecules (e.g., SOCS2) and growth factors (e.g., BMP6, PDGFA), that is exclusively induced in M-MØ in vitro and whose expression is dependent on the activation of the MAPKs ERK, p38 and JNK. Representative examples of this gene set, including CCL19,

SOCS2, BMP6 and PDGFA, are co-expressed in humans in gut and skin-resident macrophages and tumor-associated macrophages in nevi and melanoma. Thus, we have identified a novel gene set whose expression is specific for human activated homeostatic/anti-inflammatory macrophages. This finding sheds light on the mechanisms underlying the regulatory and trophic functions of this macrophage subtype.

The differentiation and functional polarization of steady state tissue-resident macrophages is controlled by M-CSF, as well as by GM-CSF, RANKL, heme or retinoic acid, whose effects induce transcription factors like PPARγ, NFATc1, SPI-C or GATA6, which then shape the appropriate transcriptomic profile needed for macrophages to accommodate to the functional demands of each specific tissue. MAFB, a bZIP transcription factor that performs essential functions during development and control organ homeostasis in the adult, is an important factor in the control of monocyte/macrophage differentiation. However, this notion primarily relies on studies performed on avian cell lines and mice macrophages, whereas the MAFB contribution to the macrophage differentiation program in human is mostly unknown. Interestingly, MAFB is greatly expressed by human anti-inflammatory M-MØ, in contrast to its very low expression found in GM-CSF-polarized pro-inflammatory macrophages. Therefore, we have addressed the determination of the whole range of MAFB-dependent genes in human M-MØ. Microarray analysis of MAFB-knocked-down macrophages revealed that MAFB positively controls the acquisition of the homeostatic/anti-inflammatory profile of M-MØ (including genes like *IL10*, *CCL2*, *CD163L1*, *HTR2B* and *CXCL12*), and impairs the expression of pro-inflammatory factors (like *CLEC5A*). Importantly, MAFB-dependent genes are co-expressed with MAFB in vivo in macrophages from the gut, dermis and melanoma samples. The control of the anti-inflammatory profile of human macrophages by MAFB is further supported by results obtained from macrophages derived from patients with Multicentric carpotarsal osteolysis (MCTO), a rare disease caused by heterozygous mutation in the MAFB gene. Our results indicate that MCTO MAFB mutations increase the MAFB protein stability, lead to an exacerbated anti-inflammatory macrophage phenotype, and impair the monocyte ability to differentiate in vitro into functional osteoclasts. Therefore, our results show, for the first time, that MAFB controls the differentiation and function of human anti-inflammatory macrophages.

In summary, this PhD thesis describes the acquisition and regulation of the transcriptional profile of human M-CSF-dependent macrophages in homeostatic, activating and pathological conditions.

RESUMEN

Los macrófagos son células del sistema inmune innato que exhiben una gran heterogeneidad fenotípica y funcional, lo que les confiere la capacidad de detectar y responder con precisión a las necesidades de su microambiente. La diferenciación y funciones de los macrófagos dependen de la integración de las señales proporcionadas por su ontogenia, el tejido donde se encuentren, la microbiota, el metabolismo y la potencial presencia de estímulos patógenicos. Los macrófagos juegan un papel esencial en desarrollo, homeostasis e inflamación y, por ello, la desregulación de funciones de los macrófagos lleva a la aparición y mantenimiento de numerosas patologías de base inflamatoria. En consecuencia, la determinación de la base molecular de la heterogeneidad funcional de macrófagos debería allanar el camino para el desarrollo de terapias anti-inflamatorias específicas de tejido.

Los macrófagos son capaces de iniciar y resolver la inflamación. La activación de macrófagos se basa en el reconocimiento de patrones moleculares asociados a patógenos (PAMP) y de peligro (DAMP) que llevan a cabo receptores como los miembros de la familia de TLR,. Dependiendo de la ontogenia, el entorno y naturaleza de las señales previas recibidas por los macrófagos, la respuesta a un estímulo puede ser pro- o anti-inflamatoria. La primera es característica de macrófagos expuestos a GM-CSF o IFNγ y resulta en la producción de TNF-α, IL-12, IL-6 e IL-23. La respuesta anti-inflamatoria, en cambio, es específica de macrófagos expuestos a M-CSF, IL-4 o glucocorticoides y conlleva la secreción de IL-10. La respuesta pro-inflamatoria de macrófagos ha sido ampliamente estudiada, en contraposición al escaso conocimiento disponible sobre la activación de macrófagos anti-inflamatorios, especialmente en humanos. Por este motivo hemos llevado a cabo la determinación del transcriptoma de macrófagos polarizados con M-CSF (M-MØ) y activados con ligandos de TLRs. Dicho análisis ha revelado la existencia de un conjunto de genes inducido por LPS exclusivamente en M-MØ, que incluye genes que codifian quimiocinas (CCL19), moléculas de señalización (SOCS2) y factores de crecimiento (BMP6, PDGFA), y cuya expressión es dependiente de la activación de las MAPKs ERK, p38 y JNK.

Además, CCL19, SOCS2, BMP6 y PDGFA se co-expresan en macrófagos humanos residentes en intestino y piel y en macrófagos asociados a nevus y melanoma. La identificación de este nuevo conjunto de genes dependiente de activación que es exclusivo de macrófagos antiinflamatorios/homeostáticos humanos contribuye de manera significativa al conocimiento de los mecanismos que subyacen a las funciones regulatorias y tróficas de este subtipo de macrófagos.

La diferenciación y polarización funcional de la mayoría de macrófagos de tejido en homeostasis depende de M-CSF, así como de GM-CSF, RANKL, el grupo hemo o el ácido retinoico. Estos factores conducen a la inducción de factores de transcripción (como PPARγ, NFATc1, SPI-C o GATA6) que regulan el perfil transcriptómico tejido-específico de macrófagos. MAFB es un factor de transcripción bZIP que realiza funciones esenciales durante el desarrollo y el control de la homeostasis de tejidos, y es crítico en el control de la diferenciación de monocitos/macrófagos. Sin embargo, este conocimiento deriva de estudios realizados sobre líneas celulares aviares y macrófagos de ratón. Por lo tanto, la contribución de MAFB en el programa de diferenciación de macrófagos en humanos es aún bastante limitada. MAFB se expresa en niveles muy elevados en macrófagos anti-inflamatorios humanos (M-MØ), en contraste con su muy baja expresión en macrófagos pro-inflamatorios polarizados por GM-CSF. Por esta razón hemos abordado el estudio del rango de genes dependientes de MAFB en macrófagos anti-inflamatorios humanos. El análisis mediante microarrays de macrófagos humanos en los que se silenció la expression de MAFB reveló que MAFB controla la adquisición del perfil homeostático/anti-inflamatorio de M-MØ (incluyendo genes como *IL10*, *CCL2*, *CD163L1*, *HTR2B* y *CXCL12*), e impide la expresión de genes asociados a la polarización pro-inflamatoria (*CLEC5A*). Por otra parte, los genes MAFB-dependientes son co-expresados con MAFB in vivo en macrófagos de intestino, dermis y melanoma. Por otra parte, la capacidad de MAFB de controlar el perfil anti-inflamatorio de macrófagos humanos se ha puesto también de manifiesto por los resultados obtenidos en macrófagos derivados de pacientes de Osteolisis carpotarsal multicéntrica (MCTO), enfermedad rara causada por mutaciones en el dominio de transactivación de MAFB. Nuestros resultados han puesto de manifesto que dichas mutaciones aumentan la estabilidad de MAFB, promueven la adquisición de un fenotipo antiinflamatorio exacerbado en los M-MØ de pacientes MCTO, y limitan la capacidad de monocitos de diferenciarse in vitro hacia osteoclastos funcionales. En conjunto, nuestros resultados demuestran por primera vez que MAFB controla la diferenciación y función de los macrófagos anti-inflamatorios humanos.

De forma global, esta tesis doctoral describe la adquisición y la regulación del perfil transcripcional de macrófagos humanos dependientes de M-CSF en homeostasis, activación y condiciones patológicas.

INTRODUCTION

Since Metchnikoff's breakthrough in the late 19th century, macrophages have been traditionally known for their critical role in innate immunity as first line responders against pathogens and tissue damage. However, the idea of what a macrophage is has greatly widened, specially in light of the advances accomplished in recent years. Nowadays, macrophages are increasingly considered as essential regulators of vertebrate biology and, consequently, as key players in the aetiology and development of many pathologies.

MACROPHAGE ONTOGENY

In recent years, previously stablished paradigms about the origin and maintenance of tissue macrophages have been drastically amended. The 'mononuclear phagocyte system' was described in 1972 by van Furth et al., who stated that hematopoietic stem cell-derived peripheral blood monocytes continuously migrate into tissues where they become terminally differentiated macrophages without proliferation ability [1]. However, it is now known that this is true for only a number of murine tissues under homeostasis, such as the intestine, dermis, heart, pancreas and peritoneum [2-5 6], whereas resident macrophages in other tissues have an embryonic origin. Microglia, brain-resident macrophages, are derived from yolk sac progenitors, whereas lung, kidney and liver macrophages derive from fetal liver monocytes. Otherwise, Langerhans cells, the epidermis macrophages, have a dual yolk sac and fetal liver origin [7-12]. Moreover, these embryonic-derived macrophage populations are now known to self-maintain by local proliferation [9; 13-15], although whether this capacity is unique to a specific population or general for all tissue macrophages is still unclear. In humans, host Langerhans cells are not replaced by donor cells in bone marrow transplant patients and monocytopenic individuals have a normal number of Langerhans cells [16-18]. These observations reinforce the studies in mice indicating that there are indeed tissue-resident macrophage populations that are independent of replenishment by circulating monocytes.

This new paradigm, however, does not apply under inflammatory conditions. Massive recruitment of monocytes to tissues occurs upon tissue injury or infection, a process that takes place simultaneously with the proliferation of resident macrophages in cases like nematode infection [19; 20]. Once inflammation has been contained, it is still unclear whether resident macrophages reestablish the total macrophage pool or the newly recruited cells take up residence by acquiring self-renewal capabilities and tissue-resident effector functions. Most likely, this will depend on the nature of the insult and the tissue where inflammation takes place [21-24].

MACROPHAGES IN INFLAMMATION

Macrophages are myeloid cells of the innate immune system that are primarily considered as "homeostasis keepers" due to their ability to sense any perturbation and to respond with a smorgasbord of activities (from tissue-dependent tasks to general immune effector functions) [25-27]. In fact, inflammation caused by either pathogens

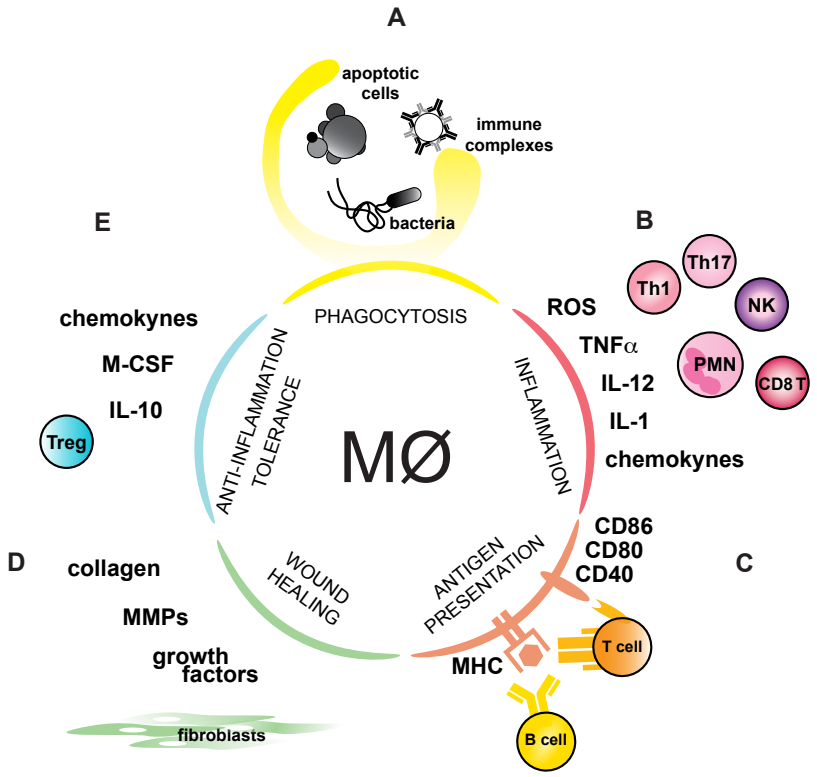

Figure 1. Macrophage functions during inflammation. (A) Macrophages take up apoptotic cells, pathogens, immune complexes and debris by phagocytosis. **(B)** Production of reactive oxygen species (ROS), proinflammatory cytokines and chemokines by macrophages leads to the recruitment of other leukocytes to the inflammed site and contribute to T cell polarization. **(C)** Macrophages present antigen through MHCI and MHCII complexes to T and B lymphocytes to initiate an adaptive immune response. Expression of co-stimulatory molecules (CD40, CD80, CD86) on the macrophage surface is essential for correct lymphocyte activation. **(D)** The reparative phase of inflammation is orchestrated by macrophages via production of growth factors to promote fibroblast proliferation as well as remodelling and deposition of new extracellular matrix. **(E)** Production of anti-inflammatory cytokines and chemokynes by macrophages dampen inflammation and promotes tolerance to endogenous or commensal antigens. TNF-α (Tumor necrosis factor alpha), IL-12 (Interleukin-12), IL-1 (Interleukin-1), Th1 (T helper cell 1), Th17 (T helper cell 17), NK (Natural killer cell), PMN (Polymorphonuclear leukocyte), CD8 T (Cytotoxic CD8+ T cell), MHC (Major histocompatibility complex), Treg (T regulatory cell), IL-10 (Interleukin-10), M-CSF (Macrophage-colony stimulating factor).

or injury may be considered as an extreme disruption of homeostasis that calls macrophages into action to restore tissue integrity and functionality.

Macrophages continuously survey their surroundings to detect anomalies, such as foreing invaders or tissue damage, and respond accordingly by initiating inflammation and by eliminating the threat by phagocytosis and production of enzymes, anti-microbial peptides and reactive oxygen species (**Figure 1A,B**). Besides, as major cytokine and chemokine producers, macrophages orchestrate inflammation and regulate the recruitment of other leukocyte populations (**Figure 1B**). Moreover, macrophages participate in the adaptive immune response by presenting antigen via

major histocompatibility complexes (MHCI and MCHII) to T and B lymphocytes, and by clearing pathogenic agents in the humoral response of B lymphocytes (**Figure 1A,C**). Finally, macrophages regulate the resolution of inflammation and wound healing processes by secreting anti-inflammatory mediators, remodelling of extracellular matrix and promoting angiogenesis (**Figure 1D,E**) [28-33].

In line with their critical role in tissue homeostasis, deregulation of the macrophage effector functions results in numerous pathologies, as best illustrated in the case of tumors. A combination of tissue-injury signals (i.e. hypoxia, extracellular matrix degradation products and apoptosis) and immune-thwarting instructions from tumour cells compell macrophages to restore homeostasis, what ends up favoring tumor growth [34-38]. As an example, breast carcinoma cells promote macrophage recruitment and survival in a M-CSF-dependent manner whereas macrophages, in turn, favour angiogenesis and tumor growth by producing epidermal growth factor (EGF) [39; 40]. Indeed, macrophage depletion results in reduced tumor growth and improved prognosis [41-44]. Other diseases where deregulated macrophage functions contribute to pathology are chronic inflammatory diseases and fibrosis. In the former, the inability to restrain inflammation by macrophages results in the prolonged production of inflammatory mediators and collateral tissue damage that causes pathologies like inflammatory bowel disease, rheumatoid arthritis, and neurologic disorders like Alzheimer disease [45-47]. Contrarily, fibrosis is the consequence of an exacerbated macrophage reparative response towards a prolonged insult [30]. In fibrosis, a sustained inflammatory stimulus promotes excessive wound healing and extracellular matrix deposition by macrophages, thus disrupting normal tissue architecture and function [48]. Therefore, understanding the mechanisms that control the immunogenic, immunoregulatory and wound healing functions of macrophages will allow for future therapies to develop.

TISSUE-RESIDENT MACROPHAGES

The most remarkable feature of macrophages is their impressive functional plasticity which reflects their ability to adapt to different environments. Irrespective of their origin, macrophages sense external cues (exogenous stimuli, prevailing cytokines and metabolites) and rearrange their epigenetic and transcriptional programs to acquire the effector functions required by the surrounding tissue. Therefore, migrating macrophage progenitors respond to different cues by differentiating into macrophages with distinct functional polarization and tissue-specific phenotypes (**Table I**) [25; 49; 50].

M-CSF and IL-34 are essential for the differentiation of tissue-resident macrophages [51]. Both cytokines signal through CSF1R, which is highly expressed by all macrophages, but exhibit distinct expression patterns. M-CSF is ubiquituously expressed by fibroblasts, osteoblasts, macrophages, endothelial and smooth muscle cells, among others, and is found in plasma at 10 ng/ml [51]. IL-34 expression is restricted to the brain and the epidermis, where it is produced by neurons and keratinocytes [51]. Thus, IL-34 is responsible for microglia and Langerhans cell differentiation, whereas M-CSF dependency is widespread for most macrophage populations [51-54]. The latter is evidenced by the fact that a mice strain with a null mutation in the M-CSF-coding gene (*Csf1*$^{op/op}$) has a broad reduction in tissue-resident macrophage numbers [54]. In the presence of M-CSF, monocytes differentiate *in vitro* into macrophages with potent tissue repair and pro-angiogenic functions, and with a strong IL-10-producing ability upon stimulation by Toll-like receptor (TLR) ligands [55-58]. Together with RANKL, M-CSF also promotes the generation of highly specialised bone-resident macrophages or osteoclasts. Specifically, osteoblast-derived RANKL and M-CSF upregulate NFATc1, MITF, FOS and NF-κB, all of which activate the transcriptional program needed for cell fusion and generation of multi-nucleated mature osteoclasts [59; 60]. GM-CSF is abundantly produced during inflammation and has a key role in the development and maintenance of alveolar macrophages [51; 61]. When migrating into the lung, fetal liver precursors are exposed to GM-CSF, what leads to induction of PPARγ expression and drives alveolar macrophage differentiation [62]. Unlike M-CSF, GM-CSF directs the *in vitro* differentiation of monocytes towards macrophages with robust antigen-presenting and immunogenic activity, and with preferential production of pro-inflammatory cytokines upon TLR stimulation [55-58].

Tissue resident macrophage differentiation is not only dependent on cytokines produced by neighbouring cells. Factors derived from microbiota's or tissue's metabolism are as well detected by macrophages and determine their functional specialisation. Metabolites such as retinoid acid, heme and oxysterols have been found to be essential, together with M-CSF, for the differentiation of peritoneal, splenic red pulp and splenic marginal zone macrophages, respectively [63-65]. In each case, metabolites are sensed by macrophages and the appropriate differentiation program is triggered by induction of GATA6 in the peritoneum, SPI-C in the red pulp and LXRα in the marginal zone.

The extreme functional plasticity of macrophages allow them to exert tissue-specific activities required for maintenance of homeostasis and the functionality of the distinct tissues and organs. In the case of the gut, intestinal muscularis mucosa macrophages regulate local tissue and systemic homeostasis through a particular interaction with enteric neurons. By a still unknown microbiota-dependent mechanism, muscularis mucosa macrophages secrete BMP2, which is bound by enteric neurons that secrete M-CSF in return for macrophage survival [66]. Interruption of this loop leads to

Table I. Tissue-resident macrophage functions, transcription factors and related pathologies.

Macrophage subset		Specific transcription factors	Homeostatic function	Pathology
Microglia		SMADs? SALL1? MEF2C? IRF8	Synaptic pruning, learning-dependent synapse formation	Neurodegeneration
Alveolar macrophage		PPARγ, BACH2	Surfactant clearance	Pulmonary alveolar proteinosis
Cardiac macrophage		ND	Phagocytose dying cardiomyocytes	Ischaemic heart disease
Kupffer cell		LXRα? SPIC?	Erythrocyte clearance, bilirubin metabolism, particulate antigen clearance from portal circulation	Fibrosis
Red pulp macrophage		SPIC	Iron recycling, erythrocyte clearance	Iron overload
Marginal zone macrophage		LXRα	Marginal zone B cell maintenance	Autoimmune disease
Lamina propria macrophages		RUNX3?	Gut tolerance	Inflammatory bowel disease
Intestinal muscularis macrophage		ND	Peristalsis	Postoperative ileus
Bone marrow macrophage		SPIC, LXRα	Regulation of HSC niche, erythroblast development, removal of aged neutrophils	Leukemia
Osteoclast		NFATC1, FOS, MITF	Bone resorption	Osteoporosis, osteopetrosis

Adapted from Wynn et al, Nature 2013 and Lavin et al, Nat Rev 2015

abnormal intestinal smooth muscle cell contractions and to defective colonic peristalsis and altered transit time. In the spleen, red pulp macrophages are continuously exposed to senescent erythrocytes and are specialised in phagocytosing and recycling heme. In this context, an improper regulation of macrophage differentiation and function leads to splenic iron overload [67]. Adipose tissue macrophages are key in regulating insulin sensitivity of adipocytes through IL-10 secretion and, thus, regulate physiological homeostasis upon nutrient intake. In obesity, metabolically stressed adipocytes

secrete inflammatory cytokines that increase macrophage recruitment and build up inflammation [68]. In the lungs, alveolar macrophages are specialised in pulmonary surfactant recycling and an imbalance in this process leads to pulmonary alveolar proteinosis [61; 69]. Osteoclasts, multinucleated macrophages of the bone, resorb bone in a finely tuned equilibrium with bone-forming osteoblasts to maintain bone integrity and calcium levels in the organism [70]. Failure in osteoclast formation, as seen in the osteoclast-deficient *Csf1*$^{op/op}$ mice strain, leads to aberrant bone architecture, with bones lacking the necessary cavities for bone marrow hematopoiesis [71].

MACROPHAGE ACTIVATION

Another aspect of macrophage functional specialisation and polarization becomes evident upon macrophage encounter with endogenous or exogenous pathogenic insults. The features of the macrophage reaction towards the stimulus is critically dependent on the surrounding environment at the moment of the insult and on previous instructions received during the macrophage's lifetime [28; 49; 72; 73]. Therefore, macrophage activation relies on the integration of signals derived from their ontogeny, differentiating factors, cytokines, metabolites and ligands for pathogen-/danger-associated molecular patterns (PAMPs/DAMPs) (**Figure 2**). As a consequence, macrophages can acquire an almost infinite number of activation (polarization) states, what has led to the hypothesis of the "spectrum model" of macrophage activation [28; 74]. In this context, macrophages are classified according to the factors which they have been primed with and to the type of response they carry out upon a pathogenic challenge [75]. For the sake of simplicity, this classification may be divided in two big groups according to the macrophage's response to the pathogenic insult. Thus, macrophages can either be pro-inflammatory or anti-inflammatory. The former secrete TNF-α, IL-12, IL-6 and IL-23 upon activation with PAMPs and DAMPs and exhibit high antigen-presenting capabilities, whereas the latter produce IL-10 and are highly phagocytic and profibrotic. Macrophages can be further classified according to the differentiating and/or activating cytokines and factors. So, macrophages exposed to IFNγ or GM-CSF become proinflammatory, whereas macrophages treated with IL-10, IL-4, IL-13, glucocorticoids or M-CSF preferentially display anti-inflammatory functions [76]. Needles to say, these *in vitro* derived macrophage populations reflect only discrete aspects of in vivo macrophages. Nevertheless, *in vitro*-polarized macrophages have proven very useful in the study of macrophage biology since many of their specific responses and behaviours have been confirmed in vivo [77]. Macrophages in the synovium of rheumatoid arthritis patients are

typically proinflammatory and transcriptionally similar to *in vitro* GM-CSF-differentiated monocyte-derived macrophages (GM-MØ) [78], whereas lamina propria macrophages that sample microbiota antigens in the intestinal lumen are anti-inflammatory and resemble IL-10-producing M-CSF-dependent monocyte-derived macrophages (M-MØ) [79; 80]. Tumor-associated macrophages tend to exhibit an ambivalent pro- and anti-inflammatory phenotype [81], probably due to the concomitant stimulation by tumor cell-derived immunosuppressive signals and by stimuli from dying cells and hypoxia.

Nowadays, however, the vast majority of the current knowledge on macrophage activation derives from studies performed on mice. Even though mouse disease models have greatly increased our understanding of the molecular basis of many pathologies, the existence of relevant differences between the mouse and human immune systems calls for more intense study of human macrophage biology [74; 82-86].

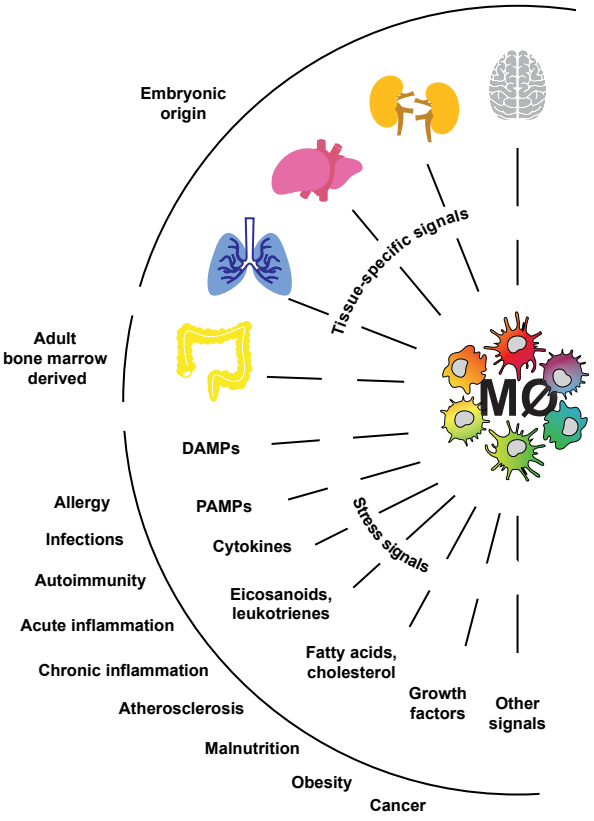

Figure 2. Multidimensional model of macrophage activation. A multidimensional model is depicted whereby macrophage activation is the result of the integration of the information provided by the microenvironment (tissue-specific signals and stress signals) and the macrophage ontogeny (developmental origin). Brain, kidney, liver and lung tissue-resident macrophages have an embryonic origin, whereas macrophages in the intestine, peritoneum and heart are continuously replenished by monocytes. Macrophage progenitors in each tissue receive specific instructions from different tissue factors. Pathologies or injuries lead to the production of stress signals that, in a localization- and kinetic-dependent manner, are integrated together with previous developmental instructions and differentially affect the outcome of the macrophage response. Adapted from Ginhoux et al, Nat. Imm. 2016.

Table II. Exogenous and endogenous TLR ligands.

	TLR1/2/6	TLR2	TLR3	TLR4	TLR5	TLR7/8	TLR9	TLR10
PAMP	Lipoproteins ($Gram^+$)	LTA ($Gram^+$) β-Glycan (fungus) GPI anchors (protozoa)	dsRNA (virus)	LPS ($Gram^-$) GPI anchors (protozoa)	Flagellin (bacteria)	ssRNA (virus)	DNA (bacteria, virus, fungus, protozoa)	ND
DAMP		HMGB1 Fibronectin Hyaluran Serum Amyloid A	mRNA	HMGB1 Fibrinogen Hyaluran Serum Amyloid A oxLDL, saturated fatty acids S100 proteins		ssRNA	mitochondrial DNA	

Adapted from Bryan et al, Critic Rev Biochem Mol Biol 2015

Toll-like receptors

Macrophages are equipped with a collection of pattern recognition receptors (PRRs) that allows them to detect pathogen-associated molecular patterns (PAMPs), such as microbial products, and danger-associated molecular patterns (DAMPs) produced or released from endogenous injured cells and tissues. Among PRRs, Toll-like receptors (TLRs) are the best characterised. TLRs are type I single spanning transmembrane proteins that are characterised by a PAMP/DAMP-recognizing Leucine-rich repeat (LRR) domain, a transmembrane helix and a cytoplasmic TLR-IL1R (TIR) domain. So far, 10 TLRs have been identified in humans and they are classified in two groups according to their cellular location. Plasma membrane TLRs (TLR1, TLR2, TLR4, TLR5, TLR6, TLR10) recognise lipids, lipoproteins and proteins, while intracellular TLRs (TLR3, TLR7, TLR8 and TLR9) recognise nucleic acids (**Table II**) [87-89]. Upon ligand recognition, TLRs dimerise and several adaptor proteins bind to their TIR domains. The most well characterised adaptor proteins include MYD88 (myeloid differentiation factor 88) and TRIF (TIR domain-containing adaptor inducing interferon beta), but MAL, TRAM and SARM also mediate TLR signalling [90]. Generally, ligand recognition by TLRs in macrophages leads to MYD88-dependent production of proinflammatory cytokines and TRIF-dependent expression of type I IFNs (**Figure 3**).

All TLRs can signal through MYD88- and TRIF-dependent pathways, except TLR3, which only signals through TRIF 90.

TLR4 signaling is initiated by binding of its co-receptor MD2 to lipopolysaccharide (LPS), its prototypical ligand that constitutes an important component of the Gram-negative bacterial cell wall (**Figure 3**). Then, the TLR4-MD2-LPS complex homodimerises and, during early signalling, MAL-MYD88 is recruited to the TLR4 TIR domains. MYD88 binds IRAK4, which sequentially phosphorylates IRAK1 and IRAK2. The MYD88-IRAK complex engages the ubiquitin ligase TRAF6 to make polyubiquitin chains that activate the TAK1 kinase. TAK1 activation triggers both the dissociation of the NF-κB inhibitor complex, leading to the release of NF-κB and its translocation to the nucleus, and also the activation of ERK, p38 and JNK mitogen-activated protein kinases (MAPKs) [91; 92]. TLR4 is later endocytosed and then signals through recruitment of the TRAM-TRIF complex, which triggers NF-κB activation and IRF3 phosphorylation [91; 92].

Macrophage activation by TLR4 ligands triggers a potent transcriptional response that depends on NF-κB, IRF3, CREB, CEBP-α and AP1 transcription factor activation. The 'classical' TLR4-mediated macrophage activation, which can be seen in macrophages generated under the influence of GM-CSF (GM-MØ), is characterised by the release of proinflammatory cytokines and type I interferons and is dependent on NF-κB, MAPK and IRF3. Conversely, LPS-TLR4 activation of macrophages generated under the influence of M-CSF (M-MØ), primarily leads to the release of IL-10 and is dependent on ERK and p38 signalling [87; 93; 94]. A myriad of studies have thoroughly assessed the molecular mechanisms and transcriptome behind the pro-inflammatory activation of murine macrophages [28; 75; 87; 95]. However, the molecular basis for the anti-inflammatory activation of macrophages has been much less studied, especially in the case of human macrophages.

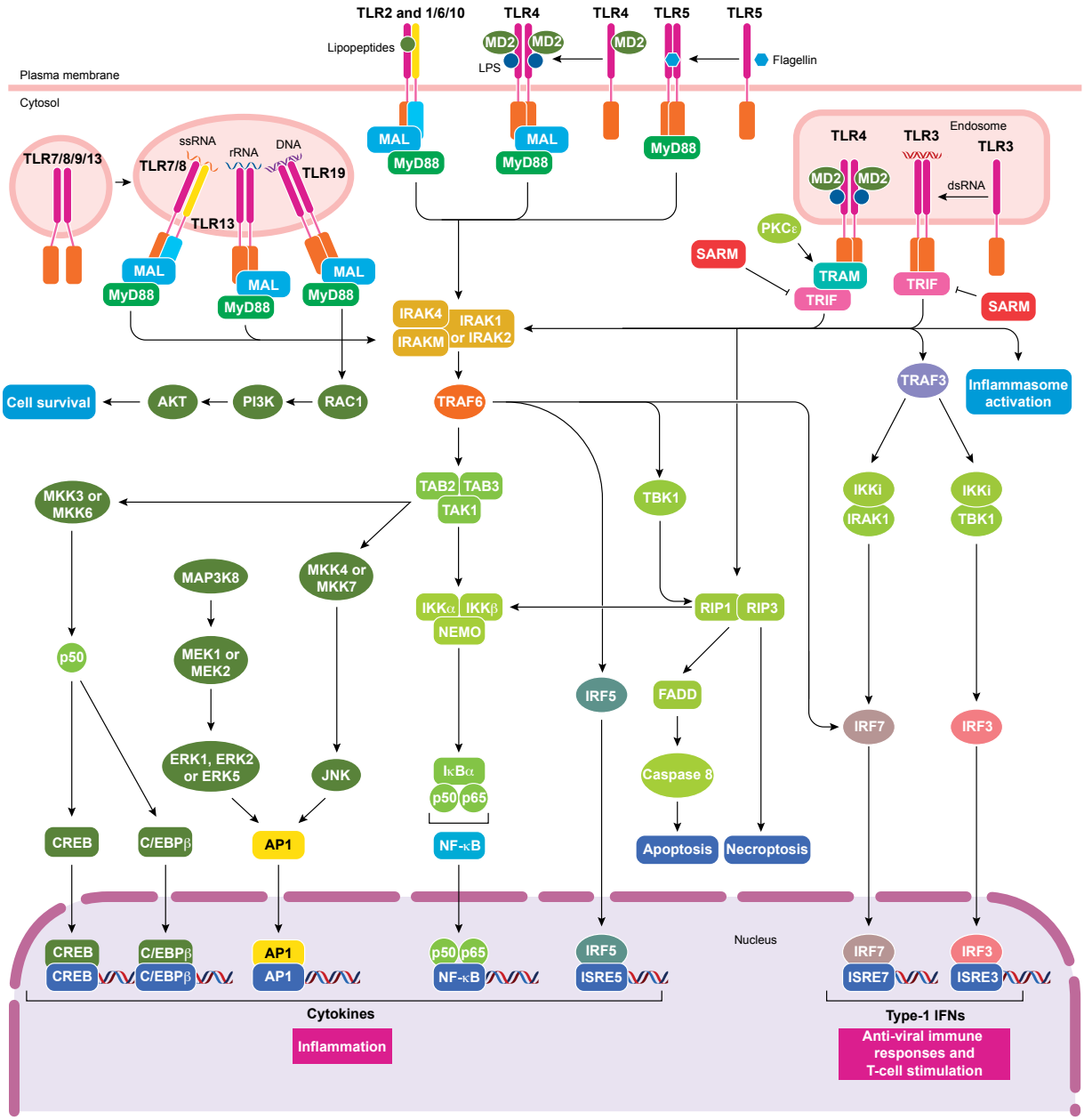

Figure 3. TLR signaling pathways. MYD88-dependent TLR signaling leads to activation of TRAF6, which activates the MAPK and NFκB pathways that lead to the expression of proinflammatory cytokine and chemokine genes. Signaling from TLR3 and endocytosed TLR4 activates IRF-dependent transcription of type-I-IFNs via the TRAM/TRIF pathway. Adapted from Ullah et al, Journal of Leukocyte Biology 2016.

MAFB

Structural features and expression

MAFB is a transcription factor that belongs to the MAF family, which is made up of 7 members, namely MAFA, MAFB, MAF and NRL (large MAFs) and MAFG, MAFF and MAFK (small MAFs) (**Figure 4**) [96]. The MAF family is part of the AP1 superfamily of transcription factors that contain basic and leucine zipper (bZIP) domains for DNA-binding and dimerisation [96]. AP1 members recognise TRE (12-O-tetradecanoyl phorbol 13-acetate (TPA)-responsive element) or CRE (cAMP-responsive element) DNA palindromic sequences. MAF members, however, contain an extended homology region that also contacts DNA and allows them to recognise TRE or CRE sequences flanked by a TGC motif, the so-called MARE (Maf-recognition element) sequences (**Figure 4A**) [96]. Interestingly, many MAF family target genes only contain half a MARE in their promoters, which highlights the ability of the MAF proteins to heterodimerize with other AP1 family members. Particularly, MAFB can heterodimerize with MAF, JUN and FOS to induce transcription [96-98], whereas it associates to other transcription factors to inhibit their function, i.e. MYB, MITF and NFATc1 [98; 99].

MAFB expression is regulated by retinoic acid and TNF-α in the monocytic cell line THP-1 [100], VEGF-C in lymphatic endothelial cells [101], IL-10 and STAT3 signalling in macrophages and the vitamin D3/Hox-A10 pathway in $CD34^+$ hematopoietic progenitors [102; 103]. MAFB is also regulated at the post-transcriptional level by phosphorylation and sumoylation (**Figure 4B**). All members of the large MAF family share similar regulatory mechanisms via phosphorylation by p38, JNK and GSK3. Like in MAF and MAFA, four residues of the MAFB transactivation domain (S66, T62, T58 and S54) are targets for GSK3 phosphorylation after a priming phosphorylation at S70 [96; 104; 105]. In an apparent contradiction, GSK3 phosphorylation of MAFs increases both transactivation activity and ubiquitylation and subsequent degradation [104; 105]. MAFB can also be phosphorylated by JNK and p38 at T62 106 and other unspecified residues [107]. Phosphorylation by JNK also regulates MAFB stability and ubiquitinilation, while sumoylation at K32 and K297 inhibits MAFB transactivation activity [98].

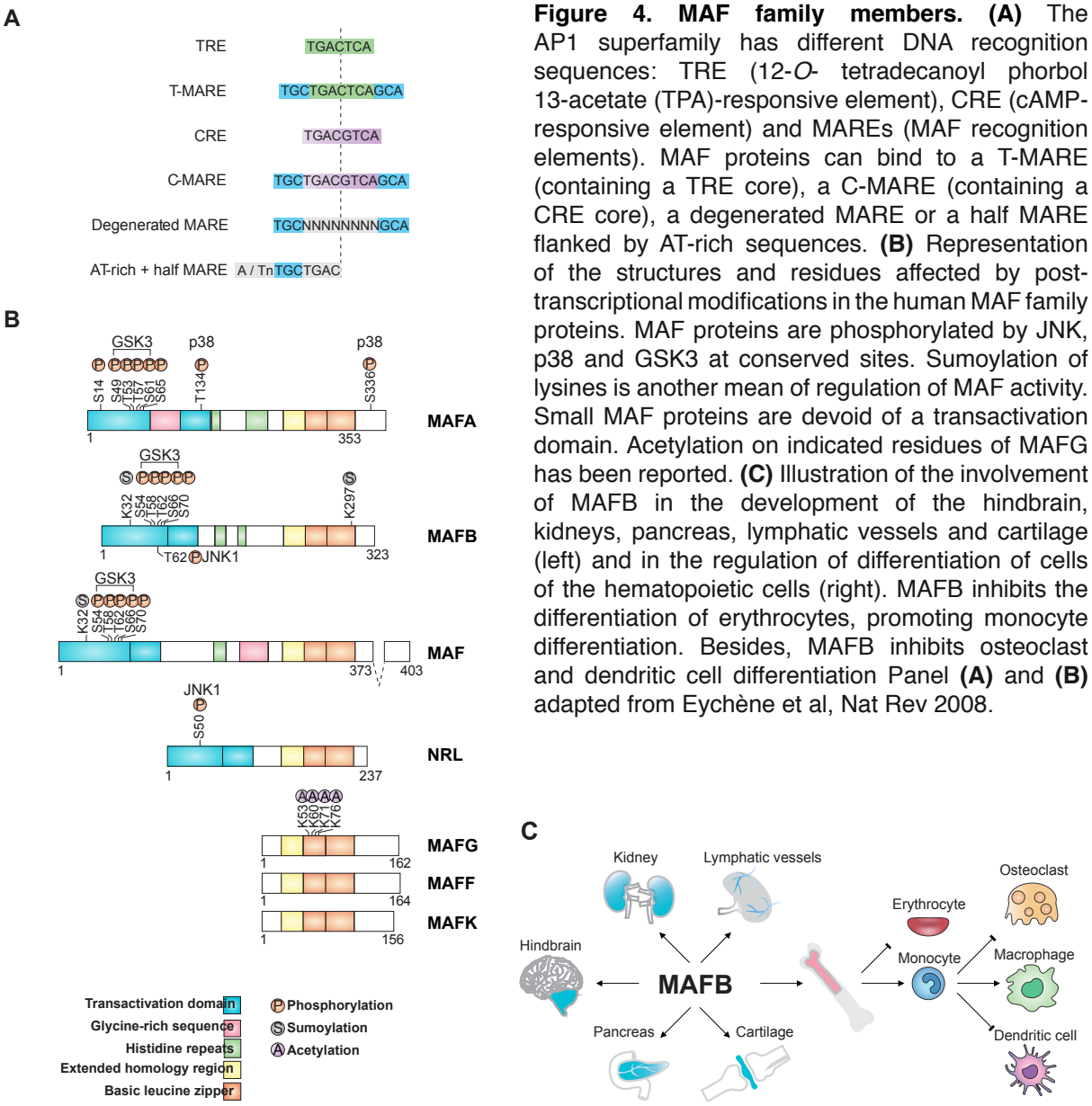

Figure 4. MAF family members. (A) The AP1 superfamily has different DNA recognition sequences: TRE (12-*O*- tetradecanoyl phorbol 13-acetate (TPA)-responsive element), CRE (cAMP-responsive element) and MAREs (MAF recognition elements). MAF proteins can bind to a T-MARE (containing a TRE core), a C-MARE (containing a CRE core), a degenerated MARE or a half MARE flanked by AT-rich sequences. **(B)** Representation of the structures and residues affected by post-transcriptional modifications in the human MAF family proteins. MAF proteins are phosphorylated by JNK, p38 and GSK3 at conserved sites. Sumoylation of lysines is another mean of regulation of MAF activity. Small MAF proteins are devoid of a transactivation domain. Acetylation on indicated residues of MAFG has been reported. **(C)** Illustration of the involvement of MAFB in the development of the hindbrain, kidneys, pancreas, lymphatic vessels and cartilage (left) and in the regulation of differentiation of cells of the hematopoietic cells (right). MAFB inhibits the differentiation of erythrocytes, promoting monocyte differentiation. Besides, MAFB inhibits osteoclast and dendritic cell differentiation Panel **(A)** and **(B)** adapted from Eychène et al, Nat Rev 2008.

MAFB functions

The functions of MAFB range from regulation of organ development and patterning during embryogenesis to control of terminal differentiation and function of adult cell lineages (**Figure 4C**). MAFB is required for proper segmentation of rhombomeres 5 and 6 of the mouse hindbrain and regulates other factors involved in hindbrain patterning [108]. Development of pancreatic α and β cell, as well as glucagon production in the adult pancreas, is regulated by MAFB [109; 110]. During lymphangiogenesis, a process regulated by VEGF-C/VEGFR-3, MAFB is activated by VEGFR-3-initiated signalling and induces

lymphatic endothelial cell-specific transcription factors and markers [101]. Moreover, MAFB has a role in skin cell differentiation [111], and contributes to chondrocyte matrix formation and development through CTGF gene expression control [112] and to podocyte generation [113-116].

In hematopoietic and immune cells, MAFB shapes responses to viral infections through regulation of type I interferon by recruitment of coactivators to IRF3 [117]. However, MAFB is best known for its role in the myeloid lineage (**Figure 4C**), where it induces monocytic differentiation in avian myeloblasts *in vitro* and represses avian erythroid cell differentiation by direct binding to Ets1 [118; 119]. This observations are supported by experiments in primary human hematopoietic progenitors, where ectopic expression of MAFB skews differentiation towards the monocytic lineage [120]. Moreover, an antagonistic equilibrium between Myb and Mafb controls proliferation of avian progenitors versus macrophage commitment [98], whereas Mafb ablation in murine hematopoietic stem cells leads to enhanced myeloid commitment [121]. Besides, PU.1 inhibits Mafb in avian myeloblasts to promote dendritic cell at the expense of macrophage differentiation [122], while in murine bone marrow-derived cells Mafb binds to Fos, Mitf and NFATc1 to inhibit osteoclast differentiation [99].

Regarding adult tissue-resident macrophages, the study of the role of Mafb has been impaired due to the fact that *Mafb*$^{-/-}$ mice die twenty-four hours after birth [123]. Nevertheless, irradiated mice that are reconstituted with fetal liver *Mafb*$^{-/-}$ hematopoietic progenitors do not show deffects in monocyte numbers in blood nor macrophage populations in spleen and peritoneum, while *in vitro*-derived *Mafb*$^{-/-}$ have an altered actin organization [124]. This mild phenotype of *Mafb*$^{-/-}$ macrophages was attributed to redundant functions of Mafb and c-Maf, being the latter upregulated after *Mafb* ablation [124]. However, double deletion of c-Maf and Mafb provides murine macrophages with self-renewal ability and adoptively-transferred double knockout monocytes are able to contribute long-term to the spleen, liver and peritoneum macrophage pool [125]. Adult mouse tissue resident macrophage-specific enhancers are enriched in MARE sequences and have high expression of *Mafb* and *c-Maf* RNA as compared to monocytes and neutrophils [21]. Altogether, a role for Mafb has been established in the differentiation of the monocyte/macrophage lineage in animal models, yet the exact nature of the implication of MAFB for human macrophage function remains to be addressed.

MAFB-related pathologies

The deregulated expression/function of MAFB affects cell, tissue and organ functions, giving rise to human pathologies. MAFB loss of function mutations have been described to cause Duane retraction syndrome, a congenital eye-movement disorder caused by defects in abducens nerve development [126]. MAFB overexpression is a common feature in multiple myeloma [127] and is linked to Dupuytren's disease [128], a fibroblastic proliferation of the palmar fascia. Besides, analysis of animal models of disease has revealed that MafB promotes atherosclerosis by inhibiting foam-cell apoptosis [129] and that MafB mutations cause kidney-associated diseases that result from altered podocyte differentiation [130]. Moreover, MafB is upregulated in alveolar macrophages in pulmonary emphysema [131] as well as in human adipocytes during adipogenesis with adverse metabolic features [132]. Finally, *MafB* knockout mice have an aberrant development of the respiratory center of the brain that causes fatal apnea immediately after birth [123].

A

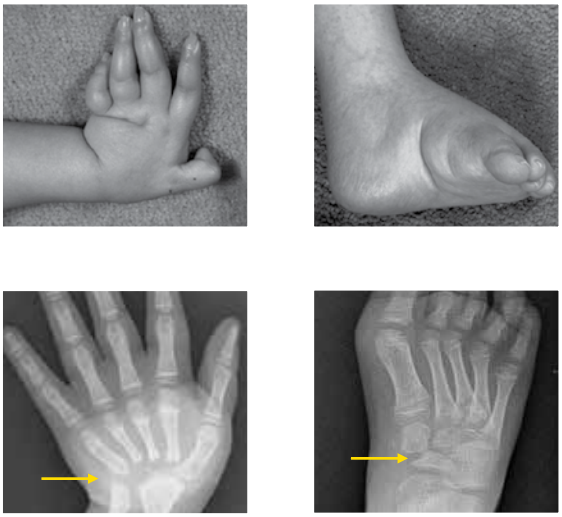

B

C

Mutation	# Probands	Reference
161C>G, Ser54Trp	1	134
161C>T, Ser54Leu	2	133
167C>T, Ser56Phe	1	137
176C>T, Pro59Leu	3	135
		134
		133
184A>C, Thr62Pro	1	133
185C>T, Thr62Ile	1	135
188C>G, Pro63Arg	2	134
		133
188C>T, Pro63Leu	2	134
194G>T, Ser65Ile	1	134
197C>G, Ser66Cys	1	133
206C>T, Ser69Leu	5	135
		133
208T>G, Ser70Ala	1	133
209C>T, Ser70Leu	3	135
		133
211C>T, Pro71Ser	3	135
		133
212C>T, Pro71Leu	1	133

Figure 5. Multicentric carpotarsal osteolysis. Pictures and radiographs of hands and feet of MCTO patients **(A)** and a control individual **(B)**. Yellow arrow marks the missing carpal (left panel) and tarsal (right panel) bones. **(C)** Reported MAFB mutations causing MCTO.

Multicentric carpotarsal osteolysis (MCTO)

MCTO is a rare autosomal dominant skeletal disorder (OMIM #166300) that is characterized by the gradual disappearance of the carpal and tarsal bones (**Figure 5A,B**) causing joint deformities and pain as the syndrome progresses during the first decades of life [133-135]. Thieffry and Sorrel-Dejerine first reported a complete description of multicentric carpotarsal osteolysis (MCTO) in 1958. Since then, only around 70 cases have been reported worldwide [134-136], probably due in part to common misdiagnoses as juvenile idiopathic arthritis. Some affected individuals may present minor craniofacial abnormalities, such as triangular faces, micrognathia and exophthalmos, as well as corneal opacity [133-135; 137]. Moreover, many patients develop nephropathy, which is usually diagnosed at terminal renal insufficiency. The mechanisms underlying the onset of nephropathy in MCTO are still unknown, although focal and segmental glomerulosclerosis have been diagnosed on rare early stage biopsies [134]. Recently, heterozygous missense mutations within a very short region (aminoacids 54-71, *see* **Figure 4B**) of the transactivation domain in MAFB have been reported to cause MCTO (**Figure 5C**) [133]. Both familial transmission and simplex cases have been detected, and MCTO is believed to be an autosomal dominant disorder.

In spite of its wide pathological relevance, the association of MAFB to specific macrophage polarization states and the identity of MAFB-regulated genes and functions in human macrophages are mostly unknown.

OBJECTIVES

1. To determine the molecular basis for the differential cytokine responsiveness of LPS-activated GM-CSF (GM-MØ) and M-CSF-primed (M-MØ) human macrophages:

1.1. To identify the signalling pathways differentially triggered by TLR activation in GM-MØ and M-MØ.

1.2. To define the transcriptomes of GM-MØ and M-MØ upon TLR4 activation with LPS.

1.3. To identify genes co-expressed with IL-10 in anti-inflammatory human macrophages *in vitro* and *in vivo***.**

2. To determine the role of MAFB in macrophage polarization:

2.1. To assess the expression of MAFB in M-MØ *in vitro* and *in vivo***.**

2.2. To determine the genes and effector functions that are controlled by MAFB in M-MØ.

2.3. To study the transcriptional and functional consequences of Multicentric carpotarsal osteolysis (MCTO)-causing MAFB mutations.

RESULTS

CHAPTER ONE

A novel set of genes that define the activation state of human anti-inflammatory macrophages

Differential cytokine LPS responsiveness of GM-MØ and M-MØ.

GM-CSF and M-CSF contribute to monocyte/macrophage cell survival and proliferation, and promote monocyte differentiation into functionally different macrophages [56; 138]. GM-CSF gives rise to macrophages (hereafter termed GM-MØ) that produce pro-inflammatory cytokines upon TLR stimulation, whereas M-CSF generates macrophages (M-MØ) with robust IL-10-producing ability in response to pathogenic stimuli [56; 57; 95]. Accordingly, human GM-MØ and M-MØ are considered as pro-inflammatory and anti-inflammatory macrophages. LPS treatment, either alone or in combination with IFNγ, is considered as the paradigmatic stimulus for acquisition of the classical macrophage polarization/activation state [75]. However, this definition does not take into account the influence that other macrophage differentiating/priming factors might have on the LPS response. To identify the molecular basis for the distinct LPS-induced cytokine profiles of GM-MØ and M-MØ we first determined their respective kinetics of LPS responsiveness at the cytokine mRNA and protein levels. Significantly elevated levels of *IL12B*, *IL6* and *IFNB1* mRNA were detected in GM-MØ after 3-5 hours of LPS exposure, a time at which *IL10* mRNA was significantly elevated in M-MØ (**Figure 6A** & **Figure 7A**). These changes preceded the significantly distinct LPS-induced cytokine profiles of both macrophage subsets: higher levels of IL-12p40 (after 12 hours), IL-6 and IFN-β (after 3 hours) in GM-MØ and higher levels of IL-10 in M-MØ (after 5 hours) (**Figure 6B**, **Figure 7B**). The distinct cytokine pattern of LPS-activated GM-MØ and M-MØ was also seen when both macrophage subtypes were stimulated by the TLR2 ligand PAM3CSK4 (**Figure 6C**, **Figure 7C**). Interestingly, although LPS-induced *TNF* mRNA levels were similar in both macrophage subtypes (**Figure 6A**, **Figure 7A**), high production was exclusively seen in GM-MØ at 12-24 hours after LPS treatment (**Figure 6B**, **Figure 7B**). The lack of TNF-α production in M-MØ, confirmed by flow cytometry and Western blot, was not secondary to IL-10 production, thus indicating that non-transcriptional mechanisms are responsible for the differential LPS-induced production expression of TNF-α by GM-MØ and M-MØ (*data not shown*).

Next, we determined at which stage during differentiation each macrophage subtype acquires their specific LPS-induced cytokine profile. In GM-MØ, the characteristic high LPS-induced TNF-α production was seen as early as 24 hours along the GM-CSF-driven differentiation, whereas high LPS-stimulated IL-10 production was detected 48 hours after monocyte exposure to M-CSF (**Figure 6D**, **Figure 7D**). Therefore, differentiating monocytes acquire the characteristic LPS-induced cytokine profile of GM-MØ (TNF-α^{high} IL-10^{low}) and M-MØ (TNF-α^{low} IL-10^{high}) at early stages along the monocyte-to-macrophage differentiation promoted by either GM-CSF or M-CSF

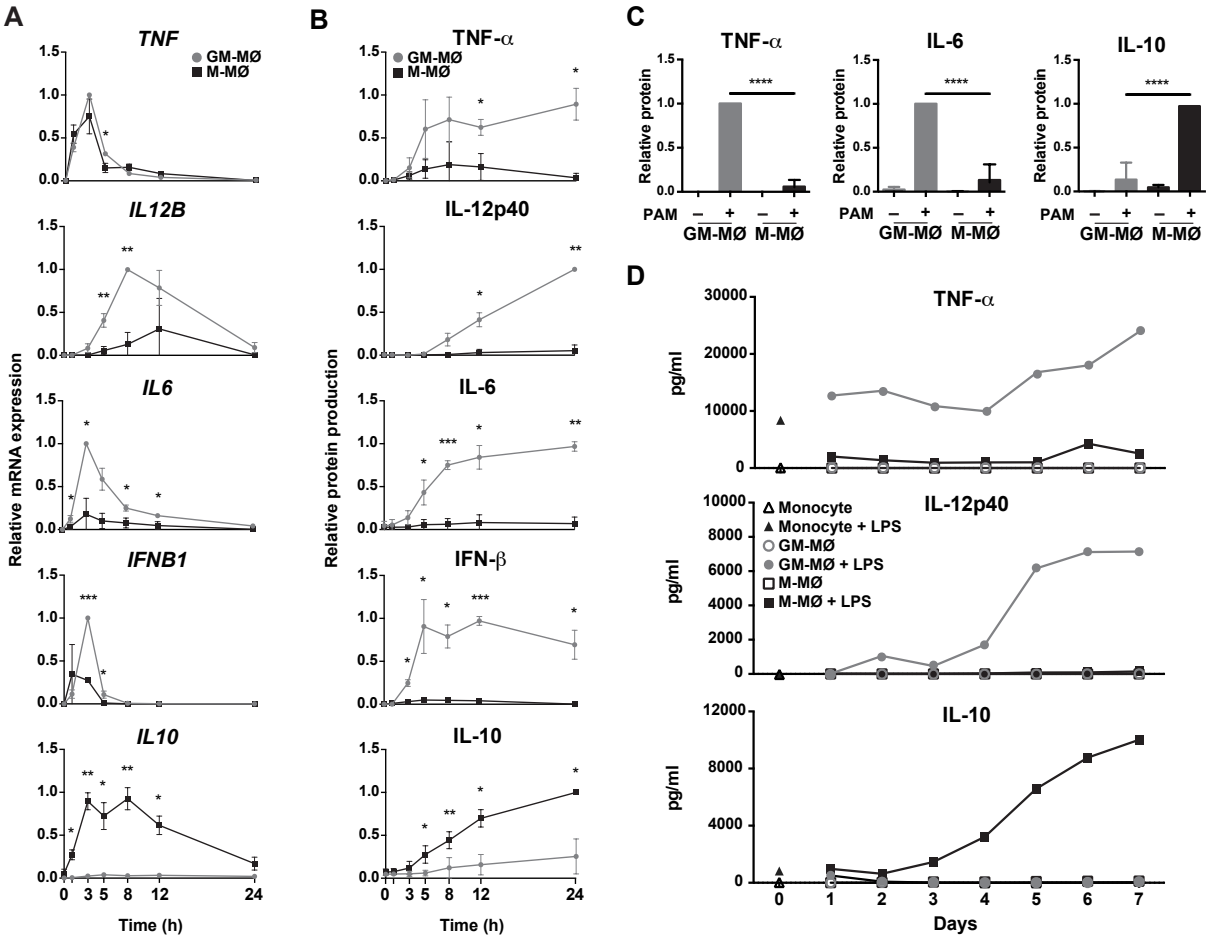

Figure 6. Differential cytokine profile of activated M-MØ and GM-MØ. (A,B) Kinetics of LPS-induced cytokine mRNA **(A)** and protein **(B)** expression of M-MØ and GM-MØ. Results are expressed relative to the maximal level of cytokine mRNA **(A)** or protein **(B)** in GM-MØ (TNF-α, IL-12p40, IL-6, IFN-β) or M-MØ (IL-10). Shown are the means and SD of three independent expreriments (n=3; *, $p < 0.05$; **, $p < 0.005$; ***, $p < 0.0005$). **(C)** PAM3CSK4 (PAM)-induced cytokine production of M-MØ and GM-MØ. Results are expressed relative to the maximal level of cytokine production in GM-MØ (TNF-α, IL-6) or M-MØ (IL-10). Shown are the means and SD of six independent experiments (n=6; *, $p < 0.05$; **, $p < 0.005$; ***, $p < 0.0005$). **(D)** LPS-induced cytokine production along the monocyte-to-macrophage differentiation of M-MØ and GM-MØ. Six experiments were done on independent monocyte samples and one of them is shown.

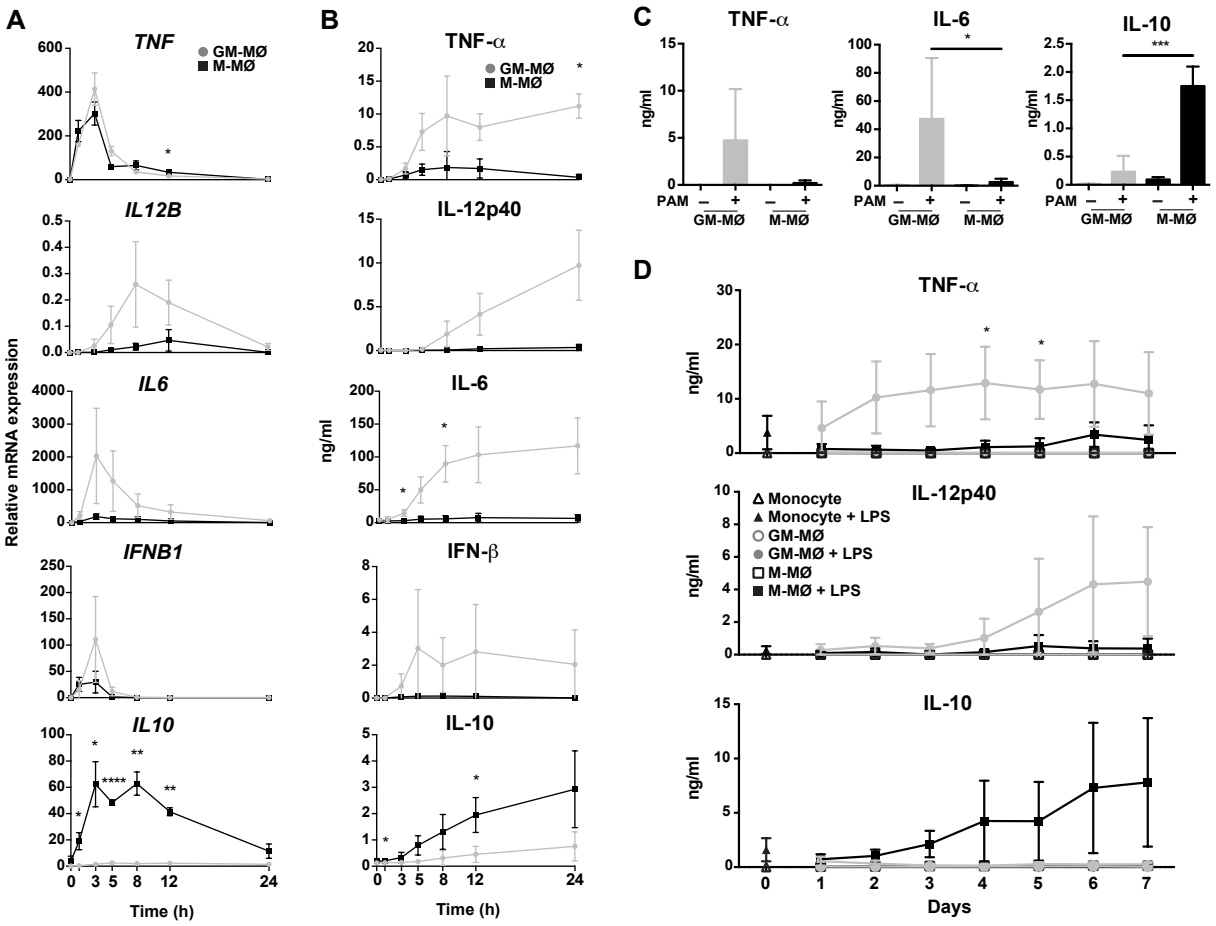

Figure 7. Differential cytokine profile of activated M-MØ and GM-MØ. (A,B) Kinetics of LPS-induced cytokine mRNA **(A)** and protein **(B)** expression of M-MØ and GM-MØ. Results indicate the relative levels of the indicated mRNA (relative to *TBP* mRNA levels) **(A)**, and the concentration of the indicated cytokines **(B)**. Shown are the means and SD of three independent experiments (n=3; *, $p < 0.05$; **, $p < 0.005$; ***, $p < 0.0005$). **(C)** PAM3CSK4-induced cytokine production of M-MØ and GM-MØ. Shown are the means and SD of six independent experiments (n=6; *, $p < 0.05$; **, $p < 0.005$; ***, $p < 0.0005$). **(D)** LPS-induced cytokine production along the monocyte-to-macrophage differentiation of M-MØ and GM-MØ. Shown are the means and SD of six independent experiments (n=6; *, $p < 0.05$).

(**Figure 6D**). In contrast, the preferential LPS-stimulated production of IL-12p40 in GM-CSF-differentiated macrophages was not acquired until later time points (4 days) (**Figure 6D**, **Figure 7D**). The delayed acquisition of the IL-12 p40 production ability by GM-MØ led us to assess whether autocrine factors contributed to the establishment of the LPS-induced cytokine profile of each macrophage subtype. To that end, GM-MØ and M-MØ were treated with LPS after exchange of their respective conditioned media. GM-MØ kept in the presence of M-MØ-conditioned medium also displayed a preferential expression of *TNF*, *IL12B*, *IL6* and *IFNB1* mRNA after LPS exposure (**Figure 8A**). Similarly, M-MØ exhibited the preferential expression of LPS-induced IL-10 mRNA and protein regardless of whether LPS stimulation took place in their own culture medium or in GM-MØ-conditioned medium (**Figure 8A,B**). Therefore, the ability of GM-MØ and M-MØ to preferentially produce pro-inflammatory (GM-MØ) or anti-inflammatory (M-MØ) cytokines in response to activating stimuli is cell-intrinsic and is not significantly modulated by the extracellular milieu or by autocrine factors accumulated along the differentiation process.

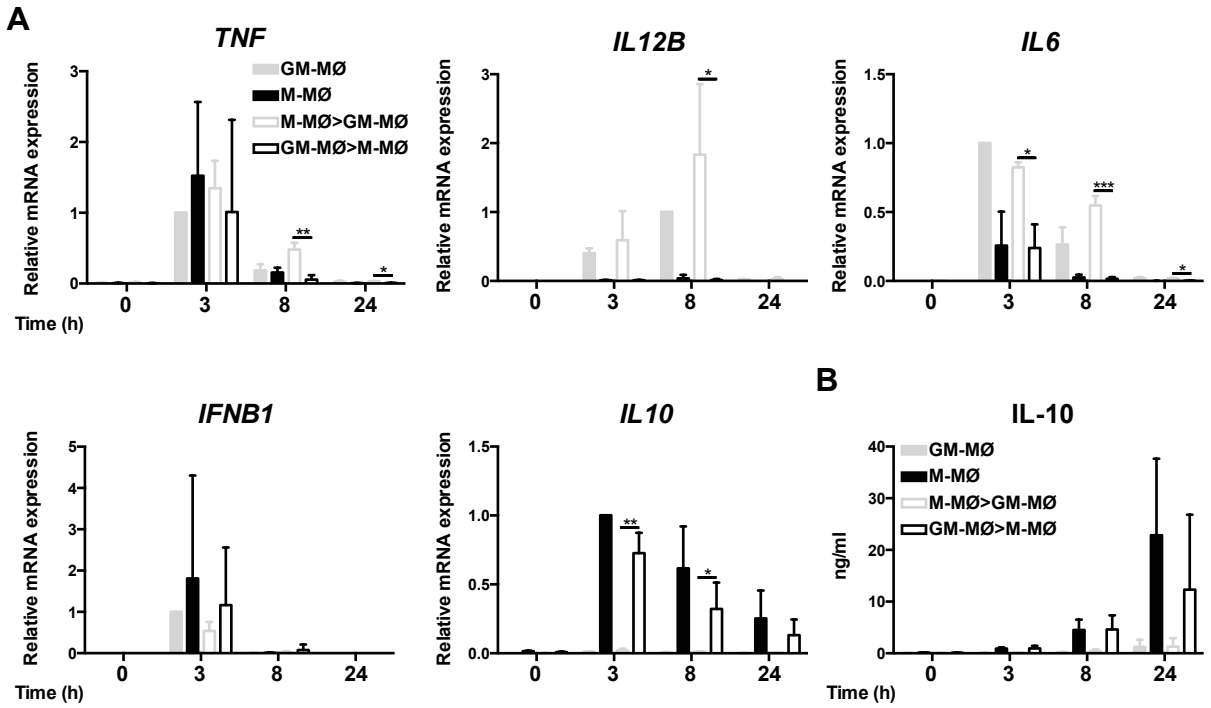

Figure 8. The differential cytokine profile of activated M-MØ and GM-MØ is cell-intrinsic. (A) LPS-induced expression of cytokine mRNA in cells kept in their conditioned media (M-MØ, GM-MØ) or whose culture medium was switched (M-MØ>GM-MØ, GM-MØ>GM-MØ) immediately before LPS stimulation. Cytokines were determined 3-24 hours after LPS exposure. Results are expressed relative to the maximal level of cytokine mRNA in GM-MØ (*TNF, IL-12B, IL6, IFN-β*) or M-MØ (*IL10*). Shown are the means and SD of four independent experiments (n=4; *, $p < 0.05$; **, $p < 0.005$; ***, $p < 0.0005$). **(B)** LPS-induced IL-10 production in cells kept in their conditioned media (M-MØ, GM-MØ) or whose culture medium was switched (M-MØ>GM-MØ, GM-MØ>GM-MØ) immediately before LPS stimulation. Shown are the means and SD of four independent experiments (n=4).

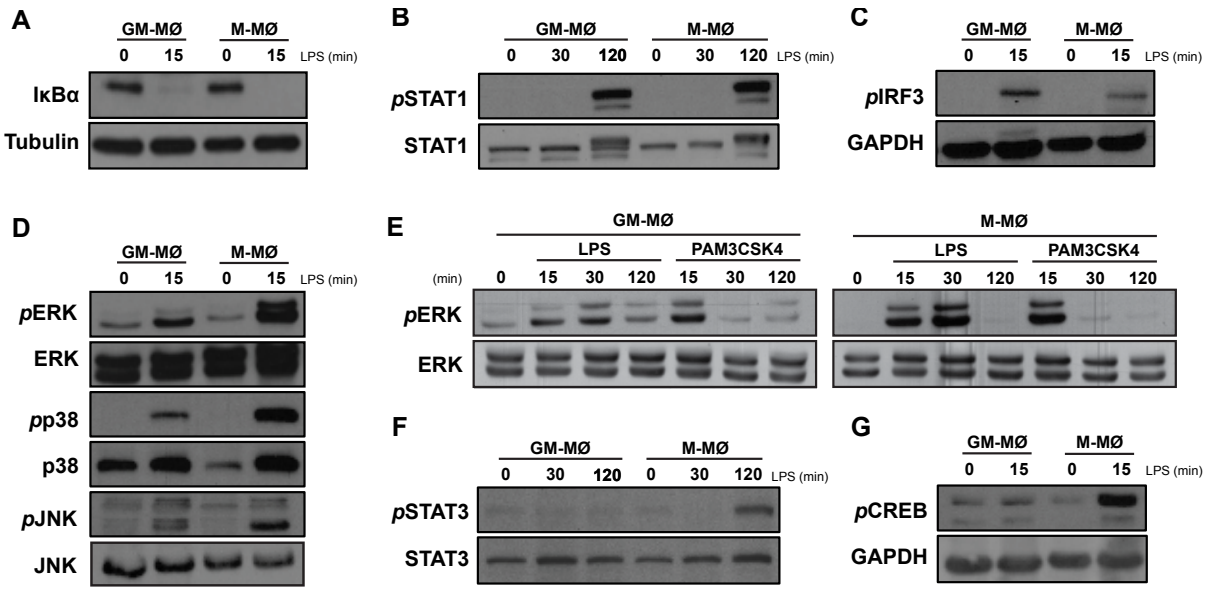

Figure 9. Differential LPS-triggered intracellular signaling in M-MØ and GM-MØ. M-MØ and GM-MØ were treated with LPS **(A-D,F,G)** or PAM3CSK4 **(E)**, and cell lysates were obtained at the indicated time points and assayed for the expression of IκBα **(A)**, phosphorylated and total STAT1 **(B)**, phosphorylated IRF3 **(C)**, phosphorylated and total ERK1/2, p38MAPK and JNK **(D,E)**, phosphorylated and total STAT3 **(F)**, and phosphorylated CREB **(G)** by Western blot using specific antibodies. Where indicated, protein loading was normalized using a monoclonal antibody against GAPDH or α-tubulin.

Differential LPS-initiated intracellular signaling pathways in GM-MØ and M-MØ.

The fact that the LPS-induced cytokine profile of GM-MØ and M-MØ was cell-intrinsic prompted us to evaluate LPS-initiated intracellular signals [139; 140] in both macrophage subsets. LPS activated the NF-κB pathway to a similar extent in both GM-MØ and M-MØ, as evidenced by the loss of IκBα at early time points after LPS treatment (**Figure 9A**). Similarly, STAT1 became activated to the same extent in both subtypes by LPS (**Figure 9B**). However, IRF3 phosphorylation, which lies below the TRAM/TRIF branch of LPS signaling [139; 140] (*see* **Figure 3**), was higher in the case of GM-MØ (**Figure 9C**, **Figure 10A,B**), a result in agreement with their higher LPS-induced production of IFN-β. Conversely, the LPS-induced phosphorylation of ERK, JNK and p38 was significantly higher in LPS-treated M-MØ (**Figure 9D**, **Figure 10C**), and a similar finding was observed after stimulation with the TLR2 ligand PAM3CSK4 (**Figure 9E**). Moreover, LPS-induced phosphorylation of STAT3 (**Figure 9F**, **Figure 10C**) and CREB (**Figure 9G**, **Figure 10C**) was exclusively detected in M-MØ. Therefore, the response of GM-MØ and M-MØ to LPS and other TLR ligands differs in terms of intracellular signaling, with a higher activation of MAPK, STAT3 and CREB in M-MØ, and a more robust phosphorylation of IRF3 in GM-MØ.

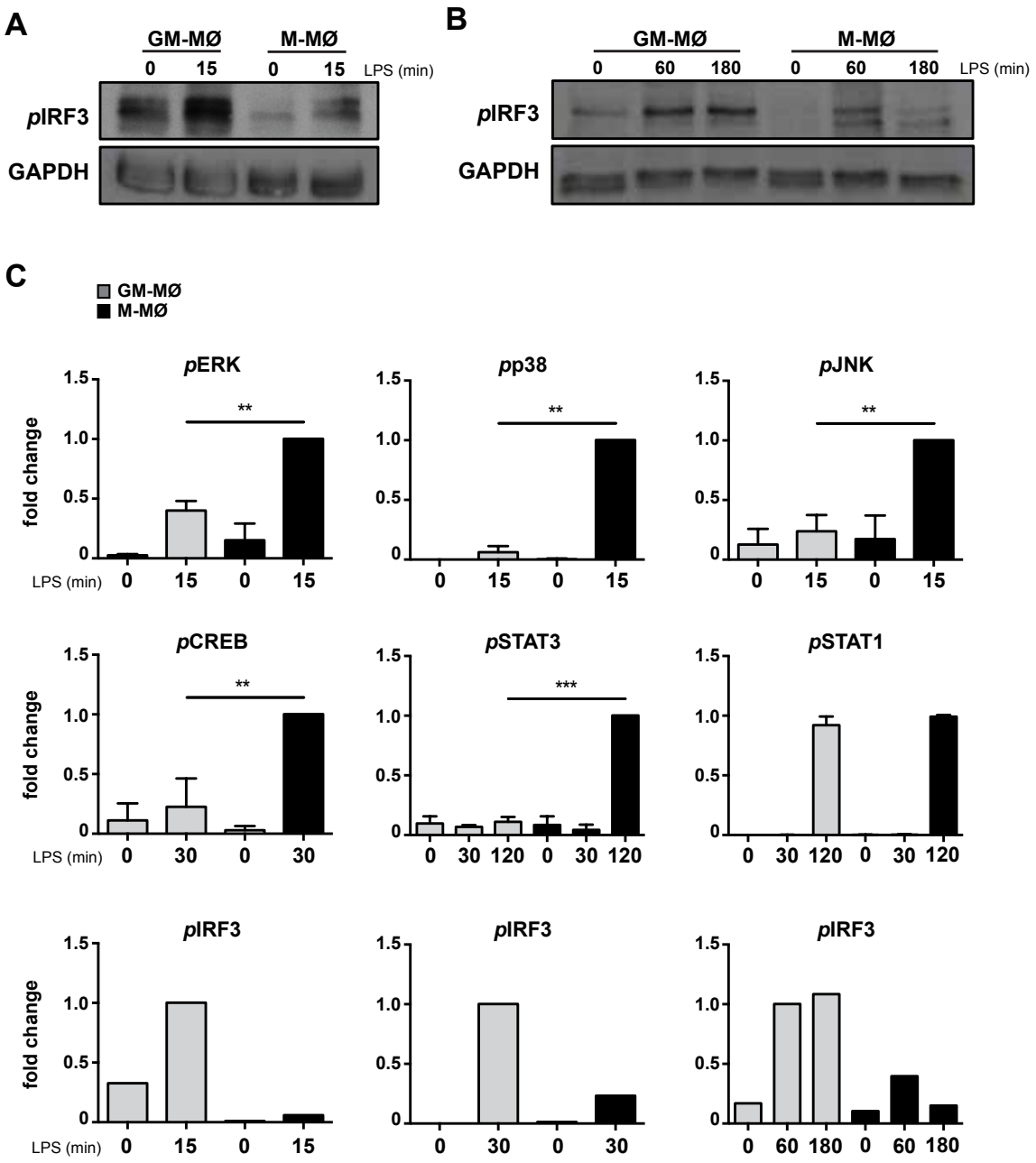

Figure 10. Differential LPS-triggered intracellular signaling in M-MØ and GM-MØ. (A,B) M-MØ and GM-MØ were treated with LPS, and cell lysates were obtained after 30 minutes **(A)** or 60-180 minutes **(B)** and assayed for the expression of phosphorylated IRF3 by Western blot. Protein loading was normalized using a monoclonal antibody against GAPDH. **(C)** Densitometric analysis of the set of experiments illustrated in **Figure 2** and in **(A,B)**. Shown are the means and SD of three independent experiments (n=3; *, $p < 0.05$; **, $p < 0.005$; ***, $p < 0.0005$). In the case of IRF3 (lower panels), phosphorylation was determined on three independent samples and at the indicated time points in each experiment.

Definition of the LPS-regulated transcriptional signature of GM-MØ and M-MØ: identification of gene sets specifically regulated by TLR agonists in both macrophage subtypes.

The limited available information on the gene signature of LPS-treated human GM-MØ and M-MØ precluded further evaluation of the transcriptional relevance of the differences in LPS-initiated signaling pathways between GM-MØ and M-MØ. Thus, we undertook the identification of the range of genes whose expression is modulated by LPS in both macrophage subsets. Microarray analysis on RNA from macrophages exposed to LPS for 4 hours (**Figure 11A** and **Table III** *included in attached CD*) reflected the differential regulation of cytokine genes in response to LPS (**Figure 11B**), and revealed the existence of gene sets differentially regulated by LPS in GM-MØ and M-MØ. Specifically, 1143 genes were up-regulated and 1545 genes down-regulated by LPS in GM-MØ, while 1906 genes were up-regulated and 2463 genes down-regulated by LPS in M-MØ (*adj p*<0.05; $\log_2$ LPS-treated/untreated >1 or <1) (**Figure 11C,D** and **Table III**). A more stringent analysis of the data (*adj p*<0.05 in one macrophage subtype and p>0.1 in the counterpart; $\log_2$ LPS-treated/untreated >2 or <-2) identified 62 genes exclusively upregulated by LPS in GM-MØ (hereafter termed activated-GM-MØ gene set), while 195 genes were upregulated by LPS only in M-MØ (hereafter termed activated-M-MØ gene set) (**Figure 11E** and **Table IV**). Besides, LPS triggered the downregulation of 40 genes in GM-MØ and 169 genes in M-MØ (**Figure 11E** and **Table IV**). A roughly similar number of genes were strongly upregulated or downregulated by LPS in both macrophage subtypes (351 and 141 genes, respectively) (*adj p*<0.05 and $\log_2$ LPS-treated/untreated >2 or <-2) (**Figure 11E** and **Table V**). Therefore, the differential LPS-responsiveness of GM-MØ and M-MØ is not limited to cytokine production, and there is a large set of genes whose expression is regulated by LPS in a macrophage subtype-dependent manner (that is, their expression is differentially modulated by LPS in GM-MØ and M-MØ). Analysis of independent samples of GM-MØ+LPS and M-MØ+LPS verified the existence of a gene set whose expression is exclusively modulated in M-MØ by LPS (**Figure 12A,B**) and also after stimulation with PAM3CSK4 (**Figure 12C**). This gene set included *CCL19* (**Figure 12D**), whose LPS-inducibility in M-MØ was confirmed at the protein level (**Figure 12E**). Along the same line, gene sets were identified whose expression is upregulated by LPS only in GM-MØ, and others whose expression is downregulated exclusively in either M-MØ or GM-MØ (**Figure 12B** and **Table IV**). Therefore, the preferential production of IL-10 by activated M-MØ, the defining feature of this macrophage subtype, is in line with the existence of an M-MØ-specific gene expression program that can be triggered by LPS and other TLR ligands.

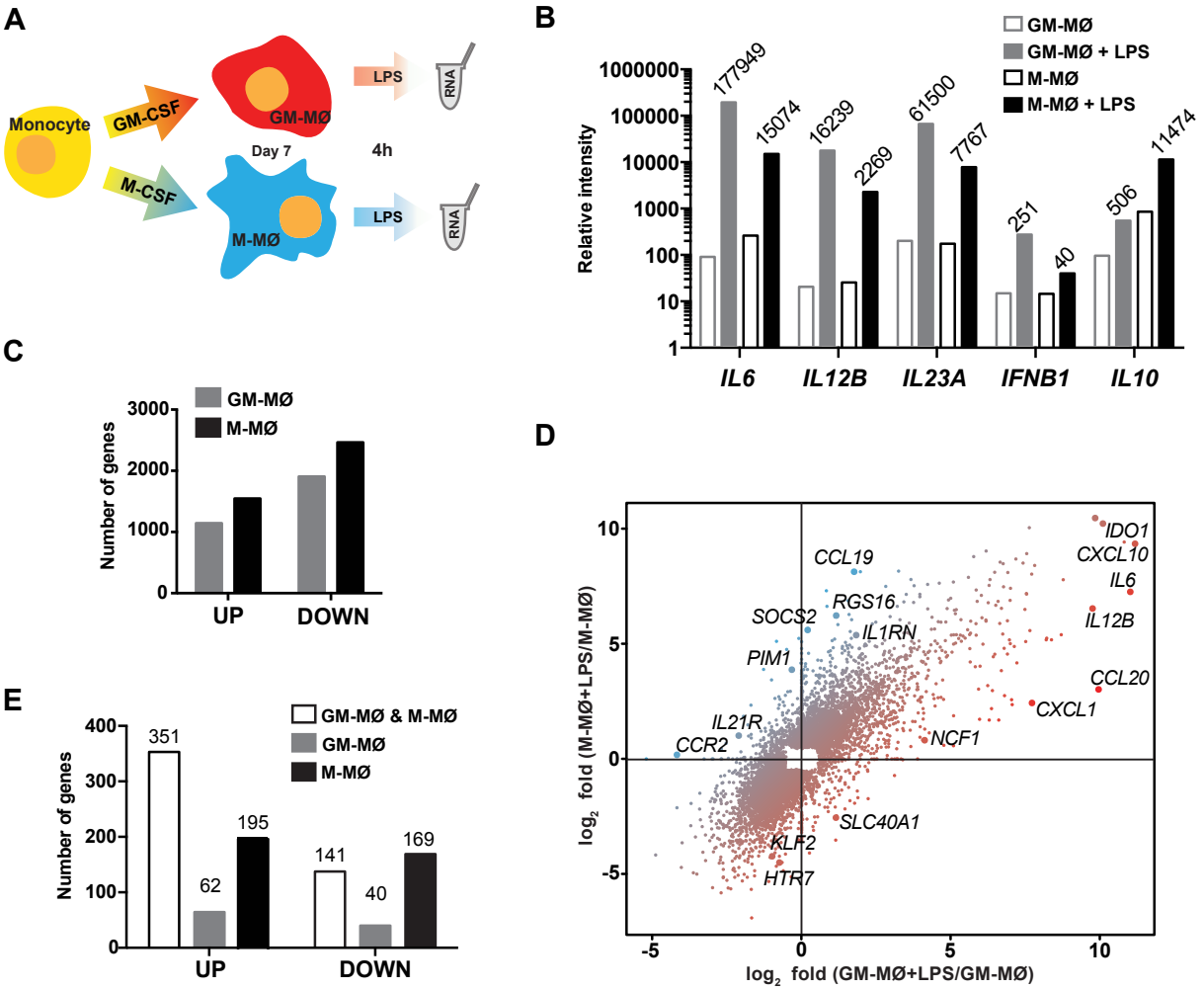

Figure 11. Determination of the gene signature of LPS-activated M-MØ and GM-MØ. (A) Experimental design. **(B)** Normalized fluorescence intensity of the indicated mRNAs in untreated and LPS-treated M-MØ and GM-MØ. **(C)** Number of annotated genes whose expression is upregulated (UP) or downregulated (DOWN) in the indicated macrophage subtypes after 4h of LPS treatment (adjusted $p < 0.05$; $\log_2$ LPS-treated/untreated >1 or <1). **(D)** Scatter plot of microarray results, showing the LPS-induced gene expression changes in GM-MØ ($\log_2$ LPS-treated/untreated GM-MØ, *x*-axis) plotted against the LPS-induced gene expression changes in M-MØ ($\log_2$ LPS-treated/untreated GM-MØ, *y*-axis). The relative position of some informative genes is indicated, with color code as indicated in panel **(A)**.

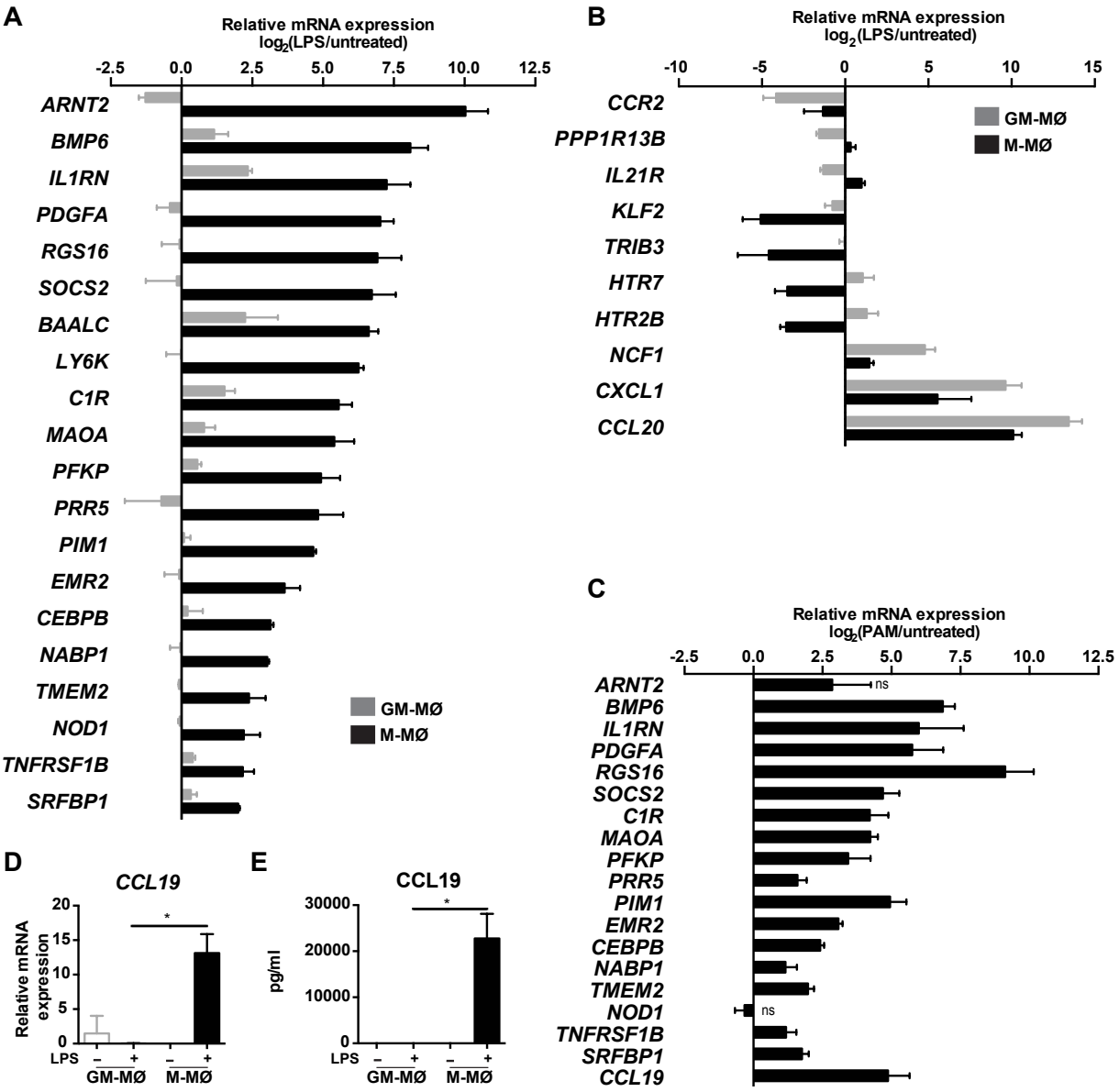

Figure 12. Validation of the M-MØ-specific LPS-activated gene signature. (A,B) Expression of the indicated genes in untreated and LPS-treated M-MØ and GM-MØ as determined by qRT-PCR on three additional independent samples. Results are indicated as the mRNA levels of each gene in LPS-treated cells relative to the level of the same mRNA in untreated cells, with all depicted changes showing at least $p < 0.05$ (n=4). Only genes whose expression is specifically upregulated by LPS in M-MØ are shown in **(A)**. **(C)** Expression of the indicated genes in untreated and PAM3CSK4(PAM)-treated M-MØ as determined by qRT-PCR on three additional independent samples. Results are indicated as the mRNA levels of each gene in PAM3CSK4-treated cells relative to the level of the same mRNA in untreated cells, with all depicted changes showing at least $p < 0.05$ (n=3), unless otherwise noted (ns: not statistically significant). **(D)** *CCL19* mRNA expression in untreated (-) and LPS-treated M-MØ and GM-MØ. Results indicate the level of *CCL19* mRNA relative to the *TBP* mRNA level in each sample (n=3; *, $p < 0.05$). **(E)** CCL19 protein levels produced by untreated (-) and LPS-treated M-MØ and GM-MØ. Shown are the means and SD of five independent expreriments (n=5; *, $p < 0.05$).

Biological function of the genes upregulated by LPS exclusively in anti-inflammatory M-MØ.

As expected from the pro-inflammatory priming of GM-MØ, the activated-GM-MØ gene set was significantly enriched in genes known to be positively controlled by LPS (*adj p* = 4.1x10^{-13}), associated with the GO Biological Process "inflammatory response" (GO:0006954, *adj p* = 1.1x10^{-4}), regulated by RelA as determined by ChIP (*adj p* = 5.5x10^{-7}), positively regulated by IL-1β (*adj p* = 5.2x10^{-10}) and negatively regulated by IL-4 (*adj p* = 1.8x10^{-3}), estrogen (*adj p* = 6.9x10^{-3}) and TGF-β1 (*adj p* = 7.8x10^{-3}) (**Figure 13A**). Conversely, the activated-M-MØ gene set included a significant number of genes regulated by EGR1 (*adj p* = 3.8x10^{-21}) and PPARγ (*adj p* = 1.8x10^{-13}) as determined by ChIP (**Figure 13B**), and a much lower association to the "inflammatory response" GO term (GO:0006954, *adj p* = 5.4x10^{-6}) (**Figure 13B**). Interestingly, the expression of a significant number of genes in the activated M-MØ gene set has been described to be enhanced by B-Raf overexpression (*adj p* = 1.8x10^{-8}) and impaired by the B-Raf inhibitor Vemurafenib (*adj p* = 6.35x10^{-6}) (**Figure 13B**), thus suggesting a link between B-Raf/MEK/ERK activation and M-MØ-specific LPS responsiveness. This prediction is, in fact, in line with the preferential activation of ERK in LPS- and PAM3CSK4-treated M-MØ (*see* **Figure 9D,E**). Moreover, the activated M-MØ was significantlly enriched in genes that are upregulated by IL-10 (*adj p* = 1.8x10^{-14}), TGF-β1 (*adj p* = 3.6x10^{-7}) and estradiol (*adj p* = 1.3x10^{-5}) (**Figure 13B**), thus supporting the existence of a strong anti-inflammatory component in the transcriptome of LPS-stimulated M-MØ.

Contribution of ERK, JNK and p38 activation to the M-MØ-specific LPS-dependent transcriptional profile.

The higher LPS-induced activation of ERK, JNK and p38MAPK, together with the enrichment of B-RAF-regulated genes within the gene set exclusively upregulated by LPS in M-MØ, prompted us to analyze the contribution of the three MAPK to the acquisition of the characteristic transcriptome of LPS-stimulated M-MØ. To that end, M-MØ were exposed to LPS in the presence of inhibitors of MEK (U0126) [141], JNK (SP600125) [142] or p38MAPK (BIRB0796) [143]. Inhibition of the activation of ERK, p38MAPK (**Figure 14A**) or JNK (**Figure 14B**) had a major impact on the characteristic LPS-induced cytokine mRNA profile of M-MØ. Specifically, simultaneous inhibition of ERK and p38 activation significantly enhanced the LPS-induced TNF mRNA levels but inhibited the LPS-induced IL10 mRNA levels (**Figure 14C**). Conversely, inhibition of JNK activation resulted in reduced TNF mRNA and IL10 mRNA levels after LPS exposure (**Figure 14D**). By contrast, siRNA-mediated knockdown of STAT3 in M-MØ

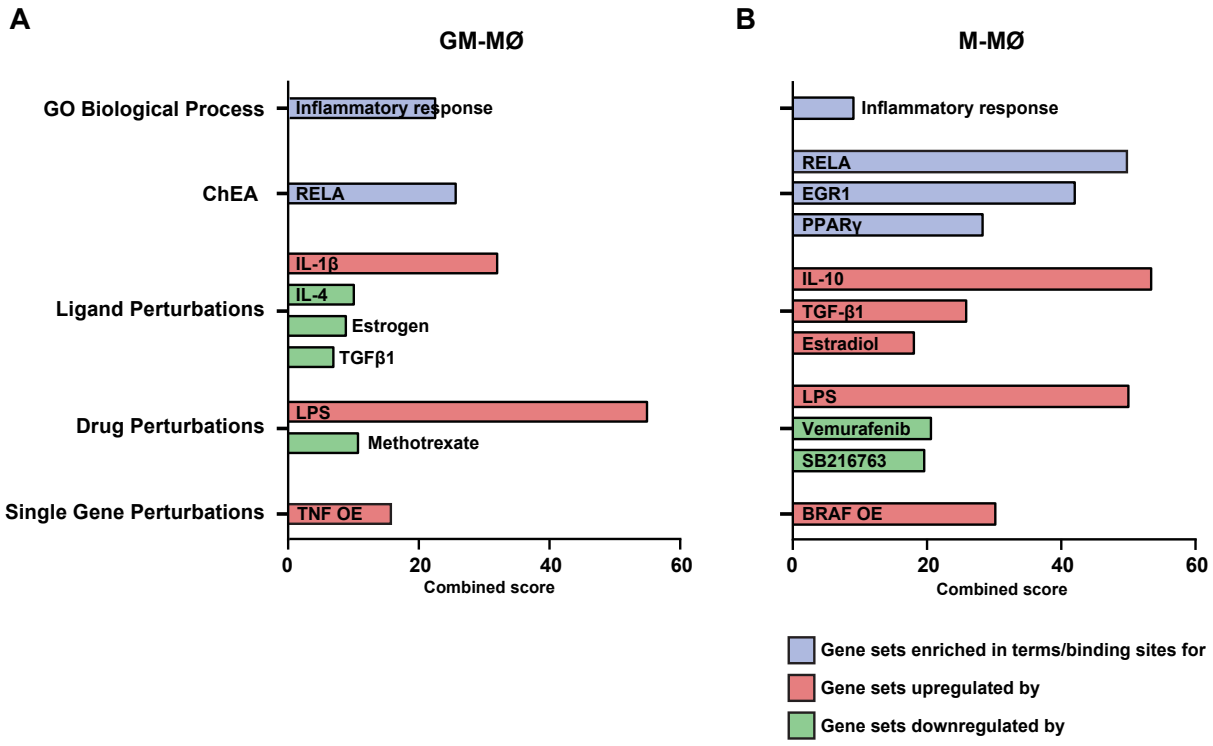

Figure 13. Gene ontology analysis of the activated-GM-MØ and activated-M-MØ gene sets. The set of genes specifically upregulated by LPS in either GM-MØ **(A)** or M-MØ **(B)** were analyzed for significant enrichment of functional activities and potential regulators using the ENRICHR tool and the indicated databases [combined score = log(p-value) x z-score]. Red and green colors indicate gene-upregulation or gene-downregulation in the indicated databases.

(**Figure 14E**) had no major effect on the LPS-stimulated cytokine mRNA expression (**Figure 14F**). Therefore, ERK, p38MAPK and JNK directly contribute to the M-MØ-specific LPS-induced cytokine profile, supporting that differences in LPS-triggered intracellular signals lie at the basis of the distinct cytokine profile of GM-MØ and M-MØ.

Based on this information, we next sought to determine the contribution of the three MAPK to the acquisition of the activated M-MØ transcriptional profile. To that end we analyzed the effect of the three inhibitors on the expression of genes exclusively upregulated (37) or downregulated (26) by LPS in M-MØ and genes upregulated by LPS in both M-MØ and GM-MØ (*see* **Table IV, V, VI**). As shown in **Figure 15A**, U0126 inhibited the LPS-induced increase of 6 genes, while inhibition of JNK or p38 impaired the LPS-induced upregulation of 14 and 21 genes, respectively. Moreover, and in line with their effect on IL10, the combined presence of U0126 and BIRB0796 significantly impaired the LPS-mediated upregulation of 24 genes (**Figure 15A**). The synergistic inhibitory effect of U0126 and BIRB0796 was particularly evident in the case of CCL19, SOCS2, BMP6 and PDGFA (**Figure 15B**), which display the most differential LPS-mediated regulation between M-MØ and GM-MØ (**Table IV**). Conversely, the inhibitors impaired the LPS-induced downregulation of 2 (U0126), 5 (BIRB0796) and 6

(SP600125) genes (**Figure 15A**). Interestingly, and in consonance with its regulation of TNF-α expression, JNK positively regulates genes that are induced by LPS in both GM-MØ and M-MØ (**Figure 15A**). Therefore, ERK, JNK and p38 significantly contribute to the acquisition of the transcriptome of LPS-stimulated M-MØ as well as to their characteristic LPS-induced cytokine profile.

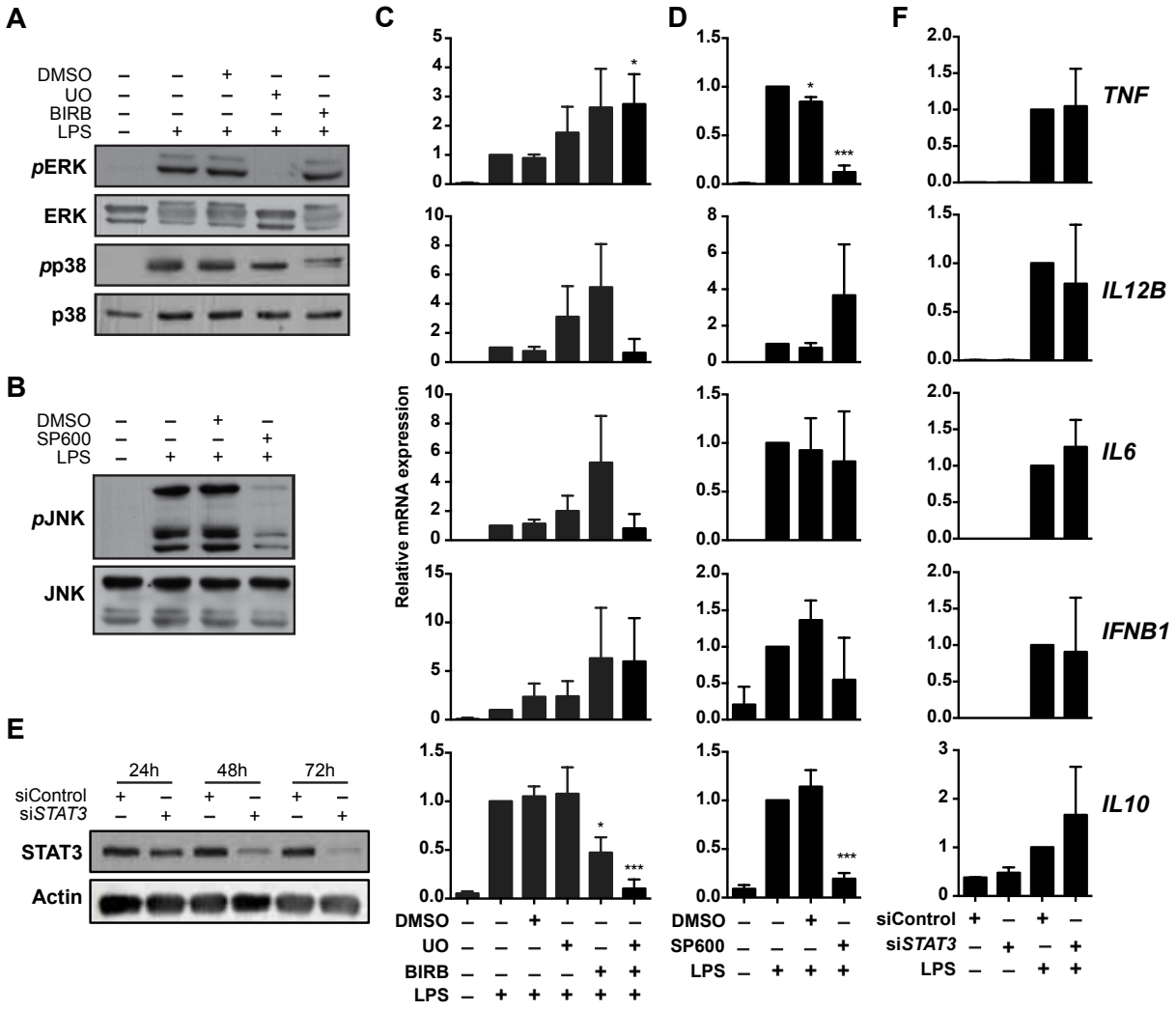

Figure 14. MAPK activation contributes to the specific cytokine profile of activated M-MØ. (A,B) ERK, p38MAPK and JNK phosphorylation in untreated and LPS-treated M-MØ and in the absence (-) or presence of the MEK inhibitor U0126 (U0), p38MAPK inhibitor BIRB0796 (BIRB) **(A),** the JNK inhibitor SP600125 (SP600) **(B)** or DMSO as a vehicle control. **(C,D)** LPS-induced cytokine production in M-MØ in the absence (-) or presence of U0126 (U0), BIRB0796 (BIRB) **(C),** SP600125 (SP600) **(D)** or DMSO as a vehicle control. Results are expressed relative to the level of each cytokine mRNA after LPS treatment. Shown are the means and SD of four independent expreriments (n=4; *, $p < 0.05$; ***, $p < 0.0005$). **(E)** STAT3 protein expression in M-MØ after transfection with either siControl or a STAT3-specific siRNA (siSTAT3) for 24, 48 or 72 hours, as determined by western blot. **(F)** LPS-induced cytokine mRNA expression production in M-MØ transfected with either siControl or siSTAT3. Results are expressed relative to the level of each cytokine mRNA after LPS treatment. Shown are the means and SD of three independent expreriments (n=3; *, $p < 0.05$; ***, $p < 0.0005$).

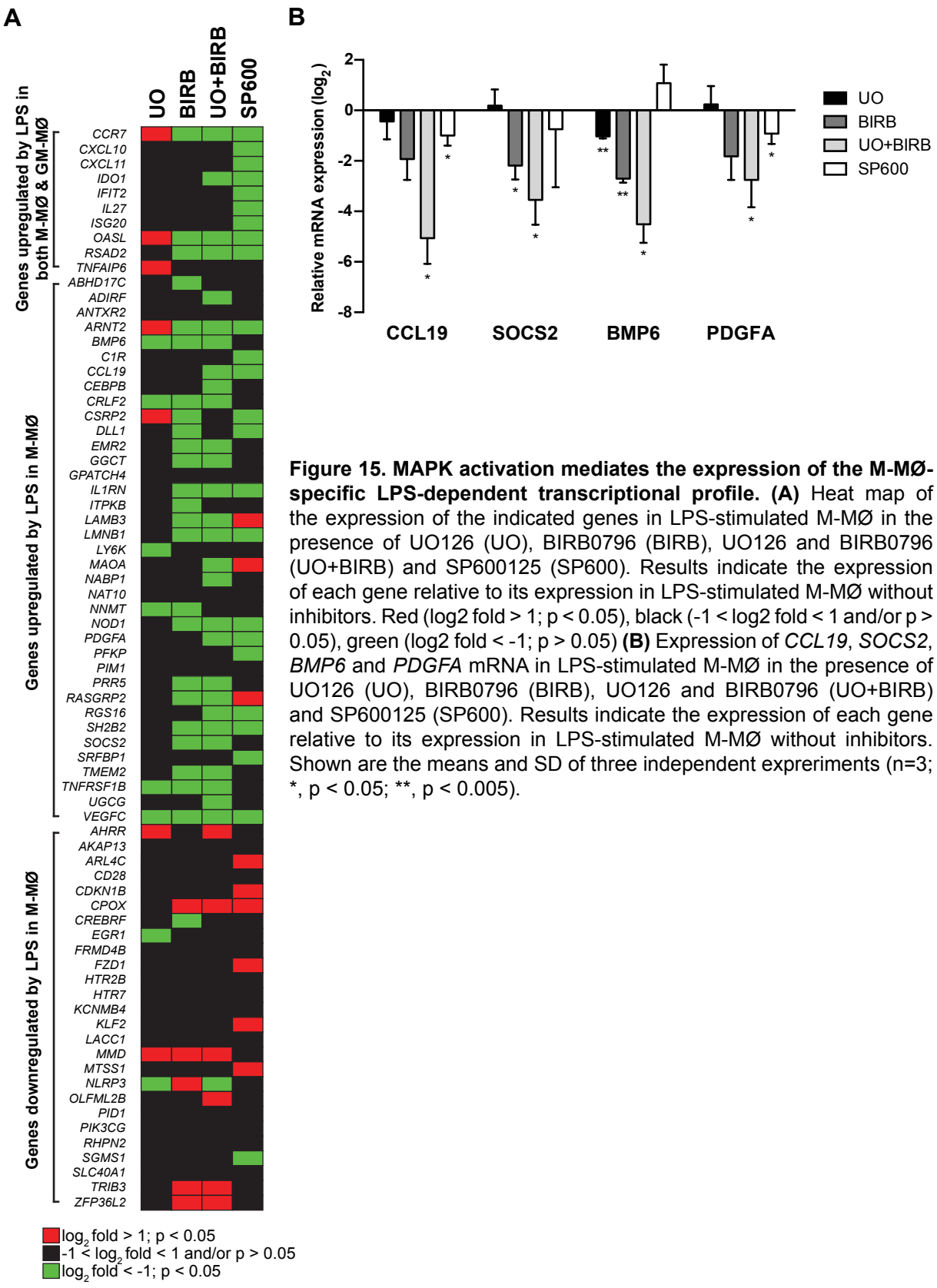

Figure 15. MAPK activation mediates the expression of the M-MØ-specific LPS-dependent transcriptional profile. (A) Heat map of the expression of the indicated genes in LPS-stimulated M-MØ in the presence of UO126 (UO), BIRB0796 (BIRB), UO126 and BIRB0796 (UO+BIRB) and SP600125 (SP600). Results indicate the expression of each gene relative to its expression in LPS-stimulated M-MØ without inhibitors. Red (log2 fold > 1; $p < 0.05$), black (-1 < log2 fold < 1 and/or $p > 0.05$), green (log2 fold < -1; $p > 0.05$) **(B)** Expression of *CCL19*, *SOCS2*, *BMP6* and *PDGFA* mRNA in LPS-stimulated M-MØ in the presence of UO126 (UO), BIRB0796 (BIRB), UO126 and BIRB0796 (UO+BIRB) and SP600125 (SP600). Results indicate the expression of each gene relative to its expression in LPS-stimulated M-MØ without inhibitors. Shown are the means and SD of three independent expreriments (n=3; *, $p < 0.05$; **, $p < 0.005$).

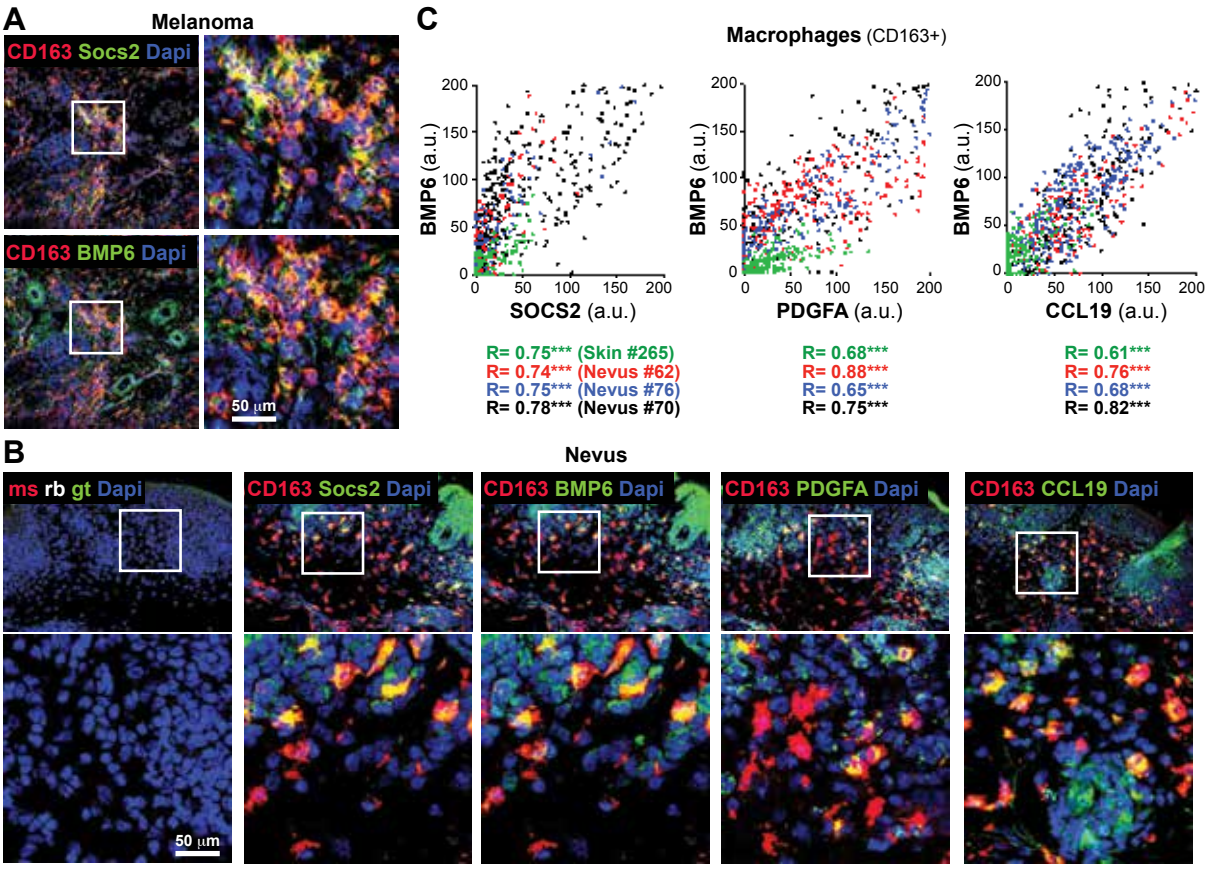

Figure 16. Human macrophages co-express genes within the activated-M-MØ-specific gene set. **(A)** Expression of SOCS2 (left) and BMP6 (right) in CD163^{+} macrophages from a primary melanoma sample, as determined by immunofluorescence and confocal microscopy. **(B)** Expression of SOCS2, BMP6, PDGFA and CCL19 in CD163^{+} macrophages from human nevi. Bottom panels illustrate a magnification of the section indicated in upper panels. Left panels show the staining produced by irrelevant non-specific and isotype-matched antibodies. **(C)** Positive correlation between the expression of SOCS2 and BMP6 (left), PDGFA and BMP6 (center), and CCL19 and BMP6 (right) in CD163^{+} macrophages from human nevi (black, red, blue) and normal skin (green).

Physiologic and pathologic relevance of the M-MØ-specific LPS-induced transcriptional profile.

The identification of the LPS-inducible M-MØ-specific gene set, whose expression primarily depends on MAPK activation, led us to explore the expression of this gene set in macrophages in vivo. As representatives of this set gene we focused on CCL19, PDGFA, BMP6 and SOCS2 because they exert potent trophic (PDGFA) [144], anti-inflammatory (SOCS2) [145-147] and matrix-synthesis stimulatory (BMP6) [148] actions that are compatible with the known effector functions of M-MØ. Tissue screening revealed the presence of BMP6^{+}/CCL19^{+}/CD163^{+} macrophages in gut (colon submucosa) and skin (*data not shown*) tissues whose tissue-resident macrophages are monocyte-derived and replaced by circulating monocytes in homeostasis [4; 149]. A percentage of CD163^{+} macrophages in primary melanoma were also found to co-express SOCS2

and BMP6 (**Figure 16A**). The simultaneous expression of PDGFA, SOCS2, BMP6 and CCL19 in $CD163^+$ macrophages was more evident in nevus (**Figure 16B**), where the expression of the four genes in $CD163^+$ macrophages exhibited a very similar distribution pattern and a good correlation (**Figure 16C**). These results confirm the co-expression of CCL19, PDGFA, BMP6 and SOCS2 in LPS-activated M-MØ, and reinforce the existence of a co-regulated set of genes that are specifically expressed upon activation of human anti-inflammatory/homeostatic macrophages.

Table IV. Genes regulated by LPS exclusively in GM-MØ or M-MØ

Adj p<0.05 in one macrophage subtype and p>0.1 in the counterpart; log_2 LPS-treated/untreated >2 or <-2 in one macrophage subtype and 'not expressed or does not change or changes in the opposite manner' in the counterpart. From top to bottom and left to right, genes are classified from more to less fold change.

Genes upregulated in GM-MØ

CCL20	*TCF4*
CXCL1	*SIGLEC1*
IL1A	*HOPX*
CXCL3	*SAT1*
IL8	*TRIL*
CXCL2	*C7orf60*
EREG	*ANO1*
WNT5A	*PID1*
NCF1	*RASGEF1B*
HHLA2	*MVB12B*
CCL15	*CLIC2*
NR4A2	*IL18*
HEY1	*PDZD2*
ADC	*C14orf182*
CXCL6	*GPR64*
ACKR3	*TLR7*
LOC283485	*SLC25A37*
TLL1	*UNC79*
GPC3	*THRB*
TAGAP	*GRASP*
CYP3A7	*JAG1*
IL19	
PDGFB	
APOL6	
CYP3A5	
ASPHD2	
IFNL1	
DHX58	
SECTM1	
C5orf56	
TMEM88	
FOXD3	
JAK2	
PKIG	
ZC3H12C	
LOC100506342	
TMEM139	
PPP1R17	
ANXA2R	
MXD1	
OTUD1	

Table IV. Genes regulated by LPS exclusively in GM-MØ or M-MØ

Adj p<0.05 in one macrophage subtype and p>0.1 in the counterpart; log_2 LPS-treated/untreated >2 or <-2 in one macrophage subtype and 'not expressed or does not change or changes in the opposite manner' in the counterpart. From top to bottom and left to right, genes are classified from more to less fold change.

Genes upregulated in M-MØ

CCL19	*LOC100509445*	*UST*	*TCHH*	*FERMT2*
RGS16	*ADAM19*	*NUPR1*	*KIAA0226L*	*FNDC4*
SOCS2	*BOC*	*STEAP3*	*EBF1*	*EGR4*
LY6K	*CXCL13*	*PRR5*	*HLX*	*HRASLS5*
BMP6	*AMIGO2*	*NCS1*	*VAV2*	*TCEA2*
CSRP2	*LMNB1*	*SYTL4*	*ADD2*	*KIAA1522*
ARNT2	*CDKN1A*	*CHRNA6*	*TUBB6*	*RAB30*
LIMS2	*DLL1*	*HSPA2*	*COL5A3*	*IL4R*
GCGR	*FRMD6*	*LAMA4*	*ANTXR2*	*CTDSP2*
GJB2	*GGT5*	*WNT1*	*VAC14*	*RBBP8*
CHI3L2	*TM4SF1*	*GZMB*	*GCKR*	*ELK1*
FFAR3	*CRLF2*	*IFNγ*	*SRFBP1*	*BACH1*
CTHRC1	*IRGM*	*PRDM8*	*ABCB5*	*VEGFA*
MMP12	*IL18RAP*	*SLC16A10*	*CD200*	*TFRC*
SPINK1	*PFKP*	*IL1RN*	*LDLRAD3*	*MMP19*
CLEC4D	*DDIT4*	*FAM60A*	*CSAG4*	*UBE2S*
SBSN	*FOSL2*	*FCAMR*	*FAM57A*	*PLOD2*
S100A3	*FAM115C*	*NXN*	*FKBP5*	*L2HGDH*
PDGFA	*LY6E*	*TMEM2*	*SH3PXD2B*	*TRIM14*
VEGFC	*BCAR1*	*GBP7*	*CDCA4*	*TPBG*
APOL4	*PLSCR4*	*GPR31*	*ITGA1*	*MYO10*
ADIRF	*CAPSL*	*ZNF462*	*TNFRSF1B*	*HNRNPLL*
C1R	*SYNPO*	*KCNN4*	*SH2B2*	*GLI3*
DUSP2	*GJA4*	*CHST2*	*CEBPB*	*PUS7*
ABHD17C	*EMR2*	*LINC00605*	*MYO5C*	*SVIL*
STRIP2	*ITGB3*	*LAMB3*	*MPP4*	*SCN9A*
IL3RA	*LRG1*	*LYPD5*	*CCR8*	*LANCL3*
PIM1	*LMCD1*	*GADD45G*	*AEN*	*VCAN*
NNMT	*FLVCR2*	*NABP1*	*ECE1*	*CDC42EP4*
KIAA1199	*ENTHD1*	*OR11A1*	*LOC154761*	*RAB15*
SLC8A3	*IL18R1*	*EPO*	*LILRA2*	*MGAT1*
MT1M	*METTL1*	*DSTYK*	*RGS20*	
EHF	*C1orf21*	*MUCL1*	*LAMA3*	
SMARCA1	*IGF2*	*GAREM*	*MYOF*	
RET	*SLC26A9*	*CBR3*	*RUNX1-IT1*	
SLCO5A1	*CCR5*	*HES1*	*SLC5A3*	
UBD	*MPP6*	*UGCG*	*CXCR5*	
C10orf10	*XLOC_014512*	*CGNL1*	*TMEM178B*	
MAOA	*PTP4A3*	*CISH*	*LOC285300*	
SLC2A1	*BAI1*	*STEAP1*	*TGM2*	
FZD6	*PDCD1LG2*	*SMAD7*	*TTC39A*	

Table IV. Genes regulated by LPS exclusively in GM-MØ or M-MØ

Adj p<0.05 in one macrophage subtype and p>0.1 in the counterpart; log_2 LPS-treated/untreated >2 or <-2 in one macrophage subtype and 'not expressed or does not change or changes in the opposite manner' in the counterpart. From top to bottom and left to right, genes are classified from more to less fold change.

Genes downregulated in GM-MØ

NFE2
CCR2
C2orf71
RAB11FIP4
ARHGEF28
FOXO6
TSEN2
ARRDC4
SLC20A1
USP2
MYB
ADRA2B
ITPRIPL1
FAM211A
CBX2
GDF15
FAM95B1
PPP1R13B
RAB36
CLMN
ST6GALNAC6
SAPCD2
STIP1
SLC46A2
KIAA0922
DISP2
CBFA2T3
XLOC_014512
KLHL30
NEURL1B
SPIN4
IL21R
LOC100130938
CECR6
ZNRF3
ALKBH2
RRS1
RPUSD1
AFAP1L1
SLC25A19

Table IV. Genes regulated by LPS exclusively in GM-MØ or M-MØ

Adj p<0.05 in one macrophage subtype and p>0.1 in the counterpart; log_2 LPS-treated/untreated >2 or <-2 in one macrophage subtype and 'not expressed or does not change or changes in the opposite manner' in the counterpart. From top to bottom and left to right, genes are classified from more to less fold change.

Genes downregulated in M-MØ

ADORA3	*LOC100240735*	*SLC22A15*	*PTPN6*	*CCDC149*
F2RL3	*ARRDC2*	*ARID3B*	*ZNF469*	*LOC100130219*
ZFP36L2	*CRHBP*	*ARHGAP6*	*MPZL2*	*ZFP14*
TRIB3	*PPM1F*	*FGD6*	*ADRB1*	*CAPS2*
HTR7	*MPPED2*	*HS3ST2*	*XLOC_010709*	*ADAMTS10*
RHPN2	*CD200R1*	*GCNT1*	*LYPD1*	
KLF2	*C12orf76*	*ANKRD50*	*NR1D2*	
MTSS1	*PPAPDC2*	*ITSN1*	*AKAP13*	
GPR155	*MS4A7*	*CKAP2*	*PINK1*	
DDIT4L	*TMEM117*	*EGR1*	*TTLL1*	
HTR2B	*DEPTOR*	*TRIM50*	*PDGFC*	
ALK	*MANBA*	*LEPREL4*	*MS4A14*	
KCNMB4	*RAB3IL1*	*HIST1H4E*	*PHF20*	
FRAT1	*CLEC4GP1*	*DNMBP-AS1*	*CEP120*	
CD28	*PCED1B*	*APBA1*	*GPR162*	
LRRK2	*ZNF217*	*GIMAP8*	*SLC45A3*	
GPRC5B	*PPARγC1B*	*UNC80*	*KLHL41*	
C10orf105	*CPOX*	*CDK19*	*RFPL1S*	
GAPT	*LYPLAL1*	*IQCD*	*MMD*	
BNC2	*CCDC152*	*CIITA*	*NOTCH4*	
MS4A4E	*RASAL1*	*GDPD1*	*PDLIM2*	
MRVI1	*WWP1*	*C16orf86*	*C6orf164*	
PIK3CG	*ZKSCAN4*	*MTL5*	*MYLK*	
HTR7P1	*ADAT2*	*SLC16A5*	*PPM1M*	
ZFP36L1	*MIS18BP1*	*ST3GAL6*	*ISCU*	
SRGAP3	*RAPH1*	*LOC100132741*	*CUX2*	
RREB1	*SCAMP5*	*HTR1F*	*ZMYND8*	
MEF2C	*DPRXP4*	*OLFML2B*	*LOC286272*	
NHS	*PCDH12*	*BDH1*	*ZNF395*	
CXCR4	*ACVR2B*	*MYOM1*	*PELI2*	
LOC340508	*TRIM45*	*CARD8*	*ZNF106*	
FAM174B	*C5AR2*	*ZNF280D*	*ING5*	
ARL4C	*CACNA2D3*	*APAF1*	*SFMBT2*	
SH3PXD2A	*LOC100129550*	*SIDT1*	*NECAB3*	
FZD2	*LACC1*	*TRPS1*	*HVCN1*	
MGC24103	*LINC00921*	*NR3C2*	*PCCA*	
LINC00294	*SLC40A1*	*AHRR*	*SASH3*	
CLCN4	*KAL1*	*ZNF581*	*COQ10A*	
EVI2A	*HAVCR2*	*SGMS1*	*KLHL13*	
SLC7A8	*LYRM9*	*HMGB2*	*RCN3*	
FRMD4B	*UBTF*	*TPRG1L*	*FARP1*	

Table V. Genes regulated by LPS in both GM-MØ and M-MØ

Adj p<0.05 and $\log_2$ LPS-treated/untreated >2 or <-2 in both macrophage subtypes. From top to bottom and left to right, genes are classified from more to less fold change.

Genes upregulated

CXCL11	*APOBEC3A*	*CCL8*	*CDC42EP2*	*TRIP10*
IDO1	*IL12B*	*IL23A*	*SLC13A3*	*MFSD2A*
IRG1	*SNAI1*	*IL2RA*	*CSF2*	*ARL5B*
CXCL10	*MIR155HG*	*CD80*	*XAF1*	*FERMT2*
LAMP3	*TNF-aIP6*	*CKB*	*CH25H*	*PPM1K*
CCR7	*HAPLN3*	*MX1*	*GRB10*	*P2RX7*
SLAMF1	*ZC3HAV1*	*EBI3*	*DUSP1*	*IL10*
OASL	*ISG15*	*ATP10A*	*TNF-aIP3*	*NKX3-1*
PTX3	*LINC00158*	*SAMD9L*	*APOBEC3B*	*SAMD4A*
IL27	*IFITM1*	*TNFSF10*	*SPSB1*	*HAS1*
LOC440896	*MCOLN2*	*HERC6*	*APOL3*	*DEFB1*
TNIP3	*MMP1*	*BAALC*	*RNF213*	*SERPINB9*
GREM1	*ITGB8*	*CCL3L3*	*CD40*	*TAP1*
IFIT2	*ADORA2A*	*CYP27B1*	*LAG3*	*FAM83H-AS1*
RSAD2	*IFIT1*	*NR4A3*	*PNPT1*	*APOL6*
IFIT3	*USP41*	*TMEM217*	*MAMLD1*	*SH2D3A*
BATF3	*HERC5*	*CCL23*	*NT5C3A*	*HSH2D*
CCL5	*CYP7B1*	*TCF7L1*	*TNFSF15*	*IRF1*
ISG20	*ELOVL7*	*LRRC32*	*IFIT5*	*TRAF3IP2*
ABTB2	*AIM2*	*IL36G*	*EXT1*	*CNKSR3*
SSTR2	*GCH1*	*ADAD2*	*KCNA3*	*FAM115C*
HES4	*GBP4*	*CSRNP1*	*PDE4B*	*FFAR2*
NIPAL4	*ZBTB32*	*MX2*	*CLIC4*	*EIF2AK2*
G0S2	*HELZ2*	*HS3ST3B1*	*LOC400043*	*GRAMD1A*
CXCL9	*HCAR3*	*AKAP2*	*PFKFB3*	*CFLAR*
IL6	*IFI44L*	*SLAMF7*	*RAB33A*	*CCM2L*
CSF3	*TNF*	*OAS2*	*PRDM8*	*RASL11A*
PDGFRL	*IFI27*	*TARP*	*GBP1P1*	*STX11*
CD274	*TMCC2*	*BATF2*	*TFPI2*	*ATF3*
IL7R	*STAT4*	*PLEKHA4*	*IRF7*	*CACNA1A*
ETV7	*RANBP3L*	*IDO2*	*GBP2*	*OAS1*
SOCS1	*CD38*	*IFIH1*	*BIRC3*	*SAMD9*
USP18	*IL15RA*	*TNFRSF9*	*RHOH*	*ACSL1*
NEURL3	*PTGS2*	*HESX1*	*IFI44*	*CD69*
GBP1	*CFB*	*TANC1*	*WTAP*	*RAPGEF2*
GBP5	*TNFSF9*	*C15orf48*	*C17orf96*	*SOD2*
SOCS3	*CMPK2*	*SLC41A2*	*MSC*	*SP140*
GFPT2	*DDX58*	*TTC39A*	*EHD1*	*PLAT*
TRAF1	*C11orf96*	*ADM*	*FAM26F*	*GPR132*
ANGPTL4	*NAMPT*	*ZC3H12A*	*GADD45B*	*SLC25A28*
INHBA	*OAS3*	*PVRL3*	*EPSTI1*	*IFI35*

Table V. Genes regulated by LPS in both GM-MØ and M-MØ

Adj p<0.05 and $\log_2$ LPS-treated/untreated >2 or <-2 in both macrophage subtypes. From top to bottom and left to right, genes are classified from more to less fold change.

Genes upregulated

B4GALT5	*KYNU*	*RNF19B*	*IFIT1B*
ICAM1	*SRC*	*NRP2*	*IGFBP4*
TDRD7	*CCNA1*	*MAML2*	*IER3*
MSANTD3	*TMPRSS13*	*LRRC3*	*SLC39A8*
ZNFX1	*C5orf56*	*NTN1*	*FUT4*
AREG	*MAP1LC3A*	*SYNE3*	*LOC285957*
SDC4	*DCP1A*	*ST7-AS1*	*PPP3CC*
OSR2	*KMO*	*DDX60*	*C2CD4B*
CD70	*SP110*	*LOC644090*	*TRIM36*
PMAIP1	*HDX*	*PRPF3*	*LYSMD2*
NFKB2	*YJEFN3*	*PELI1*	*KRTAP4-1*
HILPDA	*STAT1*	*FAS*	*ENDOD1*
CLCF1	*RND3*	*CASP7*	*TIAM2*
SRSF12	*N4BP2L1*	*NFKBIZ*	*RIPK2*
PML	*BAZ1A*	*IL4I1*	*IFITM4P*
AKT1S1	*TMEM229B*	*IL15*	*GTF2B*
TNIP1	*PI4K2B*	*NR6A1*	*ASPHD2*
CCL1	*LSS*	*MGC12916*	*IFITM3*
SLC2A6	*USP12*	*RNF144B*	*STBD1*
SNHG15	*ZHX2*	*CASP10*	*IRF4*
FLJ32255	*CCL3*	*ANKLE2*	*LHFP*
BCL2L14	*TP53INP2*	*GRAMD3*	*SLC1A2*
TMPRSS7	*NFKBIA*	*STAT5A*	*LONRF1*
SFT2D2	*APOBEC3G*	*RAP2C*	
PIM3	*ADRA1B*	*PSTPIP2*	
C12orf76	*HIF1A*	*FPR2*	
DDX60L	*CCRL2*	*NDP*	
KIAA0040	*KCNS3*	*STARD5*	
UPB1	*BLZF1*	*GTPBP1*	
USP30-AS1	*LINC00346*	*TNF-aIP8*	
MASTL	*SLED1*	*KANK1*	
MST4	*PARP14*	*CCL16*	
NFKB1	*GUCY1A3*	*LOC641510*	
BAMBI	*HCAR2*	*FZD4*	
SERPINB2	*TOR1B*	*PDLIM5*	
RTP4	*MAP3K8*	*GBP3*	
RASGRP1	*PTGIR*	*VSX1*	
NEXN	*RELA*	*CD48*	
NBN	*ETV3L*	*PPP4R2*	
MB21D1	*PANX1*	*C9orf91*	
PARP9	*TMEM171*	*SLCO3A1*	

Table V. Genes regulated by LPS in both GM-MØ and M-MØ

Adj p<0.05 and log_2 LPS-treated/untreated >2 or <-2 in both macrophage subtypes. From top to bottom and left to right, genes are classified from more to less fold change.

Genes downregulated

HHEX	*ZHX3*	*ZBTB47*	*NFATC3*
FAM78A	*SH2D3C*	*OSGEPL1*	*CAMKK1*
P2RY8	*SUFU*	*PIK3C2B*	*RSAD1*
SOWAHD	*GPR65*	*DOK2*	*CRTC1*
KLHDC8B	*PRR12*	*RHOBTB2*	*TBC1D10C*
KCNE3	*TMEM37*	*TRERF1*	*PELI3*
C15orf52	*C22orf29*	*TRIM65*	*NAIP*
RNF125	*ZCCHC24*	*PLAU*	*FAM50B*
RGS18	*GIMAP1*	*ASB13*	*SAPCD1*
RIMBP3	*PLA2G15*	*ZNF788*	*FGD5*
MYCL	*PLCXD1*	*FAM214A*	*PROC*
HEXIM2	*ABHD6*	*CEBPA-AS1*	*RFXAP*
IL16	*WDR91*	*MBLAC2*	*C16orf59*
TMEM170B	*VAV3*	*PTPN22*	*CD180*
MERTK	*C9orf139*	*GPRIN3*	*FAM156A*
DAB2	*NAPEPLD*	*RAB3A*	*TMEM223*
EEPD1	*CABLES1*	*SLC29A3*	*MKL2*
TMEM86A	*SNAI3*	*SCAI*	*ZNF573*
DBP	*MBP*	*ABHD15*	*RASSF7*
RAB42	*MID1IP1*	*PRAM1*	
FAM13A	*RNF166*	*SH3TC1*	
FAM117B	*WDR81*	*TIGD2*	
LRMP	*FRMD4A*	*ZBED3*	
TBC1D14	*ZNF652*	*ZNF589*	
RHOBTB1	*TBC1D2*	*THEM6*	
FRAT1	*FAM53B*	*NLRP12*	
MAF	*ZNF362*	*GFOD1*	
MXD4	*FAM217B*	*ZNF248*	
CEBPA	*CX3CR1*	*E2F2*	
C16orf54	*MYZAP*	*OGFOD2*	
BAIAP2-AS1	*GPAM*	*TNRC6C-AS1*	
OSBPL7	*NINL*	*CTSC*	
RAP2B	*SMYD4*	*PSTPIP1*	
SNHG12	*ABHD8*	*LOC93622*	
PANK1	*ARHGEF40*	*ASB1*	
TLR5	*GPATCH11*	*KIAA1737*	
CAMK2G	*MUM1*	*MAPKAPK5-AS1*	
DOK3	*NR2F6*	*CSRP2BP*	
PGPEP1	*CARD9*	*SPRY2*	
NT5DC2	*SAC3D1*	*RTN4R*	
TSHZ1	*ENC1*	*OSBPL11*	

Table VI. Effect of ERK, p38 and JNK inhibitors on the LPS-induced transcriptional profile of M-MØ

		UO			BIRB			UO+BIRB			SP600		
gene	geneset	p.value	fold.value	log2.fold.value	p.value	fold.value	log2.fold.value	p.value	fold.value	log2.fold.value	p.value	fold.value	log2.fold.value
CCR7	Genes upregulated by LPS in both GM-MØ and M-MØ	0.029	1.994	0.995	-0.005	0.153	-2.709	-0.035	0.150	-2.737	-0.007	0.418	-1.258
CXCL10		0.184	1.427	0.513	0.256	1.558	0.639	0.110	1.741	0.800	-0.002	0.003	-8.406
CXCL11		0.422	1.140	0.189	0.121	1.469	0.555	0.097	1.503	0.588	-0.001	0.002	-9.088
IDO1		0.201	1.171	0.228	-0.068	0.539	-0.892	-0.043	0.364	-1.458	-0.003	0.223	-2.166
IFIT2		0.034	1.304	0.383	-0.096	0.574	-0.801	-0.515	0.918	-0.123	-0.003	0.043	-4.547
IL27		0.026	1.222	0.289	0.592	1.107	0.147	-0.065	0.794	-0.332	-0.001	0.142	-2.820
ISG20		0.003	1.176	0.234	-0.080	0.854	-0.228	-0.080	0.752	-0.410	-0.001	0.129	-2.954
OASL		0.002	2.641	1.401	-0.010	0.405	-1.303	-0.011	0.600	-0.738	-0.011	0.151	-2.732
RSAD2		0.466	1.079	0.110	-0.025	0.439	-1.186	-0.009	0.370	-1.434	-0.005	0.006	-7.498
TNFAIP6		0.030	2.260	1.176	-0.517	0.954	-0.068	0.733	1.116	0.159	-0.443	0.870	-0.201
ABHD17C	Genes upregulated by LPS only in M-MØ	-0.096	0.620	-0.690	-0.009	0.224	-2.155	-0.082	0.321	-1.638	-0.574	0.966	-0.050
ADIRF		0.057	1.514	0.599	-0.238	0.648	-0.626	-0.029	0.164	-2.607	0.212	1.201	0.264
ANTXR2		-0.455	0.989	-0.016	-0.086	0.888	-0.172	-0.079	0.764	-0.387	0.111	1.123	0.167
ARNT2		0.013	2.347	1.231	-0.009	0.079	-3.669	-0.009	0.160	-2.644	-0.016	0.488	-1.035
BMP6		-0.002	0.489	-1.031	-0.001	0.154	-2.698	-0.009	0.048	-4.382	0.060	2.321	1.214
C1R		0.516	1.140	0.189	-0.059	0.571	-0.809	-0.165	0.521	-0.940	-0.001	0.205	-2.288
CCL19		-0.400	0.806	-0.312	-0.056	0.291	-1.780	-0.013	0.036	-4.808	-0.016	0.517	-0.951
CEBPB		0.077	1.117	0.160	-0.114	0.707	-0.500	-0.021	0.417	-1.261	-0.055	0.854	-0.228
CRLF2		-0.014	0.526	-0.926	-0.012	0.155	-2.690	-0.001	0.054	-4.219	-0.221	0.687	-0.541
CSRP2		0.008	3.088	1.626	-0.006	0.232	-2.106	-0.714	0.962	-0.055	-0.010	0.521	-0.941
DLL1		0.504	1.169	0.225	-0.042	0.510	-0.971	-0.113	0.609	-0.715	-0.003	0.299	-1.743
EMR2		-0.117	0.863	-0.213	-0.049	0.416	-1.265	-0.013	0.249	-2.004	-0.002	0.715	-0.485
GGCT		-0.021	0.732	-0.451	-0.001	0.453	-1.143	-0.022	0.506	-0.982	-0.375	0.852	-0.230
GPATCH4		-0.408	0.577	-0.792	-0.447	0.872	-0.197	0.311	1.383	0.467	-0.299	0.401	-1.319
IL1RN		-0.003	0.651	-0.619	-0.010	0.387	-1.370	-0.007	0.160	-2.641	-0.001	0.190	-2.393
ITPKB		0.693	1.098	0.135	-0.037	0.553	-0.854	-0.763	0.991	-0.013	-0.090	0.500	-1.000
LAMB3		-0.062	0.565	-0.824	-0.018	0.592	-0.757	-0.026	0.301	-1.731	0.019	2.296	1.199
LMNB1		-0.326	0.860	-0.218	-0.025	0.503	-0.992	-0.032	0.404	-1.306	-0.002	0.290	-1.786
LY6K		-0.010	0.130	-2.946	-0.217	0.124	-3.013	-0.103	0.034	-4.898	0.093	1.974	0.981
MAOA		0.330	1.138	0.187	-0.093	0.598	-0.742	-0.029	0.262	-1.931	0.015	1.700	0.766
NABP1		0.067	1.354	0.437	-0.054	0.329	-1.603	-0.004	0.208	-2.265	-0.328	0.908	-0.139
NAT10		-0.710	0.967	-0.048	0.226	1.211	0.276	0.216	1.323	0.403	-0.389	0.838	-0.256
NNMT		-0.050	0.494	-1.016	-0.006	0.090	-3.477	-0.143	0.096	-3.381	0.653	1.591	0.670
NOD1		-0.090	0.754	-0.407	-0.031	0.422	-1.245	-0.023	0.536	-0.900	-0.010	0.350	-1.515
PDGFA		0.630	1.271	0.346	-0.078	0.325	-1.620	-0.048	0.176	-2.508	-0.020	0.544	-0.878
PFKP		-0.095	0.873	-0.196	-0.065	0.966	-0.050	-0.192	0.819	-0.288	-0.001	0.402	-1.314
PIM1		0.211	1.672	0.741	0.744	1.142	0.192	-0.175	0.723	-0.468	-0.002	0.709	-0.496
PRR5		-0.076	0.692	-0.530	-0.013	0.362	-1.467	-0.008	0.219	-2.189	0.546	1.179	0.237
RASGRP2		-0.371	0.730	-0.454	-0.031	0.199	-2.328	-0.047	0.327	-1.614	0.021	3.008	1.589
RGS16		-0.786	0.979	-0.031	-0.111	0.591	-0.758	-0.003	0.088	-3.512	0.000	0.068	-3.882
SH2B2		-0.101	0.438	-1.193	-0.017	0.256	-1.967	-0.008	0.100	-3.324	-0.040	0.449	-1.154
SOCS2		0.655	1.223	0.290	-0.021	0.230	-2.118	-0.025	0.100	-3.321	-0.564	1.191	0.252
SRFBP1		-0.506	0.902	-0.149	-0.093	0.640	-0.644	-0.550	0.906	-0.143	-0.008	0.416	-1.264
TMEM2		-0.236	0.778	-0.363	-0.014	0.300	-1.739	-0.026	0.257	-1.962	0.697	1.438	0.524
TNFRSF1B		-0.022	0.558	-0.843	-0.016	0.348	-1.522	-0.001	0.144	-2.794	-0.909	1.012	0.017
UGCG		-0.617	0.961	-0.057	-0.110	0.462	-1.116	-0.031	0.404	-1.309	-0.487	0.961	-0.058
VEGFC		-0.019	0.578	-0.792	-0.008	0.368	-1.442	-0.023	0.130	-2.945	-0.010	0.132	-2.923
AHRR	Genes downregulated by LPS only in M-MØ	0.009	4.069	2.025	-0.650	0.944	-0.084	0.009	3.213	1.684	0.229	1.226	0.294
AKAP13		0.669	1.052	0.073	0.045	1.173	0.230	0.094	2.234	1.160	-0.009	0.635	-0.654
ARL4C		0.304	1.631	0.706	-0.579	0.921	-0.119	0.185	1.733	0.793	0.008	1.973	0.981
CD28		-0.110	0.707	-0.501	-0.346	0.822	-0.283	-0.734	0.970	-0.044	-0.003	0.633	-0.659
CDKN1B		0.923	1.013	0.019	-0.661	0.966	-0.050	-0.470	0.911	-0.135	0.000	2.034	1.024
CPOX		0.061	1.769	0.823	0.016	2.799	1.485	0.011	3.946	1.980	0.024	2.136	1.095
CREBRF		0.298	1.516	0.600	-0.018	0.477	-1.069	-0.885	1.021	0.030	0.005	1.496	0.581
EGR1		-0.015	0.210	-2.251	0.053	3.703	1.889	-0.265	0.616	-0.700	-0.500	0.913	-0.132
FRMD4B		-0.036	0.636	-0.652	0.064	1.629	0.704	0.049	1.474	0.559	-0.936	1.012	0.017
FZD1		0.281	1.533	0.617	0.005	1.474	0.560	0.634	1.168	0.223	0.030	4.363	2.125
HTR2B		0.027	1.352	0.435	0.497	1.118	0.161	0.559	1.293	0.371	-0.042	0.666	-0.586
HTR7		-0.033	0.682	-0.553	0.062	2.103	1.072	0.948	1.058	0.081	0.070	1.235	0.304
KCNMB4		0.269	1.108	0.148	-0.929	1.002	0.003	0.098	1.639	0.713	0.100	1.267	0.341
KLF2		0.205	55.054	5.783	-0.492	0.936	-0.095	0.226	151.575	7.244	0.003	5.392	2.431
LACC1		0.108	1.697	0.763	0.393	1.288	0.365	-0.527	1.741	0.800	-0.098	0.715	-0.484
MMD		0.017	2.293	1.197	0.002	3.171	1.665	0.011	6.543	2.710	0.359	1.326	0.407
MTSS1		-0.727	0.974	-0.039	0.564	1.117	0.159	0.128	1.709	0.773	0.025	2.277	1.187
NLRP3		-0.005	0.327	-1.613	0.028	1.749	0.806	-0.025	0.266	-1.912	-0.774	0.995	-0.007
OLFML2B		0.032	1.264	0.337	0.057	1.615	0.692	0.008	2.183	1.126	-0.610	0.952	-0.071
PID1		-0.117	0.738	-0.438	0.556	1.088	0.121	-0.132	0.630	-0.667	0.347	1.159	0.213
PIK3CG		-0.453	0.914	-0.130	0.114	1.360	0.444	0.189	1.742	0.800	0.054	1.401	0.486
RHPN2		0.133	1.784	0.835	-0.390	0.800	-0.322	-0.079	0.548	-0.869	-0.240	0.732	-0.449
SGMS1		0.022	1.497	0.582	-0.267	0.911	-0.135	0.049	1.375	0.460	-0.007	0.521	-0.941
SLC40A1		-0.775	0.973	-0.039	-0.131	0.545	-0.875	0.964	1.041	0.057	0.487	1.116	0.159
TRIB3		-0.063	0.587	-0.769	0.003	19.121	4.257	0.005	9.798	3.292	-0.436	0.878	-0.188
ZFP36L2		-0.364	0.952	-0.071	0.015	2.771	1.470	0.006	7.534	2.913	-0.828	1.021	0.030

UO (UO126, MEK inhibitor), BIRB (BIR0796, p38 inhibitor), SP600 (JNK inhibitor). Green and red highlight genes that are significantly up- or downregulated, respectively, after LPS stimulation by the inhibitor treatment as compared to controls ($p<0.05$ and $\log_2$LPS+inhibitor/LPS+vehicle>1 or <-1)

RESULTS

CHAPTER TWO

MAFB determines human macrophage anti-inflammatory polarization: pathological relevance for Multicentric carpotarsal osteolysis

MAFB expression in human macrophages under homeostatic and anti-inflammatory conditions.

Transcriptional analysis of M-MØ and GM-MØ identified the transcription factor-encoding *MAFB* gene as preferentially expressed in macrophages with anti-inflammatory potential (GSE27792) [138], since M-MØ express much higher levels of *MAFB* RNA than GM-MØ (19-times higher, $p<0.0005$) (**Figure 17A**). In agreement with the transcriptional data, MAFB protein expression was very high in M-MØ but barely detectable in GM-MØ (**Figure 17B**). During M-CSF-driven differentiation, *MAFB* mRNA levels dropped at early time points and peaked 24-48 hours after M-CSF treatment (**Figure 17C**, *left panel*) while high MAFB protein levels were acquired along M-MØ differentiation and reached maximum levels after 24 hours (**Figure 17C**, *right panel*). IL-34, a cytokine that drives macrophage differentiation through the M-CSF receptor [52; 53], also led to macrophages exhibiting high levels of *MAFB* mRNA (**Figure 17D**). Moreover, MAFB protein levels were upregulated in monocytes exposed to M-CSF-containing tumor cell-conditioned media (ascitic fluid) (**Figure 17E**). Therefore, M-CSF, IL-34 and M-CSF-containing ascitic fluids increase MAFB expression in human monocytes and promote the generation of macrophages with an anti-inflammatory profile, in line with our previous reports [38]. Inmunohistochemistry analysis revealed that MAFB expression is readily detected *in vivo* in tissue-resident $CD163^+$ macrophages from colon (submucosa and muscle) and skin, as well as in tumor-associated $CD163^+$ macrophages in melanoma samples (**Figure 17F**), thus confirming the expression of MAFB in tissue-resident homeostatic macrophages from certain tissues as well as in macrophages with anti-inflammatory potential under pathological conditions. Altogether, these results reveal that the expression of MAFB characterizes human macrophages with homeostatic/anti-inflammatory functions both in vitro and in vivo.

MAFB controls the acquisition of the anti-inflammatory transcriptional profile of M-MØ.

Since MAFB is the transcription factor most differentially expressed between anti-inflammatory M-MØ and pro-inflammatory GM-MØ (GSE27792) [138], its role in human anti-inflammatory human macrophage polarization was assessed. To that end, *MAFB* expression was knocked-down in M-MØ using *MAFB*-specific siRNA (siMAFB, **Figure 18A**), and the expression of the genes exhibiting the highest differential expression between GM-MØ and M-MØ was determined. The expression of most M-MØ-specific genes was found to be dependent on MAFB expression levels (**Figure 18B**), including *HTR2B*, *CCL2*, *IGF1*, *STAB1* and *CD163L1*, whose expression is associated with

macrophage homeostatic and anti-inflammatory functions [79; 150-153]. A similar result was observed in M-CSF-dependent bone marrow-derived mouse macrophages, where *Mafb* knockdown diminished the expression of genes associated to M-CSF-driven anti-inflammatory polarization like *Il10*, *Gas6* and *Ctla2b* [95] (**Figure 18D,C**). Therefore, MAFB controls the expression of genes associated to anti-inflammatory M-MØ polarization.

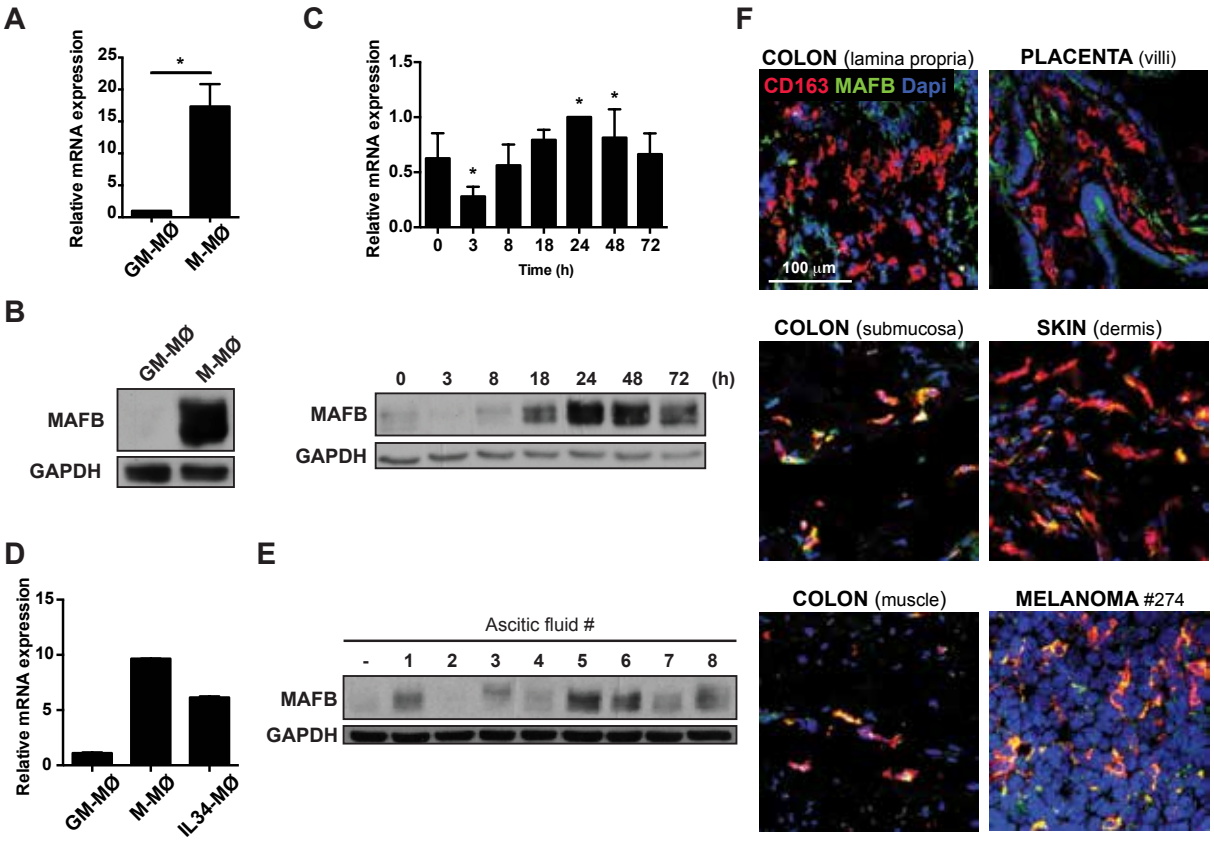

Figure 17. MAFB expression in homeostatic and anti-inflammatory macrophages *in vitro* and *in vivo*. (A) *MAFB* mRNA expression in GM-MØ and M-MØ as determined by qRT-PCR. Results are indicated as the expression of *MAFB* mRNA in M-MØ relative to the expression in GM-MØ (n=6, p = 0.0055). **(B)** MAFB protein expression in GM-MØ and M-MØ as determined by western blot. A representative experiment of three independent experiments is shown. **(C)** *MAFB* mRNA (left panel) and MAFB protein (right panel) expression in monocytes differented in the presence of M-CSF. The left panel shows the mean ± SD of the *MAFB* mRNA levels at the indicated time points and relative to the levels detected at the 24h time point (n=4; *, $p < 0.05$). The right panel illustrates the result of one of two independent experiments. **(D)** *MAFB* mRNA expression in IL34-MØ. Shown is a representative experiment run in triplicates by qRT-PCR. Results are indicated as the levels of *MAFB* mRNA relative to the levels of housekeeping *HPRT1*, *TBP* and *RPLP0* genes. **(E)** MAFB protein expression levels in untreated monocytes (lane -) and monocytes exposed for 48h to ascitic fluids from patients with tumors of distinct origin: bladder (lane 1), colon (lanes 2,3,6), stomach (lane 4), ovary (lane 5), bile duct (lane 7) and thyroid gland (lane 8). **(F)** MAFB (green) expression in CD163+ (red) macrophages in frozen samples of the indicated homeostatic and pathological tissues. DAPI staining is shown in blue. Melanoma #274 refers to a biopsy from a lymph node melanoma metastasis sample.

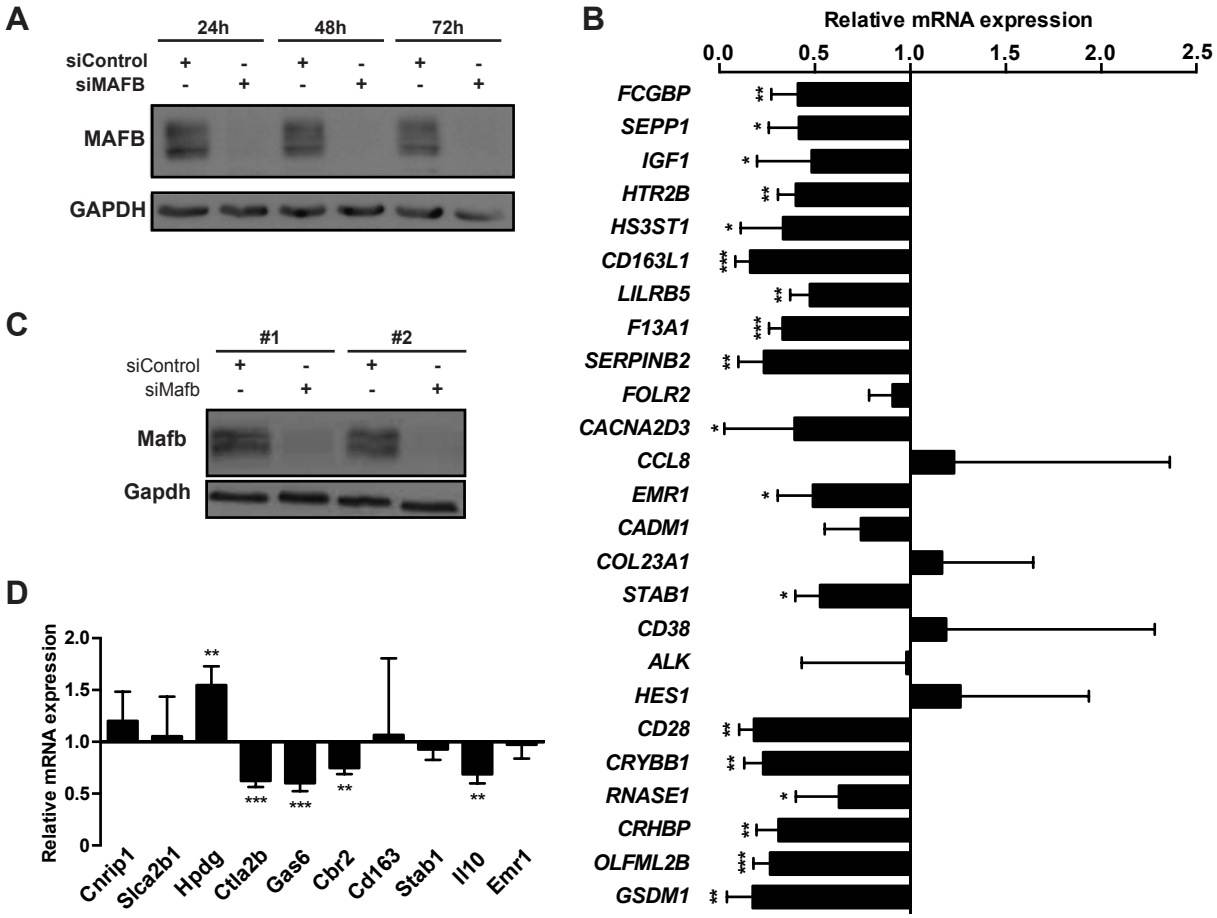

Figure 18. The expression of most M-MØ-specific genes is MAFB-dependent. (A) MAFB protein expression in M-MØ after transfection with either siControl or a MAFB-specific siRNA (siMAFB) for 24, 48 or 72 hours as determined by western blot. **(B)** Expression of the indicated M-MØ-specific genes in siRNA-transfected M-MØ for 24 hours, as determined by qRT-PCR. Results are indicated as the mRNA levels of each gene in siMAFB-transfected M-MØ relative to siControl-tranfected cells (n=4; *, $p < 0.05$; **, $p < 0.005$; ***, $p < 0.0005$). **(C)** MAFB protein expression in mouse M-MØ 24 hours after transfection with either siControl or a Mafb-specific siRNA (siMafb), as determined by western blot. Two independent experiments were performed (#1, #2) and both are shown. **(D)** Expression of the indicated murine M-MØ-specific genes in siRNA-transfected mouse M-MØ, as determined by qRT-PCR. Results are indicated as the mRNA levels of each gene in siMafb-transfected M-MØ relative to siControl-tranfected M-MØ (n=5; **, $p < 0.005$; ***, $p < 0.0005$).

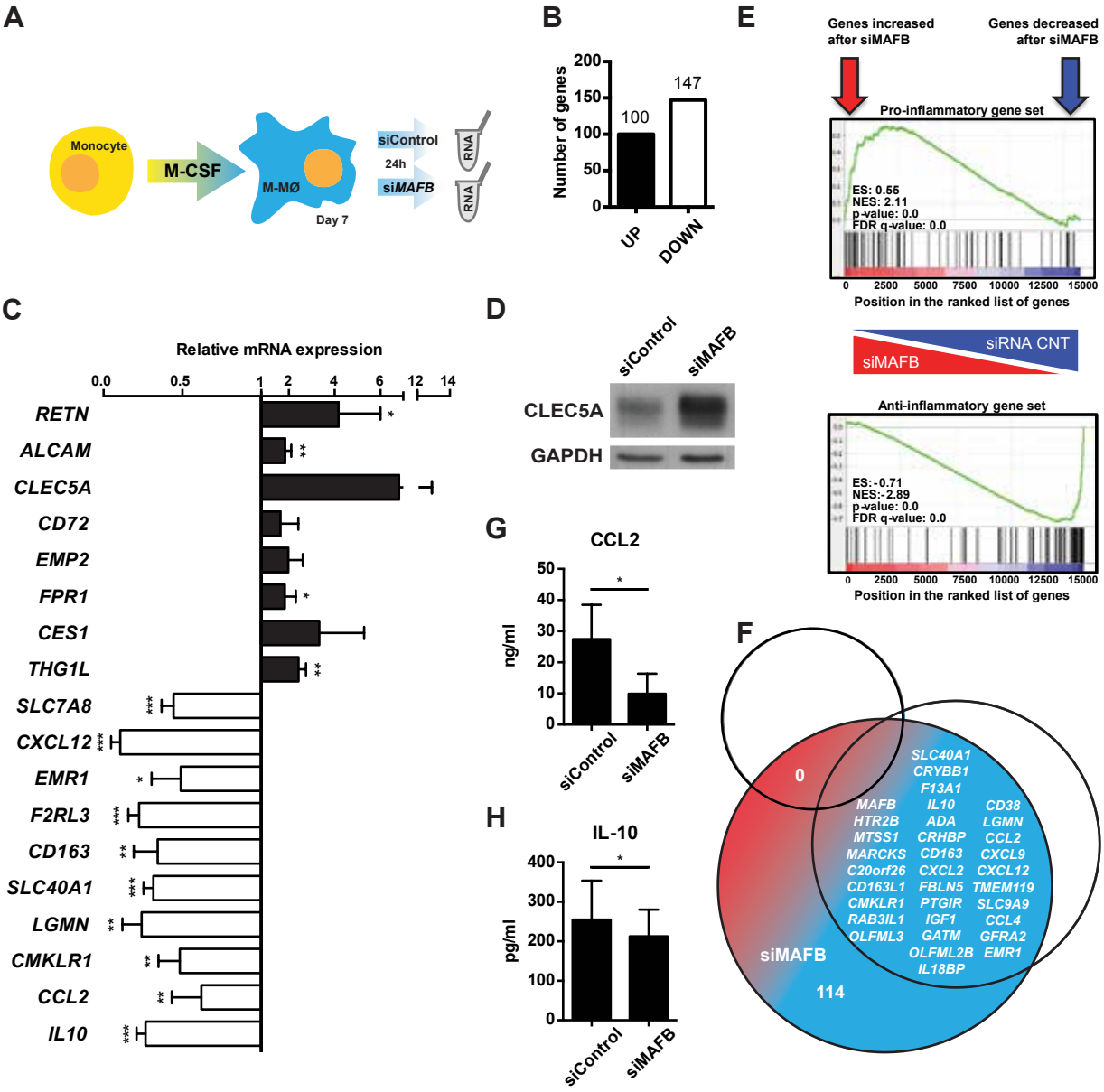

Figure 19. MAFB controls the global anti-inflammatory transcriptional signature of M-MØ. (A) Experimental design. **(B)** Number of genes whose expression is higher (UP) or lower (DOWN) in siMAFB-transfected M-MØ compared to siControl-transfected M-MØ (adjusted $p < 0.05$). **(C)** Validation of microarray results by qRT-PCR in independent samples of siMAFB-transfected and siControl-transfected M-MØ (n=4; $p < 0.05$; **, $p < 0.005$; ***, $p < 0.0005$). Results are indicated as the mRNA levels of each gene in siMAFB-transfected M-MØ relative to siControl-tranfected cells. **(D)** CLEC5A protein expression in siMAFB-transfected and siControl-tranfected M-MØ, as determined by western blot. Shown is one experiment out of three experiments performed on independent M-MØ samples. **(E)** GSEA analysis on the "t statistic-ranked" list of genes obtained from the siMAFB-M-MØ versus siControl-M-MØ limma analysis, using the proinflammatory (top) and anti-inflammatory (bottom) gene sets previously defined [142]. The red arrow indicates the location in the ranked list of those genes whose expression is higher in siMAFB-transfected M-MØ, while the blue arrow indicates the location of genes with lower expression in siMAFB-transfected M-MØ. **(F)** Venn diagram analysis of the genes with significantly lower expression in siMAFB-transfected M-MØ compared to the genes that best define the GM-MØ-specific and M-MØ-specific signatures (genes that are differentially expressed between GM-MØ and M-MØ by more than 8-fold, GSE68061) [142]. **(G, H)** CCL2 **(G)** and IL-10 **(H)** protein levels in culture media from M-MØ transfected with either siControl or siMAFB, as determined by ELISA (n=4 for CCL2, n=7 for IL-10; *, $p < 0.05$).

Notwithstanding the essential role of MAFB in the monocyte/macrophage lineage differentiation [119; 120; 125], the gene profile specifically regulated by human MAFB remained yet to be unraveled. To identify the whole range of MAFB-dependent genes in human macrophages, we determined the transcriptome of MAFB-deficient M-MØ (**Figure 19A**). Defective *MAFB* expression revealed a significantly (*adj p*<0.05) altered expression of 284 probes (247 annotated genes) in M-MØ (**Table VII**). Specifically, *MAFB* knockdown led to downregulation of 147 genes and upregulation of 100 genes in M-MØ (**Figure 19B** and **Table VII**). These results were later confirmed by qRT-PCR of selected genes, which showed that *MAFB* silencing not only reduces the expression of M-MØ-specific genes (e.g., *IL10*, *CCL2*, *EMR1*, *SLC40A1*) but also increases the expression of genes associated to GM-CSF-driven pro-inflammatory polarization (e.g., *CLEC5A*) [79] as well as other cell surface receptor-encoding genes (e.g., *FPR1*, *ALCAM*) (**Figure 19C,D**). Gene Ontology analysis (ENRICHR, http://amp.pharm.mssm.edu/Enrichr/) [154; 155] of the genes downregulated upon *MAFB* knock-down revealed a significant enrichment of genes upregulated by IL-10 (*adj p*=7.4x10^{-23}) and IFNβ (*adj p*=9.8x10^{-32}), but downregulated upon *MYB* overexpression (*adj p*=5.8x10^{-14}), thus supporting the link between MAFB and the expression of anti-inflammatory genes, and in line with the type I IFN rheostat function of MAFB [117] and the competing activities of MAFB and MYB on myeloid cell differentiation [98] (**Figure 20**). Regarding the genes whose expression significantly increases after *MAFB* knock-down, ENRICHR analysis revealed a significant enrichment of genes with functional MYB-binding sites (*adj p*=5.1x10^{-16}) as well as vitamin D3- or Retinoic acid-responsive genes (*adj p*=3.4x10-3 and 5.4x10-^{3}, respectively) (**Figure 20**), two compounds that control osteoclast proliferation and differentiation [156]. Moreover, *MAFB* knock-down downregulated the expression of 69 genes whose mouse orthologous have been identified as MAFB targets by ChIP-seq [157] (**Figure 21**), further supporting the significance of the results.

Finally, Gene Set Enrichment Analysis (GSEA) was done using the gene sets that best define pro-inflammatory GM-MØ- and anti-inflammatory M-MØ-specific signatures [138; 151]. The analysis revealed that *MAFB* knockdown significantly downregulates the expression of the genes within the "M-MØ-specific anti-inflammatory gene set" while increases the expression of the "GM-MØ-specific anti-inflammatory gene set" (**Figure 19E**). In fact, 19.4% of the genes within the M-MØ-specific gene set (33 out of 170) were significantly downregulated upon *MAFB* knockdown, including genes with known anti-inflammatory ability like *HTR2B* and *IGF1* (**Figure 19F**). Conversely, none of the GM-MØ-specific gene set (0 out of 182) were affected by MAFB silencing (**Figure 19F**). These results were validated at the protein level, as *MAFB* knockdown specifically reduced the basal production of both CCL2 (**Figure 19G**) and IL-10 (**Figure 19H**) from M-MØ. Altogether, the above results demonstrate that MAFB is a critical factor

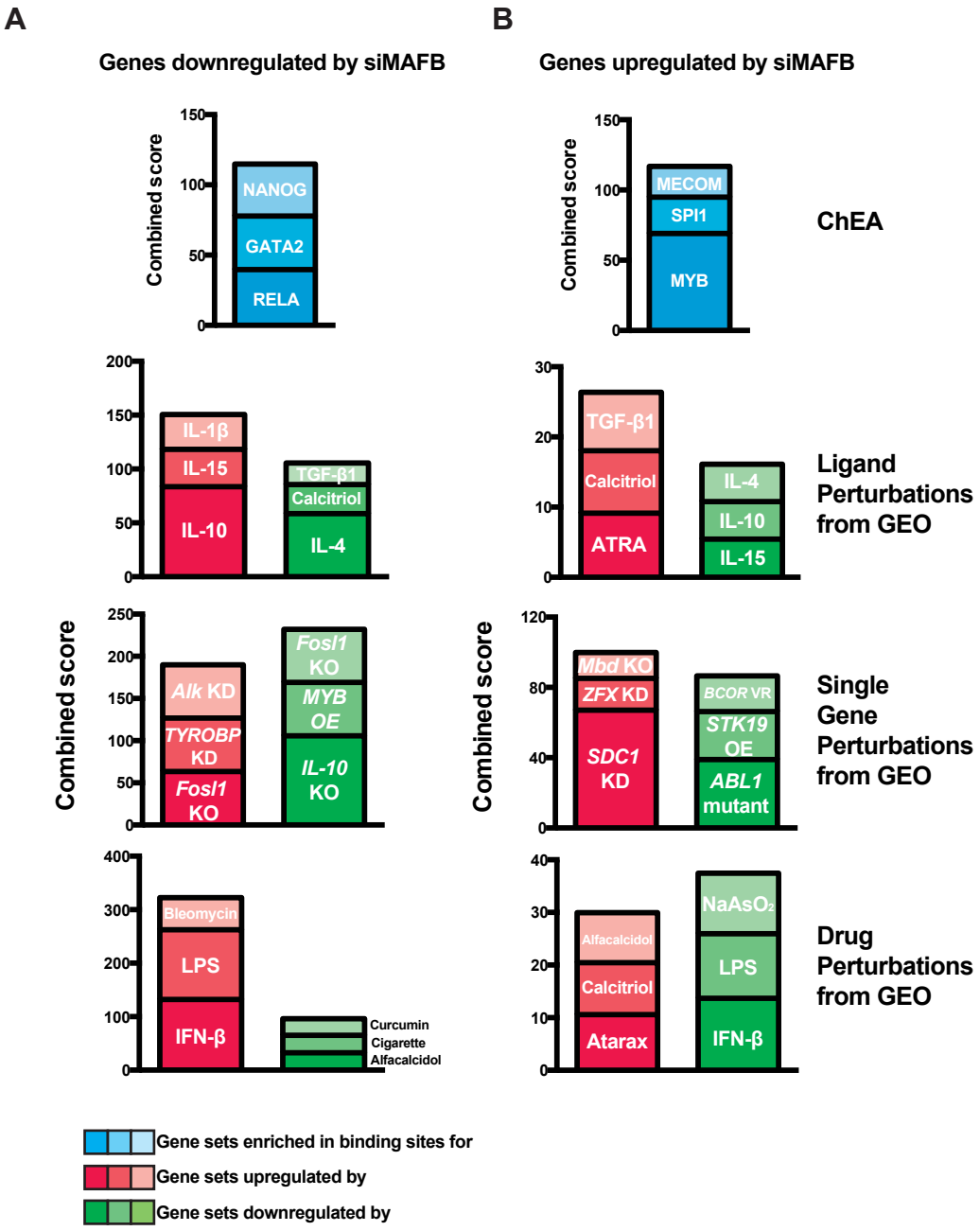

Figure 20. Gene Ontology analysis of genes whose expression is significantly modulated upon MAFB knockdown in M-MØ. (A, B) Genes significantly affected by siMAFB knockdown in M-MØ (**A**, downregulated; **B**, upregulated) were analysed for significant enrichmet of GO terms using the online tool ENRICHR. From top to bottom, the following databases were queried: ChEA, Ligand Perturbations from GEO, Single Gene Perturbations from GEO and Drug Perturbations from GEO. Color gradient intensity illustrates more to less significant hits. As suggested by the ENRICHR website, results are represented as 'Combined score' (combined score = log(*p*-value) * z-score). All the GO terms shown exhibit adjusted *p* value<0.05.

for the acquisition/maintenance of the anti-inflammatory transcriptome of human macrophages, as it positively controls the expression M-MØ-specific genes and impairs the expression of genes associated to the GM-CSF-directed pro-inflammatory polarization. Such a conclusion is also supported by GSEA of the microarray data, which revealed a significant enrichment of the "Hallmark-Inflammatory Response" and "Hallmark-Interferon gamma response", "Hallmark-Interferon gamma response" and "Hallmark-Interferon alpha response" terms in the genes upregulated after siMAFB transfection (FDR q-val = 0) and a significant enrichment of the "Hallmark-Angiogenesis" term (FDR q-val=0.011) in the genes downregulated upon *MAFB* knock-down (d*ata not shown*).

A

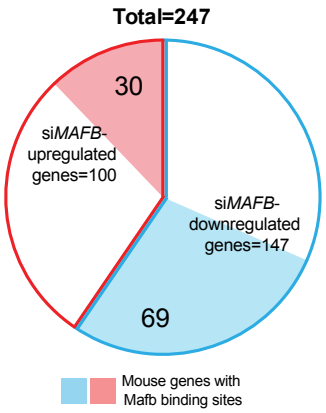

B

ChIP-seq Mafb binding sites (Human ortologues)			
Adssl1	*Abcc5*	*Gfra2*	*Stag3*
Alcam	*Ada*	*Gpr160*	*Tagap*
Alox5ap	*Adrb2*	*Htr2b*	*Tcf4*
Cd72	*Antxr1*	*Ifitm3*	*Tifab*
Cd93	*Ap2a2*	*Igf1*	*Tmem106a*
Col18a1	*Atp13a2*	*Il10*	*Tomm20*
Emp2	*C3ar1*	*Il18bp*	*Trim47*
Fam117b	*Ccl2*	*Itsn1*	*Zhx2*
Fcr1b	*Ccl4*	*Kif20b*	
Fndc3a	*Ccl5*	*Lacc1*	
Fpr1	*Cd163*	*Lag3*	
Gpx3	*Cd200r1*	*Lair1*	
Il10rb	*Cd36*	*Lgmn*	
Il17ra	*Clmp*	*Mmd*	
Itga4	*Cmklr1*	*Mtss1*	
Lsm14a	*Crhbp*	*Nln*	
Mfsd6	*Crybb1*	*Olfml2b*	
Osm	*Ctsl*	*Olfml3*	
Pcyox1l	*Cxcl1*	*Rab3il1*	
Pid1	*Cxcl12*	*Rb1*	
Ranbp2	*Epsti1*	*Rbms1*	
Scamp1	*F13a1*	*Rhobtb1*	
Selm	*F2rl3*	*Rnf19b*	
Slc11a1	*Fam26f*	*Sgms1*	
Slc16a6	*Fas*	*Siglec1*	
Srpk2	*Fbln5*	*Slc40a1*	
Steap3	*Fgd2*	*Slc7a8*	
Tgfbr1	*Gadd45g*	*Slc9a9*	
Thbd	*Gatm*	*Slco2b1*	
Vcan	*Gcnt1*	*Snx6*	

Figure 21. The mouse ortologues of a significant number of MAFB-regulated genes contain Mafb-binding sites. (A) Comparison of the number of genes significantly affected by siMAFB knockdown (147 downregulated genes; 100 upregulated genes) and the presence of Mafb-binding sites in the vicinity of their corresponding mouse ortologues, as determined by Chip-seq [115]. **(B)** List of M-MØ MAFB-regulated genes whose corresponding mouse ortologues include an experimentally verified Mafb-binding site.

The M-MØ-specific macrophage transcriptome is altered in macrophages derived from Multicentric Carpo Tarsal Osteolysis monocytes.

Addressing the role of MAFB in the adult organism has been hampered by the fact that *Mafb* KO mice die shortly after birth from apnea due to a defect in the neuronal development of the respiratory center of the brain [123]. Recently, however, mutations clustering within the amino-terminal transcriptional activation domain of MAFB have been demonstrated to cause Multicentric carpotarsal osteolysis (MCTO, OMIM# 166300), a very rare autosomal dominant disorder that causes degradation of the carpal and tarsal bones in early childhood and eventually evolves to end-stage renal failure [133-135; 137]. To date, all reported MCTO mutations affect the GSK3 phosphorylation sites within MAFB [133-135; 137], and mutations of the homologous region of MAF and NRL result in the recently described Aymé-Gripp syndrome (OMIM #601088) and retinitis pigmentosa [104], respectively. Since impaired GSK3 phosphorylation of large MAF family members leads to extended half-life and weaker transactivation potency [96; 104; 105], we hypothesized that MCTO-causing MAFB mutations would modulate MAFB levels and activity in human macrophages, thus influencing the anti-inflammatory gene signature of M-MØ. To test this hypothesis, we first generated *MAFB* expression constructs with either the Ser54Leu (161C>T) mutation, which was identified in a case of MCTO previously characterized only from the clinical point of view (hereafter termed MCTO#1) (**Figure 22A**) [158], the Pro63Arg mutation (188C>G, MCTO#2) [133; 134] or the Pro71Ser mutation (211C>T, MCTO#3) [133] (**Figure 22B**). Transfection of the three MCTO-causing MAFB mutants in HEK293T cells revealed their extended half-life upon cycloheximide treatment (**Figure 22E**), with an apparent stronger effect of mutations affecting the more C-terminal residues of the GSK3 phosphorylation sequence. This effect is also observed in monocytes and M-MØ from MCTO#1 (**Figure 22C,D**) Besides, and in agreement with previous results on MAF and MAFA mutations [96; 105], MCTO MAFB mutants exhibited reduced transactivation activity on a MAFB reporter construct (**Figure 22F**). Therefore, MCTO-causing MAFB mutations affect both the stability and the transcriptional activity of MAFB. This result is in agreement with previous results on other members of the large MAF subfamily, and might explain the increase of MAFB protein in the absence of overt changes in *MAFB* mRNA levels during M-MØ differentiation (**Figure 17C**).

Having demonstrated that MCTO-causing mutations increase MAFB protein stability, we next assessed the effect of enhanced MAFB levels on macrophage anti-inflammatory polarization through the use of monocyte-derived macrophages from MCTO patients. To that end, M-MØ and GM-MØ were generated from the MCTO#1 patient [158], and the transcriptomic profile of MCTO#1 M-MØ was determined. Comparison

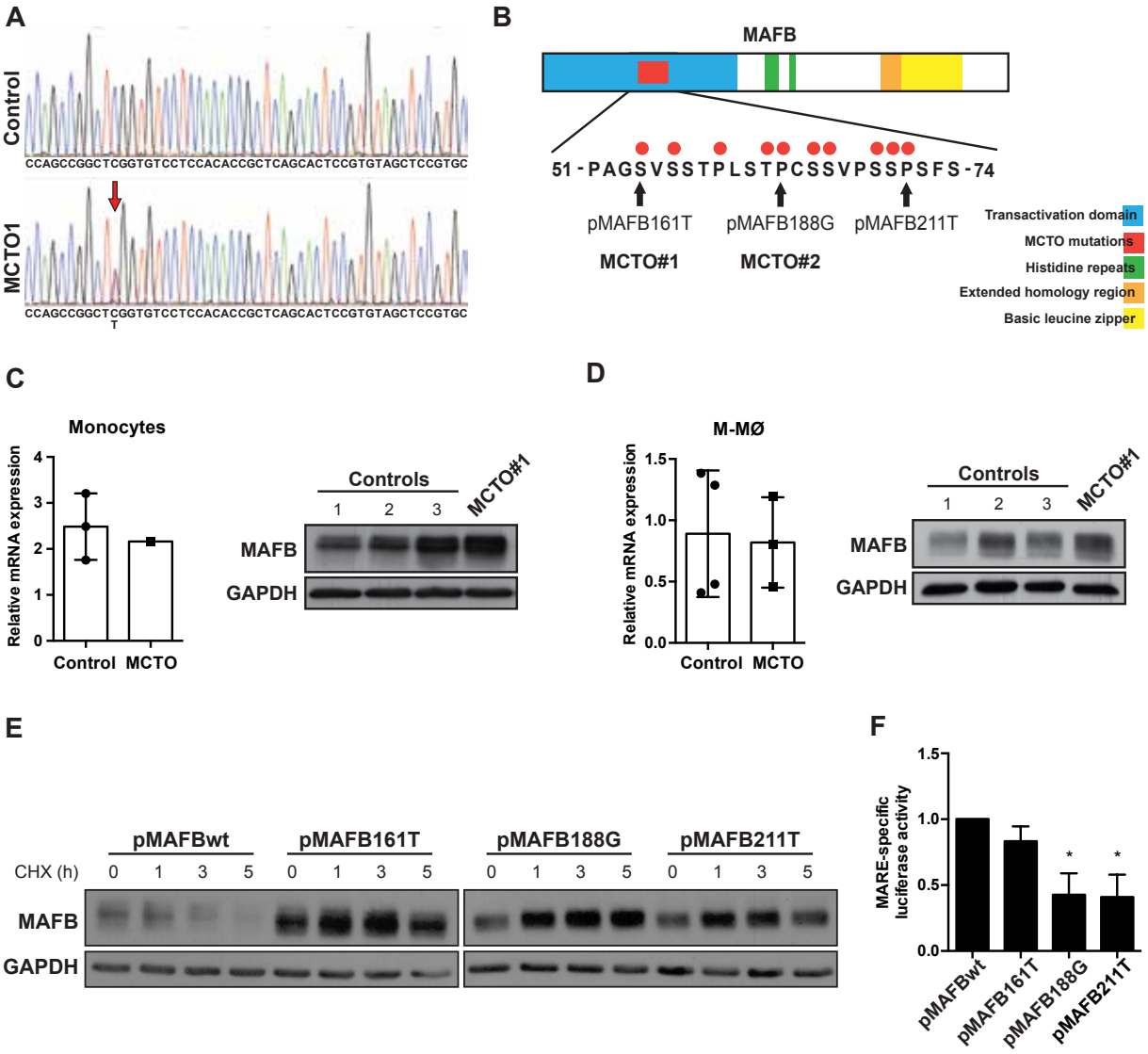

Figure 22. Mutations responsible for Multicentric carpotarsal osteolysis affect the stability and transcriptional activity of MAFB. (A) Nucleotide sequence of the mutation hotspot in the *MAFB* gene in MCTO. Sequencing of a healthy donor (top) and the MCTO#1 patient (down) is shown. Red arrow marks the heterozygous mutation (161C>T) in MCTO#1. **(B)** Representation of the MAFB protein. Red dots indicate amino acids mutated in MCTO. Black arrows indicate the amino acids mutated in the MCTO MAFB expression vectors and the amino acids affected in the MCTO#1, MCTO#2 and MCTO#3 patients. **(C-D)** MAFB mRNA and protein expression in monocytes **(C)** and M-MØ **(D)** from MCTO#1 and three healthy controls, as determined by qRT-PCR and western blot. **(E)** MAFB protein levels were determined by western blot in HEK293T transfected with the indicated expression vectors after 1-5 hours of cycloheximide (CHX) treatment. **(F)** MAFB-dependent MARE-specific transcriptional activity in HEK293T cells transfected with the indicated MAFB expression vectors. The MARE-specific luciferase activity was determined by expressing the luciferase activity produced by each MAFB construct on the 3xMARE-Luc reporter relative to the luciferase activity produced by the same expression vector in the presence of the promoter-less TATA-pXP2 plasmid. In all cases, the MARE-specific activity of each MCTO-causing MAFB mutant is referred to the activity produced by pMAFBwt (arbitrarily set to 1) (n=3; *, $p < 0.05$; For pMAFB161T, $p=0.12$).

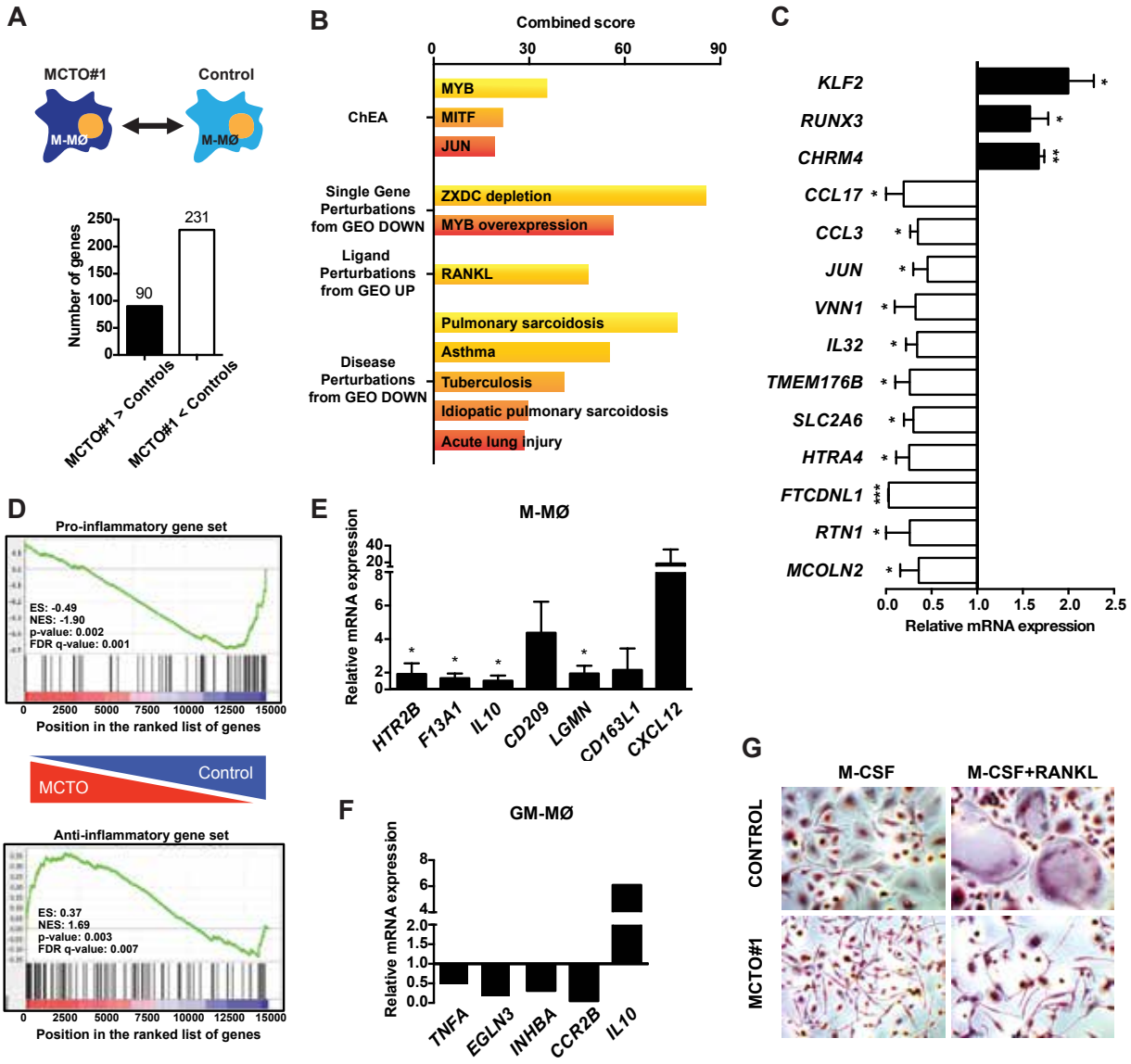

Figure 23. MCTO MAFB mutations significantly affect the M-MØ transcriptome. (A) Number of genes whose expression is higher (MCTO1>Control) or lower (MCTO1<Control) in MCTO#1 M-MØ than in control M-MØ ($p < 0.005$; adjusted $p < 0.192$; $|\log_2$ fold MCTO#1/Control$| > 0.7$), as determined by microarray analysis. **(B)** Gene ontology analysis of genes downregulated in MCTO#1, using the ENRICHR tool. The results extracted from the indicated databases are shown (combined score = log(p-value) x z-score). **(C)** Validation of microarray results by qRT-PCR in M-MØ from the three MCTO patients. Results are indicated as mean ±SD of mRNA levels in MCTO M-MØ relative to control M-MØ (n=3; *, $p < 0.05$; **, $p < 0.005$; ***, $p < 0.0005$). **(D)** GSEA analysis of the "t statistic-ranked" list of genes obtained from the MCTO#1 M-MØ versus Control M-MØ limma analysis, using the proinflammatory (top) and anti-inflammatory (bottom) gene sets previously defined. **(E)** Data are indicated as mean ±SD of mRNA levels in MCTO M-MØ relative to control M-MØ as determined by qRT-PCR (n=3; *, $p < 0.05$). **(F)** Results from a single experiment are indicated as the mRNA levels in MCTO#1 GM-MØ relative to control GM-MØ as determined by qRT-PCR. **(G)** MCTO#1 and control osteoclasts, as determined by phase contrast microscopy on cells stained for TRAP. Two independent experiments were done on monocytes from the MCTO#1 patient, and one of them is shown.

of MCTO#1 and control M-MØ gene signatures revealed the differential expression (*adj p*<0.19 or *p*<0.005) of 321 annotated genes, with 231 genes downregulated and 90 genes upregulated in MCTO#1 M-MØ (**Figure 23A**, **Table VIII**). Global analysis of the genes with lower expression in MCTO M-MØ revealed a significant enrichment of genes containing functional MYB- (*adj p*=4.5x10^{-9}), MITF- (*adj p*=7.5x10^{-13}) and JUN-binding sites (*adj p*=6.5x10^{-8}) (**Figure 23B**), a finding that fits with the known inhibitory actions of MAFB [99]. Further supporting the presence of elevated MAFB levels in MCTO M-MØ, the set of genes with lower expression in MCTO M-MØ was also significantly enriched in genes whose expression is enhanced by RANKL (*adj p*=1.9x10^{-13}), a major driver of osteoclast generation [99] (**Figure 23B**). Interestingly, the set of genes with higher expression in MCTO M-MØ was enriched in genes downregulated in systemic juvenile idiopathic arthritis (*adj p*=2.5x10^{-2}), a pathology that mimics MCTO [159]. Microarray data was further validated through qRT-PCR on independent preparations of MCTO#1 M-MØ as well as in M-MØ generated from additional MCTO#2 and MCTO#3 patients. These experiments identified 14 genes whose expression is significantly different between control and MCTO-derived M-MØ (**Figure 23C**).

The global effect of MCTO-causing MAFB mutations on the M-MØ transcriptome was also assessed by GSEA using the gene sets that best define GM-MØ- and M-MØ-specific signatures [138; 151]. As shown in **Figure 23D**, MCTO#1 M-MØ exhibited a significant reduction in the expression of pro-inflammatory (GM-MØ-specific) genes as well a significant increase in the expression of anti-inflammatory (M-MØ-specific) genes. Specifically, genes like *IL10*, *HTR2B* and *CD209*, whose expression is linked to M-MØ polarization, critically contributed to the global increase of the anti-inflammatory gene set in MCTO#1 M-MØ (**Figure 23D**). In fact, the expression of these M-MØ-specific genes was also significantly enhanced in M-MØ derived from MCTO#2 and MCTO#3 (**Figure 23E**). In line with the GSEA results, the expression of genes that best define pro-inflammatory GM-MØ polarization (*TNF*, *CCR2*, *INHBA*, *EGLN3*) [138; 152; 160] appeared reduced, while *IL10* was enhanced, in GM-MØ from MCTO#1 (**Figure 23F**). Moreover, in agreement with the inhibitory effect of the MCTO#1 MAFB mutation on the expression of RANKL-regulated genes (**Figure 23B**), MCTO#1 monocytes exposed to M-CSF and RANKL exhibited an impaired ability to differentiate into multinucleated osteoclasts as shown by microscopy analysis (**Figure 23G**), the expression of osteoclast markers (**Figure 24A**) and collagen-degradation assays (**Figure 24B**). Altogether, these results indicate that macrophages from MCTO patients exhibit an enhanced anti-inflammatory profile and that heterozygous MCTO-causing MAFB mutations drive macrophages towards the upregulation of genes associated to anti-inflammatory macrophage polarization, thus reinforcing the contribution of MAFB to the acquisition and maintenance of the anti-inflammatory gene signature in human macrophages.

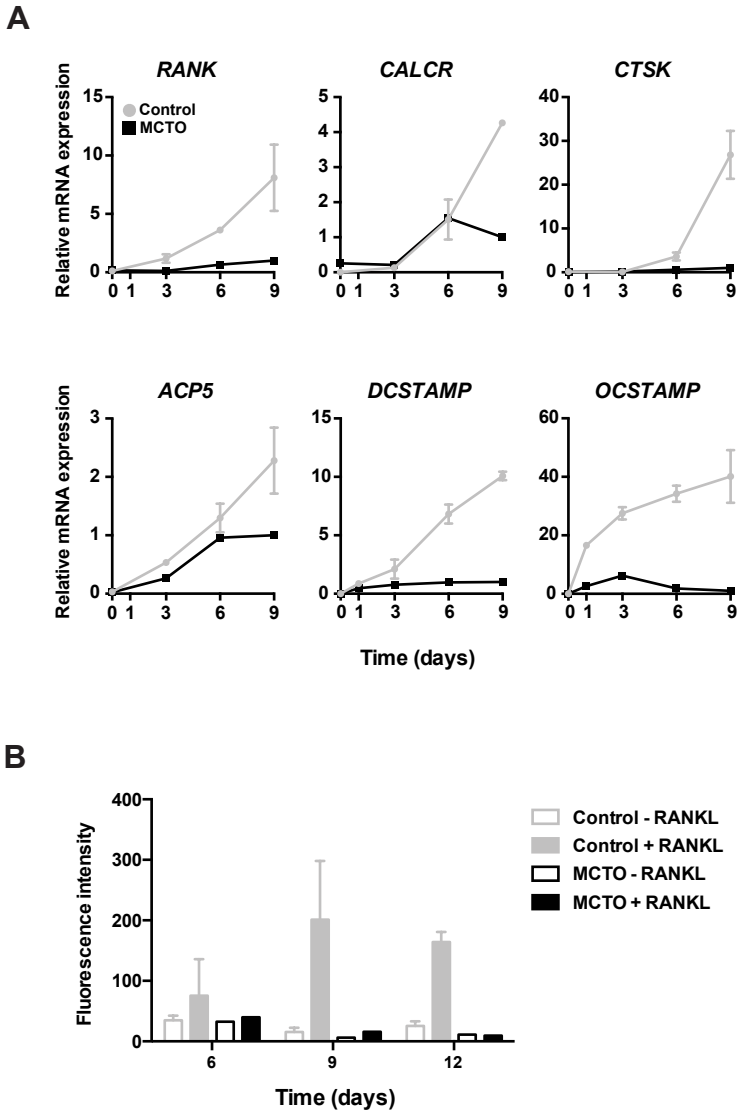

Figure 24. MCTO#1 monocytes exhibit an impaired osteoclast differentiation potential. (A) mRNA expression of osteoclast markers of *in vitro*-generated osteoclasts derived from monocytes from MCTO#1. Results from a single experiment are indicated as the mRNA levels in MCTO#1 and two healthy control osteoclasts at the indicated times during differentiation relative to *TBP* mRNA levels as determined by qRT-PCR. **(B)** Human collagen-degradation assay. Results from a single experiment are indicated as the intensity of fluorescently-labeled collagen degradation products in MCTO#1 and two healthy control osteoclasts.

MAFB also influences the LPS responsiveness of human macrophages.

Since MAFB controls the M-MØ transcriptome under basal conditions, the potential involvement of MAFB in the LPS-induced activation of M-MØ was also assessed. We have determined that M-MØ exhibit a unique transcriptional response to LPS, which is distinct from that of GM-MØ and includes the upregulation of *CCL19*, *ARNT2*, *MAOA* and *PDGFA* (**Figure 12**, **Table III & IV**). Knockdown of *MAFB* altered the LPS-responsiveness of M-MØ, as it significantly reduced the LPS-dependent upregulation

of *CCL19*, *ARNT2*, *PDGFA* and *MAOA* (**Figure 25A**). In fact, *MAFB* knockdown significantly diminished the LPS-induced expression of *IL10* (**Figure 25B**). By contrast, the LPS-mediated increase of these genes was higher in MCTO#1 M-MØ than in control M-MØ (**Figure 25C**), again illustrating the opposite consequences of *MAFB* silencing and MCTO-causing MAFB mutations. Therefore, MAFB also contributes to the acquisition of the gene expression profile of LPS-activated M-MØ.

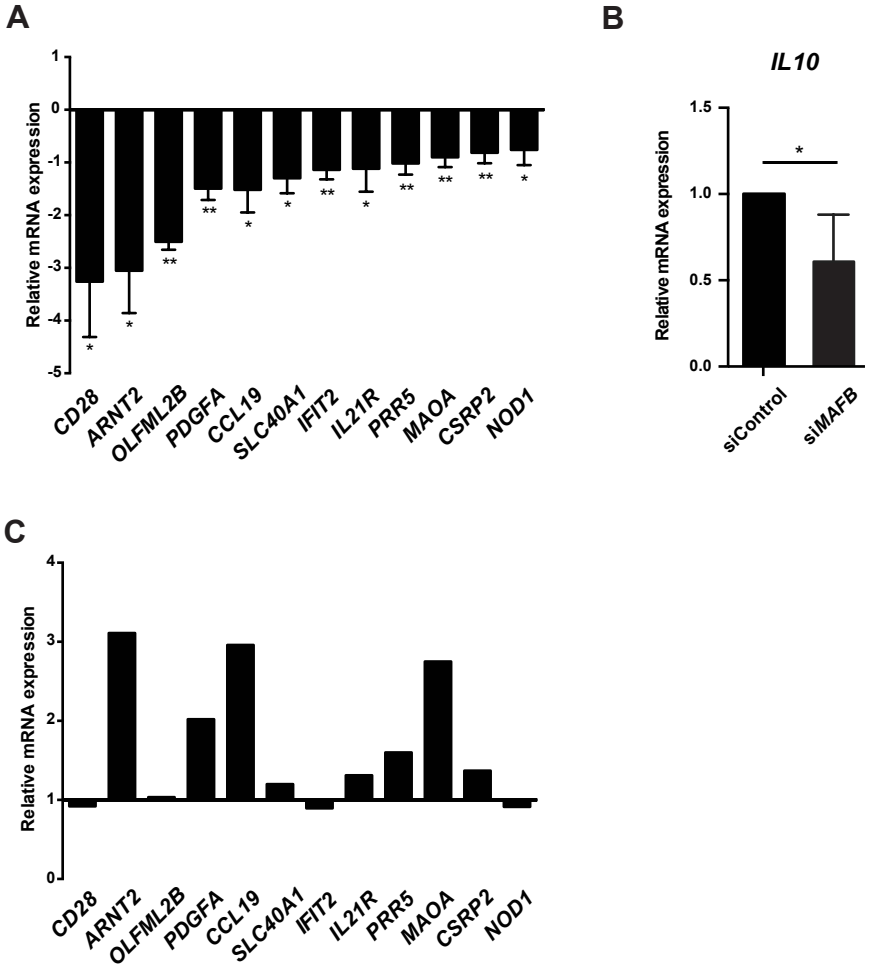

Figure 25. MAFB impacts the LPS response of M-MØ. (A) mRNA expression levels in LPS-treated (10ng/ml, 4h) siMAFB M-MØ, as determined by qRT-PCR using custom-made microfluidic gene cards. Results are indicated as the mRNA levels of each gene in LPS-treated siMAFB M-MØ relative to LPS-treated siControl M-MØ (n=3; *, $p < 0.05$; **, $p < 0.005$; ***, $p < 0.0005$). **(B)** *IL10* mRNA expression in LPS-treated siMAFB M-MØ as determined by qRT-PCR. Results are shown relative to the *IL10* mRNA level detected in siControl-transfected LPS-treated M-MØ (arbitrarily set to 1) (n=5; *, $p < 0.05$). **(C)** mRNA expression levels in LPS-treated MCTO#1 M-MØ, as determined by qRT-PCR. Results are indicated as the change in the expression of each gene in LPS-treated MCTO#1 M-MØ relative to the change of the same gene in LPS-treated control M-MØ.

Co-expression of MAFB and MAFB-regulated genes in human macrophages in vivo.

To gain evidences for the pathophysiological significance of the MAFB-dependent transcriptome in human macrophages, we next determined whether a correlation existed between the expression of MAFB and proteins encoded by MAFB-dependent genes in human macrophages in vivo. To that end we performed immunofluorescence on melanoma, where accumulation of tumor-promoting and immunosuppressive macrophages associates with a poor clinical outcome [161], as well as in other tissues (e.g., gut) where macrophages display anti-inflammatory and homeostatic functions [162]. As shown in **Figure 26A**, co-expression of MAFB and CD163L1 was observed in $CD163^+$ macrophages from colon and dermis, where MAFB expression had been previously found (*see* **Figure 17F**). Moreover, $CD163^+$ tumor-associated macrophages from melanoma samples revealed the co-expression of MAFB and the proteins encoded by MAFB-dependent genes like *HTR2B*, *CD163L1* and *CXCL12* (**Figure 26B**). The correlation between MAFB and CD163L1 expression is particularly relevant because CD163L1 expression marks anti-inflammatory IL-10 producing tissue-resident macrophages in healthy secondary lymphoid organs and gut, and also characterizes tumor-associated macrophages in melanoma [79]. Therefore, MAFB is a primary driver of the anti-inflammatory gene profile of human M-CSF-dependent macrophages, and the presence of MAFB-regulated genes provides useful markers for the in vivo identification of anti-inflammatory macrophages.

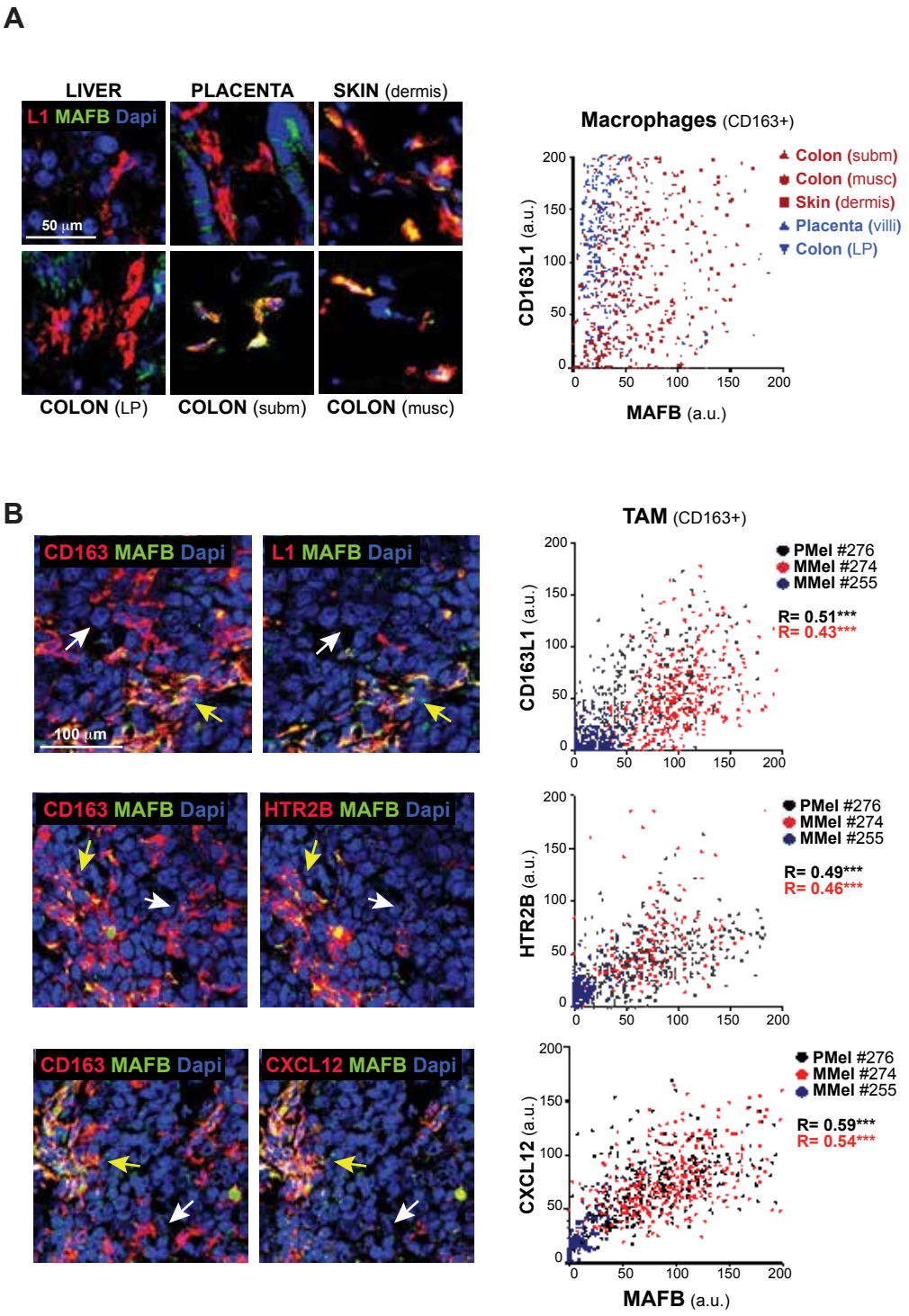

Figure 26. Human tissue-resident macrophages co-express MAFB and MAFB-dependent genes. **(A)** Immunofluorescence of MAFB (green) and CD163L1 (L1, red) in tissues, as determined by confocal microscopy. Right panel: Correlation between MAFB and CD163L1 expression in CD163+ macrophages. Red and blue mark tissues with CD163+MAFB+ or CD163+MAFB- macrophages, respectively. **(B)** Expression of the indicated proteins in samples of primary melanoma (PMel #276). Yellow arrows mark CD163+ MAFB+ CD163L1+ HTR2B+ CXCL12+ macrophages, while white arrows mark CD163+ MAFB- CD163L1- HTR2B- CXCL12- macrophages. Bottom panels show the positive correlation between MAFB expression and the expression of CD163L1, HTR2B and CXCL12 in CD163+ tumor-associated macrophages from primary melanoma (Pmel #276), lymph node metastatic melanoma (MMel #274) and skin metastatic melanoma (MMel #255) samples.

Table VII. Probes and annotated genes with altered expression in siMAFB M-MØ.

Probe	log_2FC	Avg.Exp.	t	*p* value	adj. *p* val	Gene Symbol
A_23_P17345	-2.2267	14.2667	-20.875	0.0000	0.0051	***MAFB***
A_23_P202448	-2.4133	10.3833	-18.0454	0.0000	0.0051	***CXCL12***
A_33_P3215803	-1.89	8.8617	-16.9278	0.0000	0.0051	***EMR1***
A_33_P3220837	-1.9933	15.64	-16.7766	0.0000	0.0051	***MAFB***
A_23_P376557	-1.9	10.09	-16.5567	0.0000	0.0051	***MMP25***
A_33_P3236881	-1.87	11.705	-15.9739	0.0000	0.0053	***MINOS1-NBL1***
A_23_P25994	-2.61	11.8617	-14.8108	0.0000	0.0063	***LGMN***
A_23_P164047	-1.81	10.2817	-14.7345	0.0000	0.0063	***MMD***
A_23_P41217	-1.7067	6.63	-13.3588	0.0000	0.0081	***CD200R1***
A_23_P210482	-1.5033	14.2017	-12.7094	0.0000	0.0088	***ADA***
A_33_P3400273	-1.49	7.8783	-12.603	0.0000	0.0088	***SELL***
A_23_P33723	-1.3367	15.3517	-12.2681	0.0000	0.0088	***CD163***
A_23_P2431	-1.37	12.885	-12.1283	0.0000	0.0088	***C3AR1***
A_23_P78037	-1.8067	7.9167	-12.0801	0.0000	0.0088	***CCL7***
A_33_P3330264	-1.5533	6.71	-11.9528	0.0000	0.0088	***CXCL1***
A_24_P125335	-2.8967	7.075	-11.8415	0.0000	0.0088	***CCL13***
A_23_P200073	-1.53	8.9783	-11.841	0.0000	0.0088	***PITHD1***
A_24_P379750	-1.3733	10.93	-11.7523	0.0000	0.0088	***MXD1***
A_24_P183150	-1.6567	7.4883	-11.3972	0.0000	0.0102	***CXCL3***
A_23_P435521	-1.1667	7.3467	-10.8924	0.0000	0.0112	***TMEM106A***
A_33_P3235053	-1.2433	13.575	-10.6768	0.0000	0.0115	***TRIM47***
A_33_P3395605	-1.8633	10.3683	-10.6599	0.0000	0.0115	***TMEM119***
A_23_P152838	-1.67	10.155	-10.5402	0.0000	0.0117	***CCL5***
A_33_P3712341	-1.3833	6.7317	-10.2985	0.0000	0.0129	***CXCL12***
A_23_P374322	-1.34	9.66	-10.2836	0.0000	0.0129	***LACC1***
A_33_P3317580	-1.9167	10.225	-10.0243	0.0000	0.0141	***GFRA2***
A_23_P152605	-2.57	6.9083	-9.8334	0.0000	0.0149	***GSDMA***
A_23_P252962	-1.1167	8.195	-9.792	0.0000	0.0149	***ITSN1***
A_23_P30567	-1.43	6.825	-9.7494	0.0000	0.0149	***CRHBP***
A_24_P120934	-1.1067	9.15	-9.7161	0.0000	0.0149	***GADD45G***
A_24_P335305	-1.1367	9.7017	-9.5666	0.0001	0.0158	***OAS3***
A_23_P167328	-2.7133	9.34	-9.5492	0.0001	0.0158	***CD38***
A_23_P340848	-1.2333	10.62	-9.4147	0.0001	0.0165	***PTGIR***
A_23_P46351	-1.0033	6.4383	-9.376	0.0001	0.0166	***TDRKH***
A_33_P3423941	-1.3633	9.805	-9.2828	0.0001	0.0173	***IFITM1***
A_33_P3375859	-2.1533	5.9267	-9.0743	0.0001	0.019	***CXCR2P1***
A_33_P3225512	-1.0167	9.6217	-9.0176	0.0001	0.0194	***OAS2***
A_33_P3421626	-1.0167	9.7383	-8.8972	0.0001	0.0203	***KIAA1147***
A_23_P376449	-1.18	9.4433	-8.8294	0.0001	0.0204	***XLOC_l2_002049***
A_23_P151805	-1.2467	7.1233	-8.775	0.0001	0.0204	***FBLN5***
A_23_P321388	-1.0533	7.6633	-8.677	0.0001	0.0208	***RNF19B***
A_23_P204087	-0.9133	9.4933	-8.6385	0.0001	0.0208	***OAS2***

Table VII. Probes and annotated genes with altered expression in siMAFB M-MØ.

Probe	log_2FC	Avg.Exp.	t	*p* value	adj. *p* val	Gene Symbol
A_23_P15146	-1.72	7.6367	-8.6378	0.0001	0.0208	***IL32***
A_24_P131522	-1.19	6.2783	-8.5918	0.0001	0.0208	***ANTXR1***
A_33_P3282489	-1.1767	8.205	-8.5298	0.0001	0.0208	***GCNT1***
A_23_P404821	-1.0433	8.7117	-8.5131	0.0001	0.0208	***KIAA1147***
A_23_P500381	-1.0933	10.8567	-8.4474	0.0001	0.021	***HTR7***
A_33_P3370305	-0.9733	7.6267	-8.437	0.0001	0.021	***TMEM106A***
A_23_P94533	-0.93	15.6817	-8.2637	0.0001	0.0222	***CTSL***
A_24_P257416	-1.3067	9.7567	-8.2259	0.0001	0.0223	***CXCL2***
A_23_P81441	-1.2033	12.555	-8.0955	0.0001	0.0236	***C5orf20***
A_32_P201979	-1.0533	7.6567	-8.0778	0.0001	0.0236	***HECTD2***
A_24_P173754	-0.86	8.63	-8.0121	0.0002	0.0245	***C1orf21***
A_33_P3258346	-0.8533	9.5067	-7.9963	0.0002	0.0245	***XAF1***
A_33_P3331511	-1.48	7.61	-7.9744	0.0002	0.0246	***LINC00173***
A_23_P143621	-1.35	7.105	-7.935	0.0002	0.0247	***CRYBB1***
A_33_P3252394	-0.9033	11.3017	-7.9054	0.0002	0.0247	***GADD45G***
A_23_P68031	-1.15	8.715	-7.8926	0.0002	0.0247	***STAT4***
A_23_P45871	-1.38	11.7467	-7.8643	0.0002	0.0247	***IFI44L***
A_33_P3401243	-1.56	10.3233	-7.654	0.0002	0.0278	***OLFML2B***
A_23_P129064	-1.01	11.1783	-7.4786	0.0002	0.0311	***GATM***
A_23_P126735	-1.5333	9.4967	-7.4646	0.0002	0.0311	***IL10***
A_23_P145631	-0.89	9.785	-7.45	0.0002	0.0312	***GIMAP6***
A_33_P3299898	-1.28	10.7967	-7.4115	0.0002	0.0314	***CTSLP2***
A_33_P3214586	-0.9333	6.4467	-7.3771	0.0002	0.0314	***ARTN***
A_23_P87545	-0.7833	14.1983	-7.3744	0.0002	0.0314	***IFITM3***
A_23_P116942	-0.8933	6.92	-7.3668	0.0002	0.0314	***LAG3***
A_23_P315364	-1.18	10.9533	-7.3649	0.0002	0.0314	***CXCL2***
A_24_P140788	-0.8667	8.5	-7.3546	0.0002	0.0314	***FGD2***
A_23_P205489	-1.0467	9.3933	-7.3179	0.0003	0.032	***SLC7A8***
A_33_P3348288	-1.24	9.2533	-7.3084	0.0003	0.032	***RHOBTB1***
A_33_P3317058	-0.7867	8.0867	-7.2914	0.0003	0.0322	***STAG3***
A_33_P3397840	-1.0133	8.5867	-7.2446	0.0003	0.0328	***WIPF3***
A_24_P366509	-0.9333	6.8133	-7.2179	0.0003	0.0329	***PIK3R6***
A_33_P3311863	-0.9267	6.27	-7.189	0.0003	0.0329	***AP2A2***
A_23_P61466	-1.8567	11.2817	-7.1821	0.0003	0.0329	***CD163L1***
A_23_P125680	-0.8633	7.915	-7.1501	0.0003	0.0329	***TMEM255A***
A_23_P167005	-0.8333	10.5	-7.1477	0.0003	0.0329	***GPR160***
A_33_P3371089	-1.0233	11.595	-7.1365	0.0003	0.0329	***SGTB***
A_33_P3292679	-0.7933	11.92	-7.0367	0.0003	0.034	***SNX6***
A_33_P3489737	-1.05	10.2583	-7.0362	0.0003	0.034	***NLN***
A_23_P35995	-0.8	6.78	-7.0303	0.0003	0.034	***CLMP***
A_33_P3262124	-1.1333	7.1067	-7.0034	0.0003	0.034	***MMP25***
A_33_P3234697	-0.8833	12.365	-7.0026	0.0003	0.034	***LXN***

Table VII. Probes and annotated genes with altered expression in siMAFB M-MØ.

Probe	log_2FC	Avg.Exp.	t	*p* value	adj. *p* val	Gene Symbol
A_32_P140139	-1.4967	13.5283	-7.0019	0.0003	0.034	***F13A1***
A_33_P3411075	-0.8467	12.1833	-6.982	0.0003	0.034	***FSCN1***
A_24_P33982	-0.7733	11.1167	-6.9695	0.0003	0.034	***MILR1***
A_23_P89431	-2.5	11.5433	-6.9593	0.0003	0.034	***CCL2***
A_23_P75800	-0.9467	8.3167	-6.9084	0.0004	0.0346	***RAB3IL1***
A_33_P3327847	-0.7333	10.9333	-6.8909	0.0004	0.0349	***SGPL1***
A_24_P932418	-0.87	11.4583	-6.8705	0.0004	0.0352	***AP2A2***
A_24_P131222	-0.8867	8.7567	-6.8614	0.0004	0.0352	***ATP13A2***
A_23_P102391	-1.43	10.775	-6.7868	0.0004	0.0358	***SLC40A1***
A_23_P163567	-1.3167	8.5383	-6.7838	0.0004	0.0358	***SMPD3***
A_23_P64828	-0.8567	9.8817	-6.78	0.0004	0.0358	***OAS1***
A_23_P204850	-0.8433	12.1017	-6.7778	0.0004	0.0358	***RB1***
A_23_P54000	-0.7833	11.595	-6.7767	0.0004	0.0358	***SNX6***
A_32_P54553	-1.12	6.4433	-6.7711	0.0004	0.0358	***USP41***
A_33_P3298062	-0.7467	9.6167	-6.7292	0.0004	0.0362	***ABCC5***
A_23_P105794	-1.0467	9.4367	-6.7247	0.0004	0.0362	***EPSTI1***
A_23_P7144	-2.76	7.1767	-6.7161	0.0004	0.0362	***CXCL1***
A_23_P347632	-0.93	9.3317	-6.6999	0.0004	0.0362	***MTSS1***
A_23_P16953	-0.7967	11.7383	-6.6901	0.0004	0.0362	***HTR2B***
A_33_P3355230	-0.7567	10.5483	-6.6894	0.0004	0.0362	***LAIR1***
A_24_P287043	-0.7033	13.375	-6.6429	0.0004	0.037	***IFITM2***
A_33_P3400389	-0.72	10.47	-6.6239	0.0005	0.0372	***SPATS2L***
A_24_P15502	-0.7067	12.4867	-6.6007	0.0005	0.0377	
A_23_P12554	-1.05	9.275	-6.5137	0.0005	0.0396	***PKD2L1***
A_33_P3332112	-1.2967	5.8317	-6.5107	0.0005	0.0396	***FAS***
A_33_P3222451	-1.43	6.6383	-6.5081	0.0005	0.0396	***AKT1S1***
A_23_P145657	-0.7633	10.125	-6.485	0.0005	0.0402	***STAG3***
A_33_P3228322	-0.7833	11.6083	-6.4597	0.0005	0.0402	***IL18BP***
A_33_P3264926	-0.7633	9.185	-6.4582	0.0005	0.0402	***SAMD4A***
A_23_P105465	-1.04	9.9433	-6.4014	0.0005	0.0418	***CMKLR1***
A_24_P354724	-0.6933	8.3367	-6.3635	0.0006	0.0423	***TAGAP***
A_23_P47777	-0.7633	10.215	-6.3425	0.0006	0.0429	***9-Mar***
A_33_P3346826	-1.2967	6.4883	-6.3164	0.0006	0.043	***IL32***
A_23_P75071	-0.6833	6.345	-6.3137	0.0006	0.043	***KIF20B***
A_23_P111583	-0.68	13.51	-6.3094	0.0006	0.043	***CD36***
A_32_P101860	-0.8833	11.1517	-6.2832	0.0006	0.0435	***TMEM106A***
A_33_P3380383	-1.4067	13.09	-6.2728	0.0006	0.0435	***TIFAB***
A_32_P163125	-0.92	10.8833	-6.2724	0.0006	0.0435	***SGMS1***
A_23_P18452	-2.4567	7.6617	-6.2638	0.0006	0.0436	***CXCL9***
A_33_P3393821	-0.8267	6.66	-6.2495	0.0006	0.0438	***C1R***
A_23_P97064	-0.6733	9.2767	-6.2297	0.0006	0.0439	***FBXO6***
A_23_P168951	-0.67	7.435	-6.2054	0.0006	0.0439	***ZHX2***

Table VII. Probes and annotated genes with altered expression in siMAFB M-MØ.

Probe	log_2FC	Avg.Exp.	t	*p* value	adj. *p* val	Gene Symbol
A_32_P100109	-0.71	7.2983	-6.2043	0.0006	0.0439	***REPS2***
A_24_P16124	-0.6733	11.68	-6.1964	0.0007	0.0439	***IFITM4P***
A_24_P66027	-0.94	8.7767	-6.1863	0.0007	0.0439	***APOBEC3B***
A_23_P27332	-0.8033	12.7817	-6.1835	0.0007	0.0439	***TCF4***
A_23_P145024	-0.77	8.845	-6.1787	0.0007	0.0439	***ADRB2***
A_23_P66241	-0.8967	9.4217	-6.1687	0.0007	0.0439	***MT1M***
A_24_P11315	-0.7667	6.73	-6.1491	0.0007	0.0445	***OLFML3***
A_23_P150768	-0.8167	12.3683	-6.1083	0.0007	0.0452	***SLCO2B1***
A_24_P766716	-0.9967	13.8217	-6.0885	0.0007	0.0456	***CMKLR1***
A_23_P137689	-1.45	10.0083	-6.0599	0.0007	0.0456	***OLFML2B***
A_33_P3416097	-1.7267	7.0467	-6.0528	0.0007	0.0456	***F13A1***
A_23_P56734	-0.65	11.485	-6.0447	0.0008	0.0456	***HNMT***
A_33_P3281795	-0.6567	13.1183	-6.035	0.0008	0.0456	***MGLL***
A_32_P174572	-0.68	9.6033	-6.0348	0.0008	0.0456	***HTR7P1***
A_23_P17481	-1.3067	10.7467	-6.0345	0.0008	0.0456	***SIGLEC1***
A_33_P3232955	-1.5233	8.995	-6.0198	0.0008	0.0456	***F2RL3***
A_24_P212539	-0.6833	9.485	-6.0165	0.0008	0.0456	***GALM***
A_33_P3306973	-0.8333	7.79	-6.0161	0.0008	0.0456	
A_23_P133868	-0.7233	7.795	-6.0123	0.0008	0.0456	***ZKSCAN4***
A_23_P7827	-1.4967	9.235	-6.0117	0.0008	0.0456	***FAM26F***
A_32_P4262	-1.15	6.4317	-5.9917	0.0008	0.0459	***C20orf26***
A_32_P46214	-0.8133	11.9933	-5.9824	0.0008	0.0459	***SLC9A9***
A_23_P55270	-0.7533	12.0433	-5.972	0.0008	0.0459	***CCL18***
A_33_P3253394	-0.7933	12.89	-5.9654	0.0008	0.0459	***LAIR1***
A_24_P393838	-0.6333	9.15	-5.9623	0.0008	0.0459	***TOMM20***
A_23_P214222	-0.89	14.7317	-5.9236	0.0008	0.0468	***MARCKS***
A_33_P3248967	-0.66	9.6733	-5.9163	0.0008	0.0468	***MPP5***
A_24_P304423	-0.8833	10.8817	-5.9091	0.0009	0.0469	***IGF1***
A_23_P119478	-1.92	8.92	-5.9052	0.0009	0.0469	***EBI3***
A_33_P3354607	-1.99	11.755	-5.8665	0.0009	0.048	***CCL4***
A_23_P29257	-0.8367	9.555	-5.8467	0.0009	0.0483	***H1F0***
A_24_P59667	-0.76	11.2967	-5.8433	0.0009	0.0483	***JAK3***
A_23_P100001	-0.9933	6.9367	-5.8266	0.0009	0.0484	***FAM174B***
A_24_P142118	-0.85	7.6083	-5.8207	0.0009	0.0484	***THBS1***
A_33_P3316323	-0.6533	12.4767	-5.819	0.0009	0.0484	***RBMS1***
A_23_P63896	-1.1933	8.5267	-5.8087	0.0009	0.0484	***FAS***
A_33_P3375368	-0.7067	7.5633	-5.7945	0.0009	0.0488	***GPR35***
A_32_P44394	-0.9733	6.1233	-5.7861	0.0010	0.0488	***AIM2***
A_24_P228130	-1.1467	10.95	-5.7759	0.0010	0.0488	***CCL3L3***
A_23_P67367	-0.8267	8.3833	-5.765	0.0010	0.0488	***DHDH***
A_23_P13907	-0.84	13.1267	-5.7494	0.0010	0.0492	***IGF1***
A_23_P252541	-0.6167	11.5083	-5.739	0.0010	0.0493	***RAB7B***

Table VII. Probes and annotated genes with altered expression in siMAFB M-MØ.

Probe	log_2FC	Avg.Exp.	t	*p* value	adj. *p* val	Gene Symbol
A_24_P56194	-0.6233	9.8683	-5.7388	0.0010	0.0493	***CREBL2***
A_33_P3417452	0.6067	10.17	5.7219	0.0010	0.0498	***ZGLP1***
A_23_P99397	0.6233	8.155	5.7363	0.0010	0.0493	***ZDHHC20***
A_23_P152791	0.74	8.9333	5.756	0.0010	0.0491	***SLC16A6***
A_23_P82929	0.9233	8.7483	5.7661	0.0010	0.0488	***NOV***
A_24_P124624	0.7033	7.945	5.7671	0.0010	0.0488	***OLR1***
A_33_P3321657	0.79	9.6183	5.7672	0.0010	0.0488	***HSPG2***
A_33_P3540143	0.72	11.7933	5.7853	0.0010	0.0488	***IL17RA***
A_33_P3360942	0.6433	8.1083	5.793	0.0009	0.0488	***SCAMP1***
A_33_P3272390	0.7367	7.5183	5.8112	0.0009	0.0484	***RANBP2***
A_32_P180265	0.62	7.77	5.8134	0.0009	0.0484	
A_23_P206310	0.7067	12.3733	5.8212	0.0009	0.0484	***KIAA0513***
A_23_P76823	0.92	7.56	5.8212	0.0009	0.0484	***ADSSL1***
A_24_P389491	0.67	8.7683	5.8548	0.0009	0.0482	***COQ4***
A_24_P192914	0.8933	14.5433	5.8588	0.0009	0.0482	***AMICA1***
A_23_P325690	0.71	6.9583	5.8661	0.0009	0.048	***ANKRD35***
A_23_P6413	0.85	9.735	5.8997	0.0009	0.0469	***SELM***
A_23_P154234	0.6333	11.0967	5.9184	0.0008	0.0468	***POLE4***
A_23_P501722	0.72	8.0767	5.9191	0.0008	0.0468	***TSPAN32***
A_33_P3394404	0.8067	8.1533	5.9333	0.0008	0.0468	***TSPAN32***
A_23_P26905	0.63	8.585	5.9401	0.0008	0.0467	***POLG2***
A_24_P322741	0.82	11.0233	5.9663	0.0008	0.0459	***IL10RB***
A_33_P3702055	0.7767	10.4317	5.9783	0.0008	0.0459	***SLC11A1***
A_24_P163237	0.81	7.3083	5.984	0.0008	0.0459	***STOX2***
A_24_P239811	0.7933	8.9467	5.9939	0.0008	0.0459	***UBXN11***
A_23_P211212	0.6633	7.355	6.009	0.0008	0.0456	***COL18A1***
A_32_P88905	0.6433	8.6317	6.0174	0.0008	0.0456	
A_33_P3248265	0.66	7.3933	6.0398	0.0008	0.0456	***LTB***
A_33_P3316878	1.0133	8.8233	6.0475	0.0007	0.0456	***CHPF***
A_23_P365817	0.65	11.615	6.064	0.0007	0.0456	***PPP1R14B***
A_23_P38795	1.11	11.485	6.0779	0.0007	0.0456	***FPR1***
A_33_P3215676	1.06	6.3	6.1066	0.0007	0.0452	***MANSC4***
A_23_P61487	0.89	6.855	6.1082	0.0007	0.0452	***LRRC20***
A_23_P105862	0.7133	7.31	6.109	0.0007	0.0452	***FRY***
A_33_P3209960	0.7433	7.215	6.1298	0.0007	0.0451	***RASGRP2***
A_23_P97990	0.7967	12.4783	6.1688	0.0007	0.0439	***HTRA1***
A_23_P350574	0.66	9.1167	6.1799	0.0007	0.0439	***FCRLB***
A_23_P329152	0.72	8.6667	6.1956	0.0007	0.0439	***ILF3***
A_33_P3328426	0.8467	11.65	6.2152	0.0006	0.0439	***ANO10***
A_23_P406438	0.7033	8.485	6.2179	0.0006	0.0439	***SRPK2***
A_24_P551028	0.8267	8.7	6.2383	0.0006	0.0439	***SPOPL***
A_33_P3419691	0.6867	7.66	6.2473	0.0006	0.0438	***GATS***

Table VII. Probes and annotated genes with altered expression in siMAFB M-MØ.

Probe	log_2FC	Avg.Exp.	t	*p* value	adj. *p* val	Gene Symbol
A_24_P365327	0.6633	10.665	6.2769	0.0006	0.0435	***LSM14A***
A_24_P941643	0.95	6.2717	6.323	0.0006	0.043	***PLCB1***
A_24_P71700	0.7267	10.0733	6.3314	0.0006	0.043	***ZBTB47***
A_23_P43326	0.8467	9.7367	6.3683	0.0006	0.0423	***SPTLC1***
A_23_P30275	0.83	9.505	6.3895	0.0006	0.0418	***PCYOX1L***
A_33_P3225843	0.7233	9.7883	6.3947	0.0005	0.0418	***CCDC149***
A_23_P97700	0.73	13.7883	6.3996	0.0005	0.0418	***TXNIP***
A_23_P64058	0.9633	7.2217	6.4595	0.0005	0.0402	***RASGRP2***
A_23_P166408	0.9233	9.575	6.4722	0.0005	0.0402	***OSM***
A_33_P3320212	0.7267	7.37	6.5545	0.0005	0.0388	
A_33_P3423270	0.85	5.8483	6.5598	0.0005	0.0388	***TMEM40***
A_23_P90601	1.5067	11.0867	6.6362	0.0004	0.037	***STEAP3***
A_23_P143147	0.7233	7.6983	6.6624	0.0004	0.0366	***TCFL5***
A_32_P195401	0.7633	8.4017	6.6829	0.0004	0.0362	***FAM117B***
A_23_P94095	0.8233	8.045	6.7086	0.0004	0.0362	***ANKRD46***
A_23_P206733	1.49	8.5483	6.718	0.0004	0.0362	***CES1***
A_24_P645765	0.8233	7.035	6.7607	0.0004	0.0359	***KLHL42***
A_32_P56001	0.9667	7.3733	6.776	0.0004	0.0358	***CD93***
A_33_P3272209	0.8267	8.8	6.7977	0.0004	0.0358	***MFSD6***
A_33_P3334220	0.7367	7.3383	6.8096	0.0004	0.0358	***ACACB***
A_23_P28697	0.7433	8.3817	6.9147	0.0004	0.0346	***HAAO***
A_33_P3244122	0.75	12.2717	6.9463	0.0003	0.034	***HAAO***
A_24_P252996	0.86	7.29	6.9527	0.0003	0.034	***FOLR3***
A_23_P77048	0.7567	12.0583	6.9633	0.0003	0.034	***SLC25A29***
A_23_P133474	1.0367	9.9183	7.0076	0.0003	0.034	***GPX3***
A_23_P218456	0.81	10.1517	7.0444	0.0003	0.034	***ILF3***
A_32_P172864	0.7967	9.7917	7.0897	0.0003	0.0336	***FAM102B***
A_33_P3331451	0.89	6.7317	7.1271	0.0003	0.0329	***TGFBR1***
A_23_P167276	1.03	7.9417	7.1274	0.0003	0.0329	***PAQR3***
A_24_P200000	1.0833	7.305	7.1372	0.0003	0.0329	***STEAP3***
A_23_P34597	1.0533	10.6367	7.1913	0.0003	0.0329	***CDA***
A_23_P140384	1.65	6.7617	7.1956	0.0003	0.0329	***CTSG***
A_33_P3286041	1.03	7.5617	7.2714	0.0003	0.0324	***POLR3E***
A_23_P140668	0.7867	9.0867	7.4023	0.0002	0.0314	***IDH3A***
A_23_P6099	0.9667	7.0467	7.4804	0.0002	0.0311	***PLCB1***
A_33_P3222203	0.8933	10.59	7.6506	0.0002	0.0278	***OXER1***
A_33_P3330608	0.8233	13.3217	7.7763	0.0002	0.0258	***PRAM1***
A_23_P218549	1.08	6.88	7.8104	0.0002	0.0254	***EMR3***
A_33_P3394075	1.05	7.7017	7.8705	0.0002	0.0247	***RIT1***
A_23_P23171	0.9133	7.7733	7.9169	0.0002	0.0247	***AGO4***
A_23_P104692	0.8433	9.2917	7.9393	0.0002	0.0247	***PELI3***
A_23_P25503	1.02	12.4133	8.0869	0.0001	0.0236	***FNDC3A***

Table VII. Probes and annotated genes with altered expression in siMAFB M-MØ.

Probe	log_2FC	Avg.Exp.	t	*p* value	adj. *p* val	Gene Symbol
A_23_P152181	0.9667	8.7633	8.1267	0.0001	0.0236	***POLR3E***
A_23_P304356	1.56	6.6667	8.245	0.0001	0.0222	***CLEC5A***
A_24_P248053	1.2667	8.7133	8.2627	0.0001	0.0222	***TOP1MT***
A_32_P19294	1.2967	7.505	8.2685	0.0001	0.0222	***GLT1D1***
A_24_P916614	0.93	11.6717	8.2947	0.0001	0.0222	***PTBP3***
A_23_P253791	1.09	7.0783	8.3214	0.0001	0.0222	***CAMP***
A_23_P62967	0.9633	9.6417	8.468	0.0001	0.021	***DISC1***
A_33_P3241269	1.7533	12.8	8.5092	0.0001	0.0208	***CES1***
A_32_P178966	1.0833	9.565	8.5683	0.0001	0.0208	***TMEM170B***
A_33_P3343210	1.08	6.5267	8.6082	0.0001	0.0208	***SLC25A37***
A_23_P429977	1.1367	10.965	8.6294	0.0001	0.0208	***KCNQ1***
A_23_P52676	1.2233	8.6383	8.7577	0.0001	0.0204	***CATSPER1***
A_24_P32085	0.97	7.4417	8.7619	0.0001	0.0204	***MOB3B***
A_33_P3713357	1.14	10.6933	8.8421	0.0001	0.0204	***ALCAM***
A_32_P161762	1.0767	6.485	8.9201	0.0001	0.0203	***RUNX2***
A_23_P56505	1.0133	7.5833	9.1325	0.0001	0.0187	***ITGA4***
A_33_P3353816	1.04	9.3233	9.4428	0.0001	0.0165	***ITGA4***
A_23_P92842	1.1	10.0867	9.8356	0.0000	0.0149	***SAR1B***
A_23_P122852	1.36	10.5833	10.0014	0.0000	0.0141	***SMARCD3***
A_24_P64100	1.1033	7.0817	10.1625	0.0000	0.0135	***SLC25A37***
A_23_P250245	1.5933	7.6767	10.6238	0.0000	0.0115	***CD72***
A_23_P144959	1.35	6.5817	10.7674	0.0000	0.0115	***VCAN***
A_24_P196851	1.2067	10.0933	10.8934	0.0000	0.0112	***TLN1***
A_23_P91390	1.36	10.6333	10.995	0.0000	0.0112	***THBD***
A_23_P101434	1.6533	6.4733	11.0705	0.0000	0.0112	***NLRP12***
A_23_P121956	1.2267	8.09	11.3288	0.0000	0.0102	***THG1L***
A_33_P3210561	1.4367	8.3683	11.9763	0.0000	0.0088	
A_23_P304682	1.37	6.7983	12.5537	0.0000	0.0088	***EMP2***
A_23_P106682	1.51	8.7217	13.0495	0.0000	0.0086	***EMP2***
A_33_P3350863	1.4567	6.665	13.6752	0.0000	0.0076	***RETN***
A_24_P347378	1.4767	9.5383	13.8758	0.0000	0.0076	***ALOX5AP***
A_23_P21485	1.7233	8.0683	14.5693	0.0000	0.0063	***PID1***

Table VIII. Probes and annotated genes with altered expression in MCTO#1 M-MØ

Probe	log_2FC	Avg.Exp.	t	*p* value	adj.*p val*	Gene Symbol
A_24_P213161	3.26	5.555	18.1618	0.0000	0.0161	**NLRP2**
A_23_P140384	2.72	5.76	16.5142	0.0000	0.0161	**CTSG**
A_23_P136683	5.77	12.83	16.31	0.0000	0.0161	**HLA-DQB1**
A_23_P26325	3.59	7.87	15.1319	0.0000	0.0161	**CCL17**
A_23_P164773	2.82	6.32	12.3875	0.0000	0.026	**FCER2**
A_33_P3250612	2.3	5.675	12.0732	0.0000	0.0283	**MOCS1**
A_23_P3911	2.03	9.505	10.562	0.0001	0.0437	**PLXDC1**
A_23_P94819	1.735	7.8475	10.3913	0.0001	0.0438	**RPH3AL**
A_24_P165864	1.69	6.34	10.335	0.0001	0.0438	**P2RY14**
A_24_P945113	1.87	8.695	9.8538	0.0001	0.048	**ACVRL1**
A_24_P245379	1.605	6.3775	9.8033	0.0001	0.048	**SERPINB2**
A_33_P3236881	1.685	13.0325	9.0084	0.0002	0.0554	**MINOS1-NBL1**
A_33_P3424222	2.235	14.5475	9.0045	0.0002	0.0554	**HLA-DQB1**
A_23_P119222	1.72	8.685	8.7898	0.0002	0.0573	**RETN**
A_33_P3350863	1.55	10.03	8.726	0.0002	0.0583	**RETN**
A_32_P4262	1.605	7.3525	8.6265	0.0002	0.0587	**C20orf26**
A_33_P3753757	1.445	8.7675	7.8466	0.0004	0.0763	**LOC158402**
A_24_P31235	1.295	10.1275	7.655	0.0004	0.0816	**EIF5A**
A_23_P109427	1.495	9.0425	7.4833	0.0005	0.0858	**GSTT2**
A_33_P3252695	1.22	8.895	7.4711	0.0005	0.0858	**CYTL1**
A_23_P142631	1.19	8.91	7.2773	0.0005	0.0882	**FKBP1B**
A_33_P3232557	1.2	7.44	7.2659	0.0006	0.0882	**DLGAP3**
A_24_P10657	1.28	7.025	7.2572	0.0006	0.0882	**SLC44A2**
A_23_P360209	1.28	14.385	7.2572	0.0006	0.0882	**ND3**
A_33_P3281567	1.365	8.7425	6.6268	0.0009	0.1092	**CMAHP**
A_23_P400378	1.215	11.4925	6.5977	0.0009	0.1094	**GPBAR1**
A_23_P74252	1.1	8.895	6.3907	0.0010	0.1186	**LINC00339**
A_23_P10647	1.205	8.6225	6.3718	0.0011	0.1186	**CYTL1**
A_33_P3316786	1.06	7.48	6.3203	0.0011	0.1186	**DACH1**
A_23_P30666	1.085	12.6675	6.2655	0.0011	0.1186	**TNFRSF21**
A_33_P3268472	1.05	13.205	6.2566	0.0012	0.1186	**CTSC**
A_23_P4160	1.045	6.2875	6.2546	0.0012	0.1186	**NBR2**
A_23_P43276	1.11	6.125	6.2361	0.0012	0.1186	**GPR124**
A_23_P76538	1.065	13.9625	6.2234	0.0012	0.1186	**TESC**
A_23_P351467	1.215	8.6675	6.1978	0.0012	0.1186	**CMAHP**
A_23_P330461	1.35	7.595	6.1707	0.0012	0.1186	**TMC4**
A_23_P3963	1.23	9.03	6.1165	0.0013	0.122	**CDR2L**
A_33_P3412087	1.085	9.9525	6.0145	0.0014	0.128	**CCDC170**
A_33_P3330549	1.28	7.08	5.9434	0.0015	0.128	**SLC44A2**
A_33_P3283601	1.155	8.5475	5.8636	0.0016	0.1337	**LOC389033**
A_33_P3318696	1.275	7.3925	5.8228	0.0016	0.1339	**CCBL2**
A_32_P224522	1.2	7.44	5.8162	0.0016	0.1339	**SLC25A23**
A_33_P3221748	1.03	14.035	5.7867	0.0017	0.1339	**RUNX3**

Table VIII. Probes and annotated genes with altered expression in MCTO#1 M-MØ

Probe	log_2FC	Avg.Exp.	t	*p* value	adj.*p val*	Gene Symbol
A_33_P3392892	0.985	6.4525	5.7816	0.0017	0.1339	**ULK4**
A_24_P339858	3.2	5.855	5.7793	0.0017	0.1339	**C21orf90**
A_23_P218579	1.205	8.9475	5.7675	0.0017	0.1339	**GLB1L**
A_32_P36694	0.965	7.7925	5.7643	0.0017	0.1339	**JAZF1**
A_23_P19510	2.395	12.4725	5.7443	0.0017	0.1346	**HLA-DQB2**
A_24_P331560	1.62	6.59	5.7117	0.0018	0.1356	**STS**
A_23_P126735	0.985	9.5425	5.6532	0.0019	0.1369	**IL10**
A_33_P3281572	1.04	8.2	5.6359	0.0019	0.1374	**CMAHP**
A_23_P45871	0.905	8.4775	5.4937	0.0021	0.1422	**IFI44L**
A_23_P150549	1.315	7.2825	5.4787	0.0022	0.1422	**PGA3**
A_24_P379820	0.905	7.0175	5.4713	0.0022	0.1424	**ITM2C**
A_23_P160849	0.875	15.0525	5.4007	0.0023	0.1464	**FCER1G**
A_23_P44684	0.9	7.37	5.3734	0.0024	0.1486	**ECT2**
A_23_P127663	0.935	6.7925	5.3565	0.0024	0.1501	**PRRG4**
A_23_P205489	1.065	10.5925	5.3383	0.0024	0.1503	**SLC7A8**
A_33_P3289045	1.9	7.265	5.2628	0.0026	0.154	**GSTT2B**
A_24_P402690	0.88	10.32	5.2436	0.0027	0.1558	**ITM2C**
A_23_P165989	0.865	6.8375	5.2119	0.0027	0.1566	**NEURL2**
A_23_P29303	0.915	6.7225	5.2072	0.0027	0.1566	**RRP7A**
A_23_P140563	1.235	7.6975	5.2026	0.0028	0.1566	**TTC23**
A_33_P3255677	0.97	6.685	5.2003	0.0028	0.1566	
A_33_P3260053	1.28	6.385	5.1752	0.0028	0.1581	**AIF1L**
A_23_P326893	0.985	6.0975	5.1269	0.0029	0.1593	**CCDC151**
A_23_P74088	1.715	6.2375	5.1102	0.0030	0.1607	**MMP23B**
A_24_P397294	0.935	11.5475	5.1052	0.0030	0.1607	**LTC4S**
A_33_P3387696	1.21	11.065	5.1044	0.0030	0.1607	**TMBIM4**
A_23_P217917	0.98	9.435	5.0824	0.0031	0.1621	**GSTM4**
A_33_P3214943	0.92	7.85	5.0804	0.0031	0.1621	**SPOCK2**
A_24_P243749	0.905	8.2625	5.0748	0.0031	0.1621	**PDK4**
A_24_P287043	0.86	13.105	5.0535	0.0032	0.1638	**IFITM2**
A_23_P119196	0.83	10.545	4.9885	0.0033	0.1705	**KLF2**
A_23_P252193	1.02	8.125	4.9731	0.0034	0.1705	**ITGA9**
A_23_P423309	1.355	7.8275	4.8863	0.0037	0.1762	**PCDH12**
A_23_P254842	1.055	9.9175	4.8768	0.0037	0.1765	**HDHD1**
A_23_P347632	0.865	11.3025	4.8364	0.0038	0.1784	**MTSS1**
A_24_P354724	0.915	7.9975	4.8259	0.0039	0.1784	**TAGAP**
A_33_P3276207	1	7.78	4.8155	0.0039	0.1784	**NXPE3**
A_23_P55356	0.8	8.98	4.8049	0.0040	0.1796	**VMO1**
A_23_P12733	0.78	7.38	4.8017	0.0040	0.1796	**H2AFY2**
A_33_P3395081	0.86	6.77	4.787	0.0040	0.1797	**ACSM5**
A_23_P217269	0.785	16.1425	4.7652	0.0041	0.1806	**VSIG4**
A_23_P101093	1.005	7.2725	4.7601	0.0041	0.1806	**COPZ2**

Table VIII. Probes and annotated genes with altered expression in MCTO#1 M-MØ

Probe	log_2FC	Avg.Exp.	t	*p* value	adj.*p val*	Gene Symbol
A_23_P318284	0.845	10.1525	4.7578	0.0041	0.1806	**GPD1L**
A_24_P382187	0.995	8.2075	4.7107	0.0043	0.1836	**IGFBP4**
A_23_P357760	1.3	7.095	4.6663	0.0045	0.1881	**ARSD**
A_24_P129588	0.95	7.3	4.6441	0.0046	0.1902	**FFAR4**
A_33_P3423570	0.77	10.98	4.6387	0.0046	0.1902	**METRN**
A_23_P256561	0.77	8.16	4.6263	0.0047	0.1902	**TLR6**
A_23_P371765	0.98	6.655	4.6258	0.0047	0.1902	**SPATC1L**
A_24_P373768	0.95	7.29	4.6236	0.0047	0.1902	**GIPR**
A_23_P94754	0.83	6.595	4.6042	0.0048	0.1909	**TNFSF15**
A_33_P3358957	0.81	6.365	4.5993	0.0048	0.1909	**PAPL**
A_23_P41217	1.65	9.09	4.5992	0.0048	0.1909	**CD200R1**
A_33_P3287611	0.855	7.7025	4.5954	0.0048	0.191	**KRT3**
A_23_P35444	1.165	6.4575	4.5847	0.0049	0.1912	**INA**
A_33_P3405068	-0.79	6.625	-4.5768	0.0049	0.1912	**NAV1**
A_23_P46928	-0.835	8.8475	-4.5769	0.0049	0.1912	**PFKP**
A_33_P3283828	-0.755	9.5325	-4.5769	0.0049	0.1912	**CCDC154**
A_23_P393401	-0.78	9.005	-4.5776	0.0049	0.1912	**PDXDC2P**
A_24_P96961	-0.745	8.4175	-4.5822	0.0049	0.1912	**SPSB1**
A_23_P254271	-0.87	11.145	-4.6034	0.0048	0.1909	**TUBB6**
A_33_P3214105	-0.915	6.8975	-4.6123	0.0048	0.1907	**ATF3**
A_24_P39639	-0.81	7.195	-4.6131	0.0048	0.1907	**EXOSC6**
A_33_P3223660	-0.865	7.2375	-4.6147	0.0047	0.1907	**LINC00476**
A_23_P161076	-0.975	6.5525	-4.6295	0.0047	0.1902	**CD2**
A_23_P106362	-0.88	9.385	-4.6335	0.0047	0.1902	**AQP9**
A_23_P25674	-0.785	6.6825	-4.6343	0.0047	0.1902	**CKB**
A_23_P213102	-0.92	7.51	-4.6359	0.0047	0.1902	**PALLD**
A_33_P3321781	-1.025	9.7025	-4.6418	0.0046	0.1902	**FLJ44342**
A_24_P673063	-1.21	10.68	-4.679	0.0045	0.1864	**FABP5**
A_23_P133133	-0.95	8.945	-4.6825	0.0044	0.1863	**ALPK1**
A_23_P30805	-0.78	10	-4.688	0.0044	0.186	**HIST1H4J**
A_23_P133293	-1.16	9.36	-4.695	0.0044	0.1853	**MCTP1**
A_24_P241183	-0.78	7.88	-4.6974	0.0044	0.1853	**CLEC2D**
A_33_P3362891	-0.795	10.5925	-4.7116	0.0043	0.1836	**HNRNPA2B1**
A_23_P40956	-1.475	8.2125	-4.7143	0.0043	0.1836	**GHRL**
A_33_P3245539	-0.855	6.8525	-4.7288	0.0043	0.1822	**PNMA1**
A_24_P145316	-0.795	7.9875	-4.7301	0.0043	0.1822	**DTNBP1**
A_23_P212497	-1.005	6.2075	-4.7404	0.0042	0.1813	**ACAD11**
A_24_P401870	-0.805	9.1975	-4.7463	0.0042	0.1809	**C9orf139**
A_23_P137665	-0.8	13.355	-4.7498	0.0042	0.1809	**CHI3L1**
A_33_P3268564	-1.04	8.77	-4.7537	0.0042	0.1807	**NCK2**
A_23_P157875	-0.885	14.1625	-4.7592	0.0041	0.1806	**FCN1**
A_23_P143374	-0.8	9.05	-4.77	0.0041	0.1806	**NINL**

Table VIII. Probes and annotated genes with altered expression in MCTO#1 M-MØ

Probe	log_2FC	Avg.Exp.	t	*p* value	adj.*p val*	Gene Symbol
A_33_P3279708	-0.795	9.7575	-4.7709	0.0041	0.1806	**RNU2-1**
A_33_P3216890	-1.165	7.0675	-4.7717	0.0041	0.1806	**PAG1**
A_33_P3718269	-1.07	8.495	-4.7883	0.0040	0.1797	**MIR146A**
A_33_P3296707	-0.935	6.9375	-4.7903	0.0040	0.1797	**FAM127C**
A_23_P200728	-0.875	12.9425	-4.7908	0.0040	0.1797	**FCGR3A**
A_33_P3298024	-0.795	10.1375	-4.8161	0.0039	0.1784	**ABCC3**
A_33_P3235330	-0.815	6.7075	-4.8176	0.0039	0.1784	**MTMR3**
A_33_P3645805	-0.845	12.0025	-4.8233	0.0039	0.1784	
A_33_P3390107	-1.695	9.9475	-4.8309	0.0039	0.1784	**RNA18S5**
A_23_P126486	-1.26	9.455	-4.8324	0.0039	0.1784	**CROCCP2**
A_32_P108655	-1.28	7.04	-4.834	0.0039	0.1784	**AK4**
A_33_P3324884	-0.845	8.1275	-4.8497	0.0038	0.1781	**MICAL1**
A_23_P394064	-0.945	6.9775	-4.8557	0.0038	0.1777	**PTRF**
A_33_P3269069	-1.12	7.49	-4.8629	0.0038	0.1771	**HS2ST1**
A_23_P102000	-0.825	13.1275	-4.8642	0.0037	0.1771	**CXCR4**
A_33_P3531828	-0.915	8.9375	-4.8738	0.0037	0.1765	**LARS**
A_33_P3254380	-0.95	7.26	-4.8832	0.0037	0.1762	**SLC9A7**
A_23_P14515	-0.86	6.93	-4.8832	0.0037	0.1762	**ACOT4**
A_23_P12554	-0.795	9.1375	-4.8863	0.0037	0.1762	**PKD2L1**
A_33_P3308481	-1	6.465	-4.8885	0.0037	0.1762	**HYMAI**
A_32_P83465	-0.84	15.04	-4.9032	0.0036	0.176	**NBPF10**
A_33_P3225983	-0.865	7.5725	-4.905	0.0036	0.176	
A_24_P67898	-0.95	7.8	-4.9366	0.0035	0.1719	**MGEA5**
A_32_P86763	-0.92	6.165	-4.9415	0.0035	0.1718	**TGM2**
A_33_P3338440	-0.95	6.885	-4.9428	0.0035	0.1718	
A_33_P3226542	-1.015	9.3775	-4.9471	0.0035	0.1718	**SNORD3B-1**
A_33_P3255290	-1.34	8.655	-4.9563	0.0034	0.1713	**JAKMIP2**
A_23_P15146	-1.73	7.56	-4.9581	0.0034	0.1713	**IL32**
A_33_P3372526	-0.835	6.2625	-4.9681	0.0034	0.1706	**MDH1B**
A_23_P98350	-1.18	8.455	-4.9737	0.0034	0.1705	**BIRC3**
A_33_P3336760	-0.84	6.775	-4.9743	0.0034	0.1705	**ABCB4**
A_23_P125748	-1.025	8.1725	-4.9848	0.0034	0.1705	**ZMAT1**
A_23_P427760	-0.995	7.8275	-5.0085	0.0033	0.1681	**PIWIL4**
A_23_P54918	-0.84	8.62	-5.0151	0.0033	0.1677	**LDHD**
A_33_P3567967	-1.22	10.825	-5.0374	0.0032	0.165	**FLJ11292**
A_23_P321703	-1.275	9.1625	-5.0451	0.0032	0.1644	**BCL2A1**
A_33_P3264612	-0.94	9.01	-5.0692	0.0031	0.1621	**TPCN2**
A_33_P3219572	-0.885	7.1225	-5.0731	0.0031	0.1621	
A_33_P3713357	-1.06	9.165	-5.0925	0.0030	0.1618	**ALCAM**
A_23_P138137	-1.195	8.7075	-5.1311	0.0029	0.1593	**OMA1**
A_33_P3393766	-1.485	8.6475	-5.1348	0.0029	0.1593	**C17orf96**
A_23_P47682	-0.88	7.58	-5.1367	0.0029	0.1593	**NRIP3**

Table VIII. Probes and annotated genes with altered expression in MCTO#1 M-MØ

Probe	log_2FC	Avg.Exp.	t	*p* value	adj.*p val*	Gene Symbol
A_33_P3397795	-0.86	8.3	-5.1516	0.0029	0.1583	**PCNXL4**
A_23_P210131	-0.965	7.0725	-5.1564	0.0029	0.1583	
A_33_P3381943	-1.4	7.095	-5.16	0.0029	0.1583	**DMTF1**
A_33_P3413962	-0.945	6.3775	-5.1655	0.0028	0.1583	**PFKP**
A_33_P3228102	-0.97	8.34	-5.1715	0.0028	0.1581	**NPHP3**
A_23_P56590	-0.855	9.3575	-5.1726	0.0028	0.1581	**C1D**
A_23_P500271	-0.965	13.9075	-5.1922	0.0028	0.1571	**IRF5**
A_23_P345942	-0.955	9.0825	-5.2115	0.0027	0.1566	**NDUFAF2**
A_23_P206806	-0.87	9.09	-5.2132	0.0027	0.1566	**ITGAL**
A_23_P392942	-0.92	9.47	-5.2239	0.0027	0.1566	**MSR1**
A_33_P3357580	-0.855	6.6025	-5.2332	0.0027	0.1566	**MRTO4**
A_24_P152649	-0.89	6.195	-5.2618	0.0026	0.154	**LOC644189**
A_24_P283341	-0.895	10.4025	-5.2667	0.0026	0.154	**MICAL1**
A_33_P3325558	-0.935	8.5175	-5.2894	0.0026	0.1523	**RABGAP1L**
A_24_P68908	-1.075	8.0775	-5.2957	0.0025	0.1521	**LOC344887**
A_23_P211680	-0.89	7.745	-5.3032	0.0025	0.1518	**MLC1**
A_23_P203475	-1.43	9.845	-5.3115	0.0025	0.1513	**PRKCDBP**
A_23_P63209	-1.495	8.3475	-5.3124	0.0025	0.1513	**HSD11B1**
A_33_P3413701	-1.21	10.16	-5.3142	0.0025	0.1513	**ERAP1**
A_23_P398491	-1.29	6.395	-5.334	0.0025	0.1503	**C15orf57**
A_33_P3327956	-0.9	7.9	-5.3348	0.0025	0.1503	**ZNF605**
A_23_P35066	-0.93	6.345	-5.3482	0.0024	0.1503	**SNX7**
A_23_P132956	-1.14	9.03	-5.38	0.0024	0.1484	**UCHL1**
A_23_P103672	-0.95	7.185	-5.4202	0.0023	0.1447	**NES**
A_23_P97141	-1.06	7.03	-5.4209	0.0023	0.1447	**RGS1**
A_32_P128258	-1.14	6.615	-5.4443	0.0022	0.143	**SIGLEC17P**
A_23_P22352	-1.2	9.865	-5.4525	0.0022	0.1427	**FRMD4A**
A_33_P3399571	-1.635	10.2725	-5.4577	0.0022	0.1427	**VNN1**
A_33_P3233906	-1.055	6.5925	-5.4612	0.0022	0.1427	**RAMP1**
A_24_P136551	-0.91	7.135	-5.484	0.0022	0.1422	**NPLOC4**
A_23_P85693	-0.995	8.8375	-5.4845	0.0022	0.1422	**GBP2**
A_33_P3368750	-1.36	6.155	-5.512	0.0021	0.1409	**PAQR5**
A_23_P414913	-0.915	12.3075	-5.5132	0.0021	0.1409	**GLIPR2**
A_33_P3265956	-1.02	9.3	-5.5275	0.0021	0.1404	**CBFA2T2**
A_23_P146456	-0.94	7.845	-5.5307	0.0021	0.1404	**CTSV**
A_33_P3336527	-1.51	7.86	-5.5349	0.0021	0.1404	**PDXDC1**
A_23_P414958	-0.945	9.1225	-5.5468	0.0020	0.1402	**PLXNC1**
A_33_P3275255	-0.95	7.58	-5.547	0.0020	0.1402	
A_24_P366509	-0.925	6.4325	-5.5511	0.0020	0.1402	**PIK3R6**
A_24_P351283	-0.925	6.4225	-5.5622	0.0020	0.1402	**MREG**
A_24_P238143	-0.915	8.2375	-5.5696	0.0020	0.1402	**LRRC37A2**
A_23_P108948	-1.2	8.26	-5.572	0.0020	0.1402	**MREG**

Table VIII. Probes and annotated genes with altered expression in MCTO#1 M-MØ

Probe	log_2FC	Avg.Exp.	t	*p* value	adj.*p val*	Gene Symbol
A_23_P75430	-0.94	10.99	-5.6048	0.0019	0.1376	**SMCO4**
A_33_P3287388	-1.215	9.1225	-5.6098	0.0019	0.1376	
A_23_P52207	-1.71	6.48	-5.6113	0.0019	0.1376	**BAMBI**
A_24_P416997	-0.915	7.4875	-5.6239	0.0019	0.1375	**APOL3**
A_33_P3361422	-1.03	14.355	-5.6309	0.0019	0.1374	**CYP27A1**
A_33_P3244931	-0.92	14.67	-5.6477	0.0019	0.1369	**DBI**
A_33_P3338121	-1.055	7.7875	-5.6553	0.0019	0.1369	**LAMB3**
A_33_P3514859	-1.8	6.98	-5.664	0.0019	0.1369	**LOC100506342**
A_23_P34915	-1.255	10.2675	-5.6684	0.0018	0.1369	**ATF3**
A_23_P99253	-1.31	6.625	-5.6799	0.0018	0.1369	**LIN7A**
A_23_P50508	-0.995	10.7975	-5.6829	0.0018	0.1369	**PLA2G4C**
A_33_P3345036	-0.92	6.82	-5.6835	0.0018	0.1369	**POMC**
A_23_P90626	-1.165	9.7025	-5.7109	0.0018	0.1356	**CYTIP**
A_23_P44724	-1.12	6.78	-5.7277	0.0018	0.1353	**CSRP2**
A_23_P129903	-1.185	7.5575	-5.7404	0.0017	0.1346	**TRIM16L**
A_24_P161293	-0.98	14.05	-5.7605	0.0017	0.1339	
A_23_P201808	-1.54	9.405	-5.7636	0.0017	0.1339	**PPAP2B**
A_33_P3273584	-0.965	7.5475	-5.7758	0.0017	0.1339	**SCARNA2**
A_33_P3404097	-1.25	12.955	-5.7834	0.0017	0.1339	**PGM5P2**
A_24_P931443	-0.95	10.195	-5.7876	0.0017	0.1339	**GPR68**
A_23_P384044	-1.06	6.795	-5.8191	0.0016	0.1339	**CNIH3**
A_23_P103110	-1.04	6.92	-5.8497	0.0016	0.1339	**MAFF**
A_32_P168464	-1.04	7.575	-5.8965	0.0015	0.131	**CASK**
A_23_P111804	-1.02	9.455	-5.9333	0.0015	0.128	**PARP12**
A_23_P76488	-0.995	11.6925	-5.9357	0.0015	0.128	**EMP1**
A_23_P210690	-1.005	10.7825	-5.9446	0.0015	0.128	**TRIB3**
A_33_P3382105	-1.085	9.3925	-5.9472	0.0015	0.128	
A_33_P3290443	-1.065	12.5575	-5.9547	0.0015	0.128	**SCARNA9**
A_23_P59877	-1.26	11.42	-5.9586	0.0015	0.128	**FABP5**
A_24_P248240	-1.075	6.7875	-5.9795	0.0014	0.128	**SYT11**
A_23_P426021	-1.025	7.3875	-5.9859	0.0014	0.128	**SEL1L3**
A_33_P3272231	-0.99	6.955	-5.9944	0.0014	0.128	**MFSD2A**
A_23_P408094	-1.015	9.0175	-5.9999	0.0014	0.128	**MXD1**
A_33_P3246833	-1.01	13.88	-6.0281	0.0014	0.128	**IL1RN**
A_33_P3244998	-1.035	14.1225	-6.075	0.0013	0.1244	**ODF2L**
A_24_P173754	-0.985	6.6925	-6.0797	0.0013	0.1244	**C1orf21**
A_23_P78037	-1.005	6.0125	-6.1301	0.0013	0.1216	**CCL7**
A_23_P50946	-1.205	8.8425	-6.1736	0.0012	0.1186	**RAMP1**
A_32_P356316	-1.155	13.0675	-6.1814	0.0012	0.1186	**HLA-DOA**
A_23_P125078	-1.075	11.7075	-6.1924	0.0012	0.1186	**SLC26A11**
A_33_P3333982	-2.345	13.2925	-6.1958	0.0012	0.1186	**PDE4DIP**
A_23_P146325	-1.565	7.4025	-6.2344	0.0012	0.1186	**ASAP1-IT1**

Table VIII. Probes and annotated genes with altered expression in MCTO#1 M-MØ

Probe	log_2FC	Avg.Exp.	t	*p* value	adj.*p val*	Gene Symbol
A_33_P3267263	-1.105	9.9775	-6.2511	0.0012	0.1186	**RNVU1-18**
A_23_P62764	-1.12	6.57	-6.274	0.0011	0.1186	**CCDC28B**
A_33_P3289865	-1.075	7.0475	-6.2818	0.0011	0.1186	**PLCL1**
A_23_P206501	-1.025	7.2225	-6.2824	0.0011	0.1186	**CLEC18B**
A_33_P3371305	-1.585	7.3025	-6.2882	0.0011	0.1186	**LOC644090**
A_23_P315364	-1.045	10.4025	-6.3049	0.0011	0.1186	**CXCL2**
A_33_P3454679	-1.395	7.1125	-6.3246	0.0011	0.1186	
A_23_P103932	-1.23	12.65	-6.3287	0.0011	0.1186	**FGR**
A_33_P3366120	-1.18	11.155	-6.3312	0.0011	0.1186	**FLNA**
A_23_P46936	-1.45	9.625	-6.3491	0.0011	0.1186	**EGR2**
A_33_P3342443	-1.205	9.5975	-6.3586	0.0011	0.1186	**RASA4B**
A_33_P3394140	-1.255	8.4225	-6.4173	0.0010	0.1186	**ZMIZ1-AS1**
A_23_P50678	-1.235	7.2075	-6.4217	0.0010	0.1186	**MATK**
A_23_P342131	-1.075	12.1825	-6.5435	0.0009	0.111	**CYB561A3**
A_33_P3432961	-1.215	6.1525	-6.5549	0.0009	0.111	**LOC401320**
A_33_P3354604	-2.245	6.6175	-6.5665	0.0009	0.111	**CCL4L2**
A_33_P3231414	-1.23	10.35	-6.5995	0.0009	0.1094	**LILRB1**
A_23_P326142	-1.18	6.13	-6.6255	0.0009	0.1092	**SND1-IT1**
A_23_P82929	-1.705	5.9875	-6.6267	0.0009	0.1092	**NOV**
A_24_P807031	-1.09	6.895	-6.6405	0.0009	0.1092	**ATP6AP1L**
A_24_P228130	-1.635	9.8475	-6.6616	0.0008	0.1092	**CCL3L3**
A_33_P3415191	-2.135	6.0525	-6.7043	0.0008	0.1079	**ATP8B1**
A_24_P59667	-1.185	10.7425	-6.7196	0.0008	0.1078	**JAK3**
A_24_P370472	-1.225	15.0225	-6.779	0.0008	0.1042	**HLA-DRB4**
A_33_P3269803	-1.36	6.195	-6.8258	0.0008	0.1017	**CLSTN3**
A_23_P420610	-1.19	9.11	-6.8371	0.0007	0.1017	**FCHO2**
A_33_P3363091	-1.19	7.325	-6.8644	0.0007	0.1009	**VAC14**
A_23_P55270	-2.295	8.8025	-6.8656	0.0007	0.1009	**CCL18**
A_23_P17914	-2.09	6.18	-6.8886	0.0007	0.1009	**PNPLA3**
A_24_P286114	-1.2	11.625	-6.9285	0.0007	0.0994	**SLC1A3**
A_23_P123853	-1.245	6.6775	-6.945	0.0007	0.0993	**CCL19**
A_23_P40847	-1.13	6.83	-6.9784	0.0007	0.098	**CHST2**
A_23_P398566	-1.41	7.105	-7.0751	0.0006	0.0925	**NR4A3**
A_23_P26024	-1.395	10.1325	-7.1126	0.0006	0.0911	**C15orf48**
A_23_P376557	-1.49	9.695	-7.1476	0.0006	0.0899	**MMP25**
A_23_P354805	-1.17	7.33	-7.1849	0.0006	0.0885	**KLF12**
A_23_P48056	-1.65	6.945	-7.2044	0.0006	0.0883	**CKAP4**
A_23_P79518	-1.205	7.6475	-7.2122	0.0006	0.0883	**IL1B**
A_33_P3364869	-1.355	7.4175	-7.2289	0.0006	0.0883	**NAMPT**
A_23_P146233	-1.275	11.0075	-7.2559	0.0006	0.0882	**LPL**
A_23_P74609	-1.31	6.315	-7.2711	0.0006	0.0882	**G0S2**
A_33_P3337896	-1.74	8.63	-7.2852	0.0005	0.0882	

Table VIII. Probes and annotated genes with altered expression in MCTO#1 M-MØ

Probe	log_2FC	Avg.Exp.	t	*p* value	adj.*p val*	Gene Symbol
A_33_P3342111	-2.415	6.4425	-7.3272	0.0005	0.0882	**ZNF169**
A_23_P165598	-1.85	5.9	-7.3605	0.0005	0.0882	**DAPL1**
A_23_P104464	-1.285	10.6025	-7.4573	0.0005	0.0858	**ALOX5**
A_33_P3286774	-1.245	6.4725	-7.4915	0.0005	0.0858	
A_33_P3474859	-1.405	7.8575	-7.4956	0.0005	0.0858	**LINC00537**
A_23_P8640	-1.265	6.3975	-7.5265	0.0005	0.0858	**GPER1**
A_33_P3267799	-1.25	12.87	-7.6762	0.0004	0.0816	**LILRB4**
A_33_P3323298	-1.84	8.55	-7.6815	0.0004	0.0816	**JUN**
A_33_P3280502	-1.735	7.1125	-7.7923	0.0004	0.0779	
A_33_P3412900	-1.38	7.48	-7.8736	0.0004	0.0761	**CBLN3**
A_24_P166663	-1.65	8.695	-7.9151	0.0004	0.0753	**CDK6**
A_23_P150693	-1.725	6.0975	-7.9271	0.0004	0.0753	**FJX1**
A_32_P61684	-1.475	7.4525	-7.9619	0.0004	0.0753	**PAG1**
A_33_P3296181	-1.66	8.615	-8.1221	0.0003	0.0692	**CCL3L3**
A_23_P209954	-1.6	6.11	-8.1237	0.0003	0.0692	**GNLY**
A_33_P3242543	-1.435	6.8425	-8.2866	0.0003	0.0646	**MAOA**
A_23_P42718	-3.455	7.3125	-8.2964	0.0003	0.0646	**NFE2L3**
A_33_P3234697	-1.39	10.675	-8.3486	0.0003	0.0643	**LXN**
A_33_P3405424	-1.965	13.0125	-8.4373	0.0003	0.062	**IL4I1**
A_23_P208182	-2.05	6.56	-8.4805	0.0003	0.0615	**SIGLEC10**
A_23_P57667	-1.425	11.2175	-8.5177	0.0002	0.0612	**PLXNA1**
A_33_P3233645	-1.755	9.5225	-8.6184	0.0002	0.0587	**MT1G**
A_33_P3376821	-1.64	5.85	-8.6776	0.0002	0.0587	**GZMA**
A_23_P211561	-1.435	8.5275	-8.8385	0.0002	0.0568	**MEI1**
A_23_P134176	-1.635	13.2025	-8.9076	0.0002	0.0557	**SOD2**
A_33_P3265016	-1.53	7.625	-8.9534	0.0002	0.0554	**PEX6**
A_23_P165624	-1.63	7.405	-8.991	0.0002	0.0554	**TNF-αIP6**
A_24_P299685	-2.045	6.3025	-9.1168	0.0002	0.0551	**PDPN**
A_33_P3342628	-1.57	6.555	-9.1412	0.0002	0.0551	**HES4**
A_23_P42144	-1.86	8.635	-9.344	0.0002	0.0509	**PEX6**
A_33_P3229918	-1.625	7.9125	-9.4481	0.0001	0.0493	**PTCRA**
A_33_P3367850	-2.235	7.0575	-9.5189	0.0001	0.0486	**CHRM4**
A_23_P138541	-2.115	7.1525	-9.5419	0.0001	0.0486	**AKR1C3**
A_33_P3368313	-1.94	8.445	-9.6121	0.0001	0.0486	**MT1H**
A_23_P44421	-1.77	7.535	-9.6871	0.0001	0.048	**HTRA4**
A_33_P3398912	-1.68	11.1	-9.6909	0.0001	0.048	**SLC2A6**
A_32_P187617	-2.28	7.28	-9.7278	0.0001	0.048	**TDRD3**
A_24_P355145	-1.84	6.66	-9.7714	0.0001	0.048	**DNAJC5B**
A_33_P3316273	-1.84	12.945	-9.8202	0.0001	0.048	**CCL3**
A_23_P116694	-1.88	16.005	-10.241	0.0001	0.0444	**RPS26**
A_33_P3242623	-3.005	7.9875	-10.3906	0.0001	0.0438	**SLC7A11**

Table VIII. Probes and annotated genes with altered expression in MCTO#1 M-MØ

Probe	log_2FC	Avg.Exp.	t	*p* value	adj.*p val*	Gene Symbol
A_32_P206839	-2.035	7.9875	-10.6618	0.0001	0.0433	**LOC100288911**
A_23_P122724	-2.13	11.995	-10.7029	0.0001	0.0433	**VNN2**
A_24_P233786	-1.995	9.7525	-11.3534	0.0001	0.0339	**FAM129A**
A_33_P3280157	-2.065	6.0675	-11.566	0.0001	0.0322	**SNORD116-19**
A_32_P105083	-2.135	7.2775	-11.7948	0.0000	0.0304	**FTCDNL1**
A_33_P3286157	-2.22	10.475	-12.7549	0.0000	0.0236	**TNFRSF4**
A_24_P353638	-2.125	11.3025	-12.8211	0.0000	0.0236	**SLAMF7**
A_23_P140290	-2.65	8.375	-13.4742	0.0000	0.0199	**RTN1**
A_24_P289404	-2.195	13.3825	-13.5291	0.0000	0.0199	**RPS26**
A_33_P3401902	-3.835	5.4775	-13.7896	0.0000	0.0199	**ANKRD20A2**
A_24_P49597	-2.29	9.03	-13.8329	0.0000	0.0199	
A_23_P252082	-2.315	12.5025	-13.9486	0.0000	0.0199	**TMEM176A**
A_33_P3351180	-2.63	5.99	-15.0554	0.0000	0.0161	
A_33_P3346327	-2.525	6.3825	-15.1127	0.0000	0.0161	**KGFLP1**
A_23_P23639	-2.635	7.1775	-15.123	0.0000	0.0161	**MCOLN2**
A_23_P157007	-2.68	12.96	-15.4975	0.0000	0.0161	**TMEM176B**
A_24_P852756	-3.5	10.265	-20.5929	0.0000	0.0111	**HLA-DQA2**
A_24_P281395	-3.62	7.675	-21.0311	0.0000	0.0111	
A_23_P152605	-5.43	6.58	-21.4537	0.0000	0.0111	**GSDMA**

DISCUSSION

Macrophages exhibit a huge phenotypic and functional heterogeneity (**Figure 1**, **Table I**). The macrophage ability to regulate development, homeostasis and repair is tissue-specific, a feature that reflects the existence of tissue-specific transcriptional signatures shaped by the local microenvironment [21; 25; 49; 63; 163]. This functional heterogeneity of macrophages is also evidenced by their capability to both initiating and resolving inflammation [28; 30; 32; 33]. Deregulation of macrophage functions leads to the onset of pathology [74] and, therefore, the determination of the molecular basis of macrophage functional heterogeneity should pave the way for the development of tissue-specific therapies for chronic inflammatory disorders [164]. In fact, numerous current clinical trials target either macrophages or the factors that directly regulate their polarization state [51; 164]. Further refinement and improvement of these trials require a detailed knowledge of the molecular mechanisms underlying macrophage polarization and function.

This PhD thesis addresses the study of the transcriptional profile of human macrophages that have been primed with M-CSF under homeostatic, pathologic and activating conditions. We have determined the transcriptome of M-MØ after a short-term exposure to activating agents (TLR ligands), and describe a novel gene set that exclusively identifies human IL-10-producing activated macrophages both in vitro and in vivo. The activated-M-MØ gene set includes growth factors (e.g., BMP6, PDGFA), signaling molecules (e.g., SOCS2) and chemokines (e.g., CCL19), whose co-expression is observed in vivo and depends on stimulus-induced phosphorylation of ERK and p38MAPK. Furthermore, we have described the whole range of MAFB-dependent genes in IL-10-producing anti-inflammatory M-MØ. The analysis of the MAFB-dependent gene set, combined with the gene signature of macrophages derived from MCTO patients, has allowed us to demonstrate that the MAFB transcription factor controls the acquisition of the transcriptional signature and effector functions that characterize anti-inflammatory human macrophages both *in vivo* and *in vitro*.

Human M-MØ activation

Several recent reports have demonstrated the validity of the “spectrum model” of macrophage polarization [28; 72], which implies that macrophages in tissues (tissue-resident and incoming) can display a wide array of activation states whose acquisition is ultimately driven by the integration of signals from surrounding extracellular stimuli, cytokines and factors controlling macrophage differentiation [74; 77]. However, the analysis of the transcriptional macrophage heterogeneity and the various macrophage activation states [72; 75; 95; 165] have been mainly adressed on mouse tissue-resident cells

and on macrophages primed towards the pro-inflammatory side, mostly after long-term exposure to activating stimuli [72]. Therefore, it is of utmost importance to determine the factors that underlie human macrophage heterogeneity under homeostatic and pathological conditions and to define the transcriptional basis of other alternative modes of human macrophage activation.

Nevi are very common bening tumors of melanocytes [166-168]. Nevi and mostly diplastic nevi are risk factors for the development of melanoma, as well as familial history and ultra-violet radiation [167]. Even though nevi are considered as risk factors, the development of melanoma from a diplastic nevus rarely occurs [167]. The diagnosis of melanocytic lesions depends on semiquantitative observations of five different features: assymetry, border irregularity, color, diameter and evolution. Indeed, according to these parameters, benign diplastic nevi usually exhibit melanoma features and may lead to misdiagnosis [166-168], what calls for additional studies to establish clearer criteria for recognizing high-risk lesions. Expression of proteins encoded by the activated-M-MØ gene set has been found in macrophages in gut (colon submucosa), skin, nevus and melanoma. The expression of the activated-M-MØ gene set in colon and skin CD163$^+$ macrophages might be related to the fact that, unlike other tissues, resident macrophages in colon and skin are replenished by monocyte-derived macrophages [7; 74; 169]. In the case of nevi, the co-expression of the four proteins CCL19, SOCS2, BMP6 and PDGFA suggests that, like TAM [161; 170], macrophages in nevi might exhibit an anti-inflammatory (trophic and immune-regulatory) profile. Although no detailed phenotypic characterization of macrophages within nevi has yet been reported, it is posible that the population of proliferating melanocytes in nevi might also skew the polarization of surrounding macrophages towards the anti-inflammatory/trophic side. Alternatively, melanocytic nevi display several properties of senescent cells (activated BRAF expression, proliferative arrest, and expression of p16INK4A and senescence-associated acidic β-galactosidase) [171], whose clearance is executed by macrophages both during development [172;173] and within tumors [174;175]. Since senescent cells release the alarmin HMGB1 [176], a ligand for TLR2, TLR4 and TLR9 [177; 178], it is tempting to speculate that the expression of the activated M-MØ gene signature in CD163$^+$ macrophages in nevi is driven by senescent melanocyte-derived HMGB1. This hypothesis is in line with the recent demonstration that HMGB1 drives IL-10 production in M-CSF+IL-4-polarized mouse macrophages and that low HMGB1 expression correlates with low levels of CD163$^+$ cells and absent IL-10 expression in human nevi [179].

The presence of the *CCL19* and *SOCS2* genes within the activated-M-MØ gene set, and their exclusive expression in IL-10-producing human macrophages, is specially worth noting as they might significantly contribute to the immunosuppressive

and anti-inflammatory actions of activated M-MØ. *CCL19* encodes a ligand for CCR7 [180], the chemokine receptor that determines T lymphocyte recirculation and dendritic cell migration into lymph nodes [181]. Although the two known CCR7 ligands (CCL19 and CCL21) are equally capable of promoting intracellular signaling, only CCL19 binding to CCR7 leads to receptor desensitization [182-185]. Therefore, CCL19 produced by activated M-CSF-primed macrophages might impair emigration of dendritic cells and T lymphocytes from tissues towards the lymph nodes, thus inhibiting the generation of immune responses. This activity would be compatible with the immunoregulatory (IL-10-producing) ability of activated M-CSF-dependent macrophages. Besides, since both GM-MØ and M-MØ upregulate CCR7 upon LPS stimulation but CCL19 is only produced by LPS-stimulated M-MØ, this differential expression might constitute an autocrine mechanism for preventing CCR7-dependent anti-inflammatory macrophage motility and emigration from inflamed tissues.

Regarding *SOCS2*, which encodes the Suppressor of Cytokine Signalling 2 (SOCS2) protein [186], its differential regulation in GM-MØ and M-MØ might contribute to the distinct cytokine and gene profile of both macrophage subtypes under resting and activated conditions. In agreement with its STAT5-mediated GM-CSF inducibility [186], *SOCS2* mRNA levels are higher in GM-MØ than in M-MØ (**Table III**). However, although *SOCS2* is upregulated after TLR activation in human monocyte-derived dendritic cells [147], its expression is greatly upregulated by LPS only in M-MØ. In fact, LPS-activated M-MØ exhibit significantly much higher levels of *SOCS2* than GM-MØ or LPS-activated GM-MØ (**Table III**). This is particularly relevant because SOCS2 acts as an anti-inflammatory factor that promotes TRAF6 degradation [187], inhibits TLR4 signaling in macrophages [146], mediates the anti-inflammatory actions of lipoxins [188; 189] and Interferon type I [145], and its levels are diminished in inflammatory pathologies [190]. Therefore, the higher levels of SOCS2 in GM-MØ (compared to M-MØ) might promote a stronger TRAF6 degradation and, consequently, the weaker LPS-induced phosphorylation of the three MAPK we have observed in GM-MØ (**Figure 9**). Along the same line, and if the same mechanism holds true after LPS treatment, the elevated levels of SOCS2 could favor the attainment of a state of refractoriness to TLR stimulation in LPS-activated M-MØ.

The induction of growth factors like BMP6 and PDGFA in activated M-MØ highlights a different functional aspect of M-CSF-primed macrophages. Tissue resident macrophages are known for their critical homeostatic and trophic roles during tissue development as well as tissue maintenance and repair after injury in the adult organism. Besides, the trophic roles of macrophages are known to promote tumor growth and metastasis [191]. In this regard, PDGFA is expressed in neural, lung and

intestinal tissues during development where it regulates proliferation, migration and tissue remodeling [192]. Moreover, the PDGF family has long been recognized as having a critical role in tumorigenesis. In fact, several PDGF signaling antagonists have been developed to treat a variety of malignant diseases [193] and recent reports show success in the use of sunitinib, a PDGFR kinase inhibitor, in the treatment of melanoma [193; 194]. Therefore, the production of PDGFA by in vivo nevus-associated macrophages might contribute to the progression of skin proliferative diseases. Indeed, PDGFA from melanoma conditioned-media is responsible for the activation of fibroblasts that leads to hyaluronan deposition and metalloproteinase secretion, which promote melanoma cell growth and metastasis [195; 196].

BMP6 regulated systemic iron homeostasis by inducing the hormone hepcidin, which leads to increased intracellular iron in cells by binding and driving the degradation of the iron exporter SLC40A1 (ferroportin) [197; 198]. Iron is essential for electron exchanges in core biological cellular processes, such as the electron transport chain to produce ATP in mithochondria or the production of ROS in inflammation [199]. Thus, iron availability affects cell growth and inflammatory responses [200; 201]. Tumor cells are especially dependent on iron to maintain their high proliferation levels and are able to reprogram iron metabolism to favor iron influx [202]. Therefore, the presence of BMP6 in nevus and melanoma macrophages might reflect a mechanism whereby proliferative cells promote BMP6 production by macrophages in order to favor tumor growth. This is further supported by the elevated levels of BMP6 found in serum from breast cancer patients [203]. Moreover, increased intracellular iron has an anti-inflammatory effect on macrophages [201; 204] from which tumor cells also benefit. In fact, *in vitro* activated M-MØ not only upregulate *BMP6*, but also downregulate *SLC40A1* and, contrarily, GM-MØ upregulate *SLC40A1* upon LPS stimulation (**Figure 11D** and **Table III**). Altogether, redirecting iron metabolism by inducing BMP6 expression in macrophages might be an advantageous strategy of malignant cells to sustain tumor development.

ARNT2 (aryl hydrocarbon receptor nuclear translocator 2) is a member of the bHLH-PAS family that includes AHR, HIF and SIM transcription factors [205]. ARNT2 is a close homolog of ARNT, however, their expression patterns differ greatly [205; 206]. ARNT is ubiquitously expressed whereas ARNT2 is only expressed in neurons and kidney and its functions remain nowadays mostly unknown [205; 206]. In the nervous system ARNT2 has been described to dimerize with SIM1 and NPAS4 to regulate appetite and neuronal firing and *Arnt2* ablation in mice results in perinatal death, similar to mice with a targeted mutation in SIM1 [205; 206]. HIF1A has also been shown to form active dimers with ARNT2 and likely affect hypoxia responses in neurons [206; 207]. In vitro assays originally showed a similar capacity of ARNT and ARNT2 to bind to AHR and induce transcription

of *CYP1A1* after TCDD activation of AHR [208]. However, later studies carried out in cell lines revealed that ARNT2 is not able to induce AHR-dependent transcription [209]. It has been suggested that different AHR ligands might induce different AHR conformations that in turn affect its affinity to bind ARNT and ARNT2 [210]. Thus, different cellular contexts could modulate AHR dimerization to different partners. Nonetheless, this issue has not been further addressed. Surprisingly, unlike *ARNT*, *ARNT2* is expressed at low levels in steady state M-MØ and is greatly induced upon activation of M-MØ, whereas its expression in GM-MØ is very low (**TableIII**, **Table IV**, **Figure12A**). Besides, *HIF1A* is more highly expressed (2-fold) in M-MØ than GM-MØ, both under steady state and LPS-stimulating conditions (see **Table III**). We previously reported that an increase in HIF1A in M-MØ exposed to hypoxia primes M-MØ to increase the production of pro-inflammatory cytokines after a successive activation with LPS [211]. Regarding *AHR*, its expression is slightly higher in M-MØ, but is downregulated upon LPS stimulation, and our preliminary results show that AHR has different roles in the regulation of the polarization and LPS response of GM-MØ and M-MØ (*data not shown*). All things considered, this is the first time, to our knowledge, that *ARNT2* expression has been reported in leukocytes and we hypothesize that ARNT2 might have an unexpected role in macrophage polarization and activation through regulation of HIF1A and AHR function.

Altogether, the definition of the transcriptomic profile of activated M-MØ after a short exposure to LPS has allowed us to expand our knowledge on the regulation of the characteristic anti-inflammatory response of M-MØ.

MAFB-directed human macrophage anti-inflammatory polarization

The importance of the transcription factor MAFB in development and homeostasis is widely accepted. MAFB is critical for the development of the hindbrain, pancreas, kidneys, cartilage and lymphatic vessels (*see* **Figure 4**) [101; 108-110; 112; 113]. Moreover, maintenance of kidney and pancreas functions are dependent on MAFB [110; 114], and its function as an oncogene in multiple myeloma has been described [212-214]. In murine monocytes and macrophages, MAFB has been established as a master regulator of their differentiation [121; 125]. Nonetheless, the available knowledge about the genes and functions in macrophages that are regulated by MAFB is surprisingly limited. This might be mostly due by the fact that MAFB deficient mice die shortly after birth [123], making the work with murine models very cumbersome. All things considered, and knowing that MAFB was preferentially expressed in M-MØ compared to GM-MØ (**Figure 17**), we decided to determine the genes and functions regulated by MAFB in human anti-

inflammatory macrophages under steady-state and activating conditions. Moreover, we validated our results with macrophages derived from MCTO patients that carry mutations in the transactivation domain of MAFB, what constitutes an excellent genetic tool to further study the role of MAFB in human macrophage biology.

In addition to reported genes regulated by MAFB in mouse myeloid cells, like *CCL2* [100], and in line with the preferential expression of *MAFB* in IL-10-producing macrophages, the MAFB-dependent transcriptome of human M-MØ under resting conditions includes genes with known anti-inflammatory effects as well as genes whose expression is associated with the acquisition of anti-inflammatory activity by human macrophages (**Table VII**). Among the first group it is worth mentioning IL-10, the paradigmatic anti-inflammatory cytokine [215], CCL2, that recruits monocytes towards inflamed tissues and impairs the production of inflammatory cytokines [152; 216; 217], and HTR2B, whose ligation skews macrophage differentiation towards the anti-inflammatory side [150]. The presence of *CD163L1* within the MAFB-dependent gene set is especially relevant because CD163L1 expression primarily marks tissue-resident macrophages with IL-10-producing ability [79]. In fact, the presence of CD163L1 on macrophages appears to be concomitant with that of the CD209 lectin, a receptor whose ligation also potentiates IL-10 production from macrophages [38]. Along the same line, MAFB also positively regulates the expression of the *EMR1* gene, whose mouse ortologue (the F4/80 receptor-encoding *Emr1* gene) is required for the induction of regulatory T cells in peripheral tolerance [218] and whose expression depends on the Mafb-heterodimerizing factor c-Maf [113; 219]. Conversely, MAFB negatively regulates the expression of genes associated to pro-inflammatory polarization like *CLEC5A*, which codes for a lectin preferentially expressed in TNF-α-producing macrophages in secondary lymphoid organs and in lamina propria macrophages from inflammatory bowel disease patients [79]. The gene ontology analysis of the transcriptome of MCTO and siMAFB-transfected M-MØ has lent further support to the link between MAFB expression and macrophage anti-inflammatory polarization. GSEA revealed that *MAFB* knockdown leads to a global downregulation of genes preferentially expressed in anti-inflammatory macrophages ("anti-inflammatory gene set") and to a significant upregulation of the "pro-inflammatory gene set". Furthermore, and in agreement with the higher half-life of MCTO-causing MAFB mutants, the MCTO M-MØ gene signature shows the opposite effect, with a global upregulation of the "anti-inflammatory gene set". Besides, the set of genes positively regulated by MAFB is significantly enriched in genes upregulated by IL-10 and downregulated upon *IL10* gene ablation (**Figure 20**). All the above findings indicate that MAFB controls the expression of a large set of molecules that either contribute, or are associated to, the anti-inflammatory ability of IL-10-producing human macrophages (IL-10, CCL2, HTR2B, CD163L1, EMR1), thus

identifying MAFB as a critical determinant for the acquisition of the anti-inflammatory profile of steady-state human macrophages.

Moreover, MAFB confers anti-inflammatory ability to M-MØ also under activating conditions, such as LPS stimulation (**Figure 25**). MAFB-deficient M-MØ exhibit a decreased expression of *IL10* after LPS treatment. Furthermore, MAFB positively regulates the induction of the activated-M-MØ gene set described in **Figure 12**. Specifically, LPS-mediated induction of *CCL19* and *PDGFA*, which are expressed in nevus-associated macrophages, is dependent on MAFB whereas MCTO-derived M-MØ have an increased induction of *CCL19* and *PDGFA* as compared to controls. Together, these results hint at a role for MAFB in the regulation of the response to an inflammatory challenge by macrophages and highlight the increased anti-inflammatory potential of MCTO-derived M-MØ. However, whether MCTO patients show an impaired ability to deal with infectious diseases or alergies has not yet been addressed.

Recently, fate-mapping studies on the murine macrophage ontogeny concluded that tissue-resident macrophages in the brain, epidermis, liver and lungs have an embryonic origin and are not replenished by monocytes in the steady state [7-12], whereas tissue-resident macrophages in the intestine, dermis, heart, pancreas and peritoneum are monocyte-derived [2-6]. These observations lead to questioning whether macrophages from various origins would have specific functions dictated by particular differentiating factors. In this regard, and as shown in **Figure 26**, we have seen expression of MAFB in human tissue-resident macrophages from the colon and dermis, whereas macrophages from placenta and liver samples don't have detectable levels of MAFB. This observation is intriguing since all of the above macrophage populations are tissue-resident, homeostatic macrophages and dependent on CSF1R ligands for their differentiation [51; 54]. However, only macrophages from tissues where continuous replenishment by monocytes occurs (colon and dermis) are MAFB-positive, as opposed to tissues where resident macrophages have been described to be of embryonic origin (placenta and liver). We therefore surmise that MAFB might not only define anti-inflammatory macrophages, but it might specifically mark anti-inflammatory/homeostatic macrophages that derive from monocytes in humans *in vivo*. This hypothesis would also be in agreement with the known ability of MAFB to restrict myeloid cell proliferation [121] and the fact that murine tissue-resident macrophages that have an embryonic origin are known to self-renew [9; 13-15].

Pathological relevance of MAFB-driven macrophage polarization

Although we have used MCTO-derived macrophages mainly as a genetic tool to unravel the role of MAFB in anti-inflammatory human macrophage polarization, the information we have gathered on macrophages derived from MCTO monocytes might shed light on the pathogenic mechanisms operating in MCTO and other diseases that share either similar etiologies, such as diseases caused by mutations in MAFB or other MAF familiy members, or similar symptoms, namely diseases where osteolysis is a defining pathological feature. Duane retraction syndrome [126], Aymé-Gripp syndrome [104], and retinitis pigmentosa [220] are caused by MAFB loss of function, MAF and NRL mutations, respectively. Specifically, mutations that cause Aymé-Gripp syndrome and retinitis pigmentosa cluster in the same homologous region as MCTO mutations, which is necessary for GSK3 phosphorylation of MAF family members. Thus, the study of MCTO-derived macrophages may allow us to unravel the pathological consequences of a deffective GSK3 function. Alternatively, other rare osteolytic syndromes exist that, despite extensive efforts, have yet unknown causes, namely, Multicentric osteolysis, nodulosis and arthropathy (MONA, OMIM #259600), Winchester syndrome (OMIM #277950) and Gorham-Stout disease (OMIM #123880). The osteolysis observed in these diseases and in MCTO might be due to common misregulated mechanisms for which the study of MCTO-derived macrophages and osteoclasts may be of great value.

In the case of MCTO, we have identified a number of genes whose expression is altered not only in MCTO-derived macrophages but also in peripheral blood monocytes from the three analyzed MCTO patients (*data not shown*). Although analysis of additional patients is still required to propose their use as potential MCTO diagnostic markers, a disease commonly misdiagnosed [159], our results suggest that MCTO-causing mutations impact on the generation of monocytes and affect their later differentiation into fully functional tissue-resident macrophages, as exemplified by their inability to differentiate into functional osteoclasts in response to M-CSF and RANKL in vitro. Whether the profound anti-inflammatory skewing of MCTO-derived M-MØ is responsible for their inability to generate osteoclasts *in vitro* is an issue that we are currently pursuing. Along the same line, the genes downregulated in MCTO-derived M-MØ include a significant proportion of MYB- and ZXDC-regulated genes, two factors that participate in monocyte-to-macrophage differentiation, M-CSF-driven macrophage polarization [221; 222] and even positive regulation of *CCL2* gene expression [221].

MMP25 expression is downregulated in siMAFB-transfected M-MØ and in MCTO M-MØ. This feature resembles the ability of mouse Mafb to control the expression of MMP-9 and -12 in alveolar macrophages [131], and MMP-13 in neonatal chondrocytes [112]. The MAFB-MMP-25 link might also have pathological relevance because MMP-25 directly activates MMP-2 [223], a metalloproteinase whose mutation is responsible for MONA, a rare autosomal recessive disorder also characterized by multicentric osteolysis [224; 225]. Moreover, mutations in the MT1-MMP-encoding *MMP14* gene are now known to be responsible for Winchester syndrome, a pathology similar to MONA and whose clinical symptoms include severe osteolysis in the hands and feet and generalized osteoporosis and bone thinning [224]. Since MMP14 also activates MMP-2 [226-228], it is tempting to speculate that the altered expression of MMP-25 that we have observed in MCTO monocyte-derived macrophages might be relevant to the pathology in MCTO. The finding that MMP-14 and MMP-2 are responsible for the fibroblast-mediated contraction in Dupuytren's disease [229], a disease where MAFB is significantly upregulated [128] further supports the validity of this hypothesis. Gorham-Stout disease, also known as vanishing bone disease, is characterized by massive localized osteolysis that can arise in any bone and that is preceded by an enormous increase in lymphatic vascularization of the bone [230]. Although the precise etiology of Gorham-Stout disease remains unclear, it is believed that the increase of lymphangiogenesis is related to the lysis of the bone. In this regard, a recent report has described MAFB as an important transcription factor in the generation of lymphatic vessels [101]. Thus, one could hypothesize that a deregulation of MAFB function, as occurs in MCTO, might be responsible for the increase in lymphatic vessel formation and an abnormal osteoclast function in Gorham-Stout disease.

Our results on *in vitro* monocyte-derived macrophages clearly points to a link between M-CSF-driven differentiation and *MAFB* expression: M-CSF-driven macrophage differentiation results in high levels of *MAFB*, while the presence of GM-CSF lowers the basal levels of *MAFB* found in human monocytes. This result agrees with the ability of murine MafB to antagonize the phenotypic alteration of microglia induced by GM-CSF [231]. Whether the MAFB/GM-CSF antagonism operates in all types of macrophages is still unknown. However, we have observed that MCTO mutations limit the acquisition of GM-CSF-inducible genes in GM-MØ, a finding that might be relevant in the case of macrophage whose development is critically dependent on GM-CSF (lung alveolar macrophages) [61]. Although no lung-associated pathology has been so far reported in MCTO patients, it is worth noting that a significant number of genes aberrantly expressed in pulmonary diseases (pulmonary sarcoidosis, asthma and tuberculosis) exhibit an altered expression in MCTO M-MØ (**Figure 23B**), a finding that might be related to the fact that mature alveolar macrophages, identified as

intermediate positive for the *Emr1*-encoded F4/80, are reduced in the bronchoalveolar lavage of mice expressing a dominant-negative MafB in macrophages [131]. Given these antecedents, the analysis of further MCTO patients it is certainly worthy as a means to get a deeper knowledge of the molecular mechanisms operating in this and other MAF family- and osteolytic-related syndromes as well as to more clearly delineate the role of MAFB in the acquisition of the human macrophage anti-inflammatory profile.

CONCLUSSIONS

1. The response of GM-MØ and M-MØ to LPS and other TLR ligands differs in terms of intracellular signaling, with a higher activation of MAPK, STAT3 and CREB in M-MØ, and a more robust phosphorylation of IRF3 in GM-MØ.

2. The preferential production of IL-10 by activated M-MØ, the defining feature of this macrophage subtype, is in line with the existence of an M-MØ-specific gene expression program characterized by a strong anti-inflammatory component that can be triggered by LPS and other TLR ligands.

3. ERK, p38MAPK and JNK directly contribute to the M-MØ-specific LPS-induced transcriptomic and cytokine profile, supporting that differences in LPS-triggered intracellular signals lie at the basis of the distinct transcriptomic responses of activated GM-MØ and M-MØ.

4. The co-expression of *CCL19*, *PDGFA*, *BMP6* and *SOCS2* observed in LPS-activated M-MØ is also found in macrophages in melanoma and nevi, thus reinforcing the existence of a co-regulated set of genes that are specifically expressed upon activation of human anti-inflammatory/homeostatic macrophages.

5. The expression of MAFB characterizes human macrophages with homeostatic/anti-inflammatory functions both in vitro and in vivo.

6. MAFB is a critical factor for the acquisition/maintenance of the anti-inflammatory transcriptome of human macrophages, as it positively controls the expression M-MØ-specific genes and impairs the expression of genes associated to the GM-CSF-directed pro-inflammatory polarization.

7. MCTO-causing MAFB mutations affect both the stability and the transcriptional activity of MAFB and drive MCTO macrophages towards the upregulation of genes associated to anti-inflammatory macrophage polarization leading to a global increase of the expression of anti-inflammatory M-MØ-specific genes, thus reinforcing the contribution of MAFB to the acquisition and maintenance of the anti-inflammatory gene signature in human macrophages.

8. MCTO-causing MAFB mutations impact on the generation of monocytes and affect their later differentiation into fully functional tissue-resident macrophages, as exemplified by their inability to differentiate into functional osteoclasts in response to M-CSF and RANKL in vitro.

9. MAFB also contributes to the acquisition of the specific gene expression profile of LPS-activated M-MØ.

10. MAFB is a primary driver of the anti-inflammatory gene profile of human M-CSF-dependent macrophages, and the presence of MAFB-regulated genes provides useful markers for the *in vivo* identification of anti-inflammatory macrophages.

EXPERIMENTAL PROCEDURES

Generation of monocyte-derived macrophages.

Human Peripheral Blood Mononuclear Cells (PBMC) were isolated from buffy coats from normal donors over a Lymphoprep (Nycomed Pharma, Oslo, Norway) gradient according to standard procedures. Monocytes were purified from PBMC by magnetic cell sorting using anti-CD14 microbeads (Miltenyi Biotec, Bergisch Gladbach, Germany) (>95% $CD14^+$ cells). Monocytes (0.5 x 10^6 cells/ml, >95% $CD14^+$ cells) were cultured in RPMI 1640 supplemented with 10% fetal bovine serum (FBS) for 7 days in the presence of 1000 U/ml GM-CSF, 10 ng/ml M-CSF (ImmunoTools, Friesoythe, Germany) or 10 ng/ml IL-34 (Biolegend, CA, USA) to generate GM-CSF-polarized macrophages (GM-MØ) or M-CSF-polarized macrophages (M-MØ), or IL-34-polarized macrophages (IL34-MØ), respectively. Cytokines were added every two days. Cells were cultured in 21% O2 and 5% CO2. Monocyte-derived osteoclasts were generated by culturing monocytes for 12 days on glass coverslips or in an Osteolyse Assay Kit (Lonza, MD, USA) in the presence of M-CSF (25 ng/ml) and RANKL (30 ng/ml). After fixing, osteoclast generation was verified by staining for tartrate-resistant acid phosphatase (TRAP) using the Leukocyte Acid Phophatase kit (Sigma Aldrich). Generation of monocyte-derived macrophages from Multicentric carpotarsal osteolysis (MCTO) patients was done using a similar procedure and following the Medical Ethics committee procedures of Hospital Clínico Universitario, Santiago de Compostela (patient MCTO#1) and of Hôpital Necker Enfants Malades, Paris (patients MCTO#2 and MCTO#3). MCTO#1 patient was found to contain a Ser54Leu (161C>T) mutation, whereas patients MCTO#2 and MCTO#3 contain a Pro63Leu (188C>T) mutation [134]. For *MAFB* and *STAT3* knockdown, M-MØ (10^6 cell/ml) were transfected with a *MAFB*- or *STAT3*-specific small interfering RNA (siMAFB and siSTAT3, 50 nM) (Thermo Fisher Scientific) using Hiperfect (Qiagen). As a control, cells were transfected with a non-specific siRNA (siControl, Thermo Fisher Scientific). After transfection, cells were cultured for the indicated times in RPMI 1640 supplemented with 10% FBS. For macrophage activation, cells were treated with 10 ng/ml E. coli 055:B5 lipopolysaccharide (LPS, Sigma-Aldrich, MO, USA) or 10µg/ml N-Palmitoyl-S-[2,3-bis(palmitoyloxy)-(2RS)-propyl]-[R]-cysteinyl-[S]-seryl-[S]-lysyl-[S]-lysyl-[S]-lysyl-[S]-lysine (PAM3CSK4, Invivogen, CA, USA). For intracellular signaling inhibition, macrophages were exposed to p38MAPK inhibitor BIRB0796 (0.1 µM) [143], MEK inhibitor U0126 (2.5 µM) [141] or JNK inhibitor SP600125 (30 µM) [142] for 60 min before treatment with LPS. Macrophage supernatants were assayed for the presence of cytokines using commercial ELISA kits for human TNF-α, IL12p40, CCL2 (BD Biosciences, CA, USA), IL-6 (Sigma-Aldrich, Steinheim, Germany), CCL19 (PBL Assay Science, NJ, USA) and IL-10 (Biolegend, CA, USA) according to the protocols supplied by the manufacturers. Where indicated, monocytes were exposed to tumor ascitic fluids of different origins [38] that were kindly provided by Dr. Mª Isabel Palomero

(Oncology Department, Hospital General Universitario Gregorio Marañón). Mouse bone marrow-derived macrophages were generated using human M-CSF (10 ng/mL; ImmunoTools).

Quantitative real-time RT-PCR.

Total RNA was extracted using the NucleoSpin RNA/Protein kit (Macherey-Nagel, Düren, Germany), retrotranscribed, and amplified using the Universal Human Probe library (Roche Diagnostics, Mannheim, Germany). Oligonucleotides for selected genes were designed according to the Roche software for quantitative real-time PCR (Roche Diagnostics, Mannheim, Germany). Assays were made in triplicate and results normalized according to the expression levels of *TBP* or *18S* for macrophage or monocyte samples, respectively. Custom-made microfluidic gene cards (Roche Diagnostics) were designed to analyze the expression of genes whose expression is differentially modulated by LPS in GM-MØ and M-MØ. Specifically, the gene cards included 10 genes upregulated by LPS in both GM-MØ and M-MØ, 16 genes upregulated by LPS exclusively in GM-MØ, 37 genes upregulated by LPS exclusively in M-MØ, 3 genes downregulated by LPS exclusively in GM-MØ, and 20 genes downregulated by LPS exclusively in M-MØ. Assays were made in duplicate on three independent samples of each type, and the results normalized according to the mean of the expression level of endogenous reference genes *HPRT1*, *TBP* and *RPLP0*. In all cases the results were expressed using the ΔΔCT method for quantitation.

Western blot.

Cell lysates were obtained in RIPA buffer (10 mM Tris-HCl pH 8, 150 mM NaCl, 1% NP-40, 2 mM Pefabloc, 2 mg/ml aprotinin/antipain/leupeptin/pepstatin, 10 mM NaF, and 1 mM Na3VO4). 10 μg of cell lysate was subjected to SDS-PAGE and transferred onto an Immobilon polyvinylidene difluoride membrane (Millipore). Protein detection was carried out using antibodies against phosphorylated and total ERK1/2, p38MAPK and JNK (Cell Signaling, MA, USA), phosphorylated and total STAT1 and STAT3 (BD Biosciences, CA, USA), and IκBα, phosphorylated IRF3 and phosphorylated CREB (Cell Signaling), MAFB (sc-10022, Santa Cruz, CA, USA), CLEC5A (MAB2384, R&D Systems, MN, USA). Samples for CLEC5A detection were assayed under non-reducing conditions. Protein loading was normalized using a monoclonal antibody against

GAPDH (sc-32233, Santa Cruz, CA, USA), α-actin (Sigma-Aldrich), or β-tubulin (sc-58667, Santa Cruz, CA, USA).

Microarray analysis.

Global gene expression analysis was performed on RNA obtained from three independent samples of untreated (M-MØ or GM-MØ) or LPS-treated human monocyte-derived macrophages (4h, M-MØ+LPS or GM-MØ+LPS). For siMAFB and MCTO microarrays, RNA was obtained from siControl-transfected M-MØ, siMAFB-transfected M-MØ (three independent samples), and M-MØ generated from either MCTO#1 or from two healthy individuals. In the case of M-MØ from MCTO#1, two RNA aliquots were analyzed in parallel. RNA was isolated using the NucleoSpin RNA/Protein kit (Macherey-Nagel, Düren, Germany) and analyzed with a whole human genome microarray from Agilent Technologies (Palo Alto, CA). Only probes with signal intensity values >60% quantile in at least one condition were considered for the differential expression and statistical analysis. Statistical analysis for differential gene expression was carried out using empirical Bayes moderated t test implemented in the limma package (http://www.bioconductor.org). The p values were further adjusted for multiple hypotheses testing using the Benjamini-Hochberg method to control the false discovery rate [232]. All the above procedures were coded in R (http://www.r-project.org). Data from siMAFB and MCTO microarrays were deposited in the Gene Expression Omnibus (http://www.ncbi.nlm.nih.gov/geo/) under accession no. GSE84622. The differentially expressed genes were analysed for annotated gene sets enrichment using the online tool ENRICHR (http://amp.pharm.mssm.edu/Enrichr/) [154; 155]. Enrichment terms were considered significant when they had a Benjamini-Hochberg-adjusted p value <0.05. For gene set enrichment analysis (GSEA) [233], the previously defined “Pro-inflammatory gene set” and “Anti-inflammatory gene set” [151], which contain the top and bottom 150 probes from the GM-MØ versus M-MØ limma analysis of the microarray data in GSE68061 (ranked on the basis of the value of the t statistic) were used.

MAFB expression vectors, site-directed mutagenesis and reporter assays.

The coding sequence of MAFB was amplified by PCR from reverse-transcribed cDNA from a healthy donor and was sequenced to confirm the absence of mutations. The oligonucleotides used for amplification of the MAFB coding region were 5’-CGGAATTC-CGATGGCCGCGGAGCTGAGC-3’ and 5’- GCTCTAGAGCTCACAGAAAGAACTCG-GGAGAG-3’, which include EcoRI and XbaI restriction sites for subsequent cloning

into EcoRI- and XbaI-cut pCDNA3.1(+) expression vector (pMAFBwt). Site-directed mutagenesis was carried out using the QuikChange site-directed mutagenesis kit (Stratagene, CA, USA) to generate MAFB expression constructs with the Ser54Leu mutation (161C>T, found in MCTO#1 patient) (pMAFB161T), the Pro63Arg mutation (188C>G) (pMAFB188G) [134] or the Pro71Ser mutation (211C>T) (pMAFB211T) [133]. The oligonucleotides used for mutagenesis were S54LF (5'-CACGCCTGCAGCCAGCCG-GCTTGGTGTCCTCCAC-3'), S54LR (5'-GTGGAGGACACCAAGCCGGCTGGCT-GCAGGCGTG-3'), P63RF (5'-CCGCTCAGCACTCGGTGTAGCTCCGTGCCCTC-GTC-3'), P63RR (5'-GACGAGGGCACGGAGCTACACCGAGTGCTGAGCGG-3'), P71SF (5'-GTAGCTCCGTGCCCTCGTCGTCCAGCTTCAGCCCGACCGAAC-3') and P71SR (5'-GTTCGGTCGGGCTGAAGCTGGACGACGAGGGCACGGAGCTAC-3'). The resulting plasmids were verified by sequencing.

To check the transcriptional activity of MAFB MCTO-causing mutations, HEK293T cells were seeded in 24-well plates at 4 x 10^4 cells/well and transfected with SuperFect (Qiagen) with 200 ng of each expression vector and 1 μg of the 3xMARE-Luc reporter vector. Each transfection also included 25 ng of a construct expressing the Renilla luciferase for normalization of transfection efficiency. After 24 hours, firefly and Renilla luciferase activities were determined by using the Dual-Luciferase Reporter Assay System (Promega). The 3xMARE-Luc reporter construct was generated by inserting three multimerized MAF-Recognition Element (MARE) [97] into HindIII- and XhoI-cut pXP2-TATA plasmid. The sequences of the oligonucleotides used to generate the 3xMARE-Luc construct were 5'-agctttcgacccgaaaggTGCTGAcgTCAGCAgctagccctcgacccgaaag-gTGCTGAcgTCAGCAgctagccctcgacccgaaaggTGCTGAcgTCAGCAgctagcccc-3' and 5'-tcgaggggctagcTGCTGAcgTCAGCAcctttcgggtcgagggctagcTGCTGAcgTCAG-CAcctttcgggtcgagggctagcTGCTGAcgTCAGCAcctttcgggtcgaa-3', where capital letters indicate the MAFB-binfding sites.

To assess the protein stability of MAFB MCTO-causing mutants, HEK293T cells were transfected with 1 μg of pMAFBwt, pMAFB161T, pMAFB188G or pMAFB211T plasmids using SuperFect (Qiagen). After 24h cells were treated with 10 μg/ml cycloheximide and cell lysates generated at the indicated times using RIPA buffer.

Fluorescence confocal microscopy.

Human biopsied samples were obtained from patients undergoing surgical treatment and following the Medical Ethics committee procedures of Hospital General Universitario Gregorio Marañón. Frozen samples were cryosectioned (5 μm), fixed with acetone, blocked with human immunoglobulins and simultaneously stained with different primary antibodies at 1-5 µg/ml. Imaging was performed with the glycerol ACS APO

20x NA 0.60 immersion objective of a confocal fluorescence microscope (SPE, Leica Mycrosystems). For quantification of in vivo protein expression, mean fluorescence intensities of the proteins of interest (SOCS2, BMP6, CCL19, PDGFA, MAFB, CD163L1, HTR2B and CXCL12) were quantified at segmented $CD163^+$ macrophages using the FIJI software (National Institute of Health, USA), and background subtracted data from at least three different fields displayed as scatter plots (GraphPad). The antibodies used were the following: mouse monoclonal anti-CD163 (K0147-4, MBL, MA, USA), rabbit polyclonal anti-PDGFA and rabbit polyclonal anti-SOCS2 (sc-127 and sc-9022, Santa Cruz, CA, USA), goat polyclonal anti-BMP6 (AF507, R&D Systems, MN, USA), rabbit polyclonal anti-CCL19 (13397-1-AP, Proteintech, IL, USA), goat polyclonal anti-MAFB (sc-10022, Santa Cruz, CA, USA), rabbit polyclonal anti-CD163L1 (HPA015663, Sigma-Aldrich, MO, USA), rabbit polyclonal anti-CXCL12 (P87B, Peprotech, NJ, USA) and rabbit polyclonal anti-HTR2B (sc-25647, Santa Cruz, CA, USA).

Statistical analysis.

For comparison of means, and unless otherwise indicated, statistical significance of the generated data was evaluated using the Student t test. In all cases, $p<0.05$ was considered as statistically significant.

REFERENCES

1. van Furth, R., Cohn, Z.A., Hirsch, J.G., Humphrey, J.H., Spector, W.G., and Langevoort, H.L. (1972). The mononuclear phagocyte system: a new classification of macrophages, monocytes, and their precursor cells. Bulletin of the World Health Organization 46, 845-852.

2. Calderon, B., Carrero, J.A., Ferris, S.T., Sojka, D.K., Moore, L., Epelman, S., Murphy, K.M., Yokoyama, W.M., Randolph, G.J., and Unanue, E.R. (2015). The pancreas anatomy conditions the origin and properties of resident macrophages. The Journal of experimental medicine 212, 1497-1512.

3. Bain, C.C., Bravo-Blas, A., Scott, C.L., Gomez Perdiguero, E., Geissmann, F., Henri, S., Malissen, B., Osborne, L.C., Artis, D., and Mowat, A.M. (2014). Constant replenishment from circulating monocytes maintains the macrophage pool in the intestine of adult mice. Nature immunology 15, 929-937.

4. Tamoutounour, S., Guilliams, M., Montanana Sanchis, F., Liu, H., Terhorst, D., Malosse, C., Pollet, E., Ardouin, L., Luche, H., Sanchez, C., et al. (2013). Origins and functional specialization of macrophages and of conventional and monocyte-derived dendritic cells in mouse skin. Immunity 39, 925-938.

5. Epelman, S., Lavine, K.J., Beaudin, A.E., Sojka, D.K., Carrero, J.A., Calderon, B., Brija, T., Gautier, E.L., Ivanov, S., Satpathy, A.T., et al. (2014). Embryonic and adult-derived resident cardiac macrophages are maintained through distinct mechanisms at steady state and during inflammation. Immunity 40, 91-104.

6. Kim, K.W., Williams, J.W., Wang, Y.T., Ivanov, S., Gilfillan, S., Colonna, M., Virgin, H.W., Gautier, E.L., and Randolph, G.J. (2016). MHC II+ resident peritoneal and pleural macrophages rely on IRF4 for development from circulating monocytes. The Journal of experimental medicine.

7. Hoeffel, G., Wang, Y., Greter, M., See, P., Teo, P., Malleret, B., Leboeuf, M., Low, D., Oller, G., Almeida, F., et al. (2012). Adult Langerhans cells derive predominantly from embryonic fetal liver monocytes with a minor contribution of yolk sac-derived macrophages. The Journal of experimental medicine 209, 1167-1181.

8. Ginhoux, F., Greter, M., Leboeuf, M., Nandi, S., See, P., Gokhan, S., Mehler, M.F., Conway, S.J., Ng, L.G., Stanley, E.R., et al. (2010). Fate mapping analysis reveals that adult microglia derive from primitive macrophages. Science (New York, NY 330, 841-845.

9. Hashimoto, D., Chow, A., Noizat, C., Teo, P., Beasley, M.B., Leboeuf, M., Becker, C.D., See, P., Price, J., Lucas, D., et al. (2013). Tissue-resident macrophages self-maintain locally throughout adult life with minimal contribution from circulating monocytes. Immunity 38, 792-804.

10. Sheng, J., Ruedl, C., and Karjalainen, K. (2015). Most Tissue-Resident Macrophages Except Microglia Are Derived from Fetal Hematopoietic Stem Cells. Immunity 43, 382-393.

11. Hoeffel, G., Chen, J., Lavin, Y., Low, D., Almeida, F.F., See, P., Beaudin, A.E., Lum, J., Low, I., Forsberg, E.C., et al. (2015). C-Myb(+) erythro-myeloid progenitor-derived fetal monocytes give rise to adult tissue-resident macrophages. Immunity 42, 665-678.

12. Guilliams, M., De Kleer, I., Henri, S., Post, S., Vanhoutte, L., De Prijck, S., Deswarte, K., Malissen, B., Hammad, H., and Lambrecht, B.N. (2013). Alveolar macrophages develop from fetal monocytes that differentiate into long-lived cells in the first week of life via GM-CSF. The Journal of experimental medicine 210, 1977-1992.

13. Ghigo, C., Mondor, I., Jorquera, A., Nowak, J., Wienert, S., Zahner, S.P., Clausen, B.E., Luche, H., Malissen, B., Klauschen, F., et al. (2013). Multicolor fate mapping of Langerhans cell homeostasis. The Journal of experimental medicine 210, 1657-1664.

14. Davies, L.C., Rosas, M., Smith, P.J., Fraser, D.J., Jones, S.A., and Taylor, P.R. (2011). A quantifiable proliferative burst of tissue macrophages restores homeostatic macrophage populations after acute inflammation. European journal of immunology 41, 2155-2164.

15. Varol, C., Landsman, L., Fogg, D.K., Greenshtein, L., Gildor, B., Margalit, R., Kalchenko, V., Geissmann, F., and Jung, S. (2007). Monocytes give rise to mucosal, but not splenic, conventional dendritic cells. The Journal of experimental medicine 204, 171-180.

16. Mielcarek, M., Kirkorian, A.Y., Hackman, R.C., Price, J., Storer, B.E., Wood, B.L., Leboeuf, M., Bogunovic, M., Storb, R., Inamoto, Y., et al. (2014). Langerhans cell homeostasis and turnover after nonmyeloablative and myeloablative allogeneic hematopoietic cell transplantation. Transplantation 98, 563-568.

17. Collin, M.P., Hart, D.N., Jackson, G.H., Cook, G., Cavet, J., Mackinnon, S., Middleton, P.G., and Dickinson, A.M. (2006). The fate of human Langerhans cells in hematopoietic stem cell transplantation. The Journal of experimental medicine 203, 27-33.

18. Bigley, V., Haniffa, M., Doulatov, S., Wang, X.N., Dickinson, R., McGovern, N., Jardine, L., Pagan, S., Dimmick, I., Chua, I., et al. (2011). The human syndrome of dendritic cell, monocyte, B and NK lymphoid deficiency. The Journal of experimental medicine 208, 227-234.

19. Serbina, N.V., Jia, T., Hohl, T.M., and Pamer, E.G. (2008). Monocyte-mediated defense against microbial pathogens. Annual review of immunology 26, 421-452.

20. Jenkins, S.J., Ruckerl, D., Cook, P.C., Jones, L.H., Finkelman, F.D., van Rooijen, N., MacDonald, A.S., and Allen, J.E. (2011). Local macrophage proliferation, rather than recruitment from the blood, is a signature of TH2 inflammation. Science (New York, NY 332, 1284-1288.

21. Lavin, Y., Winter, D., Blecher-Gonen, R., David, E., Keren-Shaul, H., Merad, M., Jung, S., and Amit, I. (2014). Tissue-resident macrophage enhancer landscapes are shaped by the local microenvironment. Cell 159, 1312-1326.

22. Zigmond, E., Samia-Grinberg, S., Pasmanik-Chor, M., Brazowski, E., Shibolet, O., Halpern, Z., and Varol, C. (2014). Infiltrating monocyte-derived macrophages and resident kupffer cells display different ontogeny and functions in acute liver injury. J Immunol 193, 344-353.

23. Bleriot, C., Dupuis, T., Jouvion, G., Eberl, G., Disson, O., and Lecuit, M. (2015). Liver-resident macrophage necroptosis orchestrates type 1 microbicidal inflammation and type-2-mediated tissue repair during bacterial infection. Immunity 42, 145-158.

24. Ajami, B., Bennett, J.L., Krieger, C., McNagny, K.M., and Rossi, F.M. (2011). Infiltrating monocytes trigger EAE progression, but do not contribute to the resident microglia pool. Nat Neurosci 14, 1142-1149.

25. Okabe, Y., and Medzhitov, R. (2016). Tissue biology perspective on macrophages. Nature immunology 17, 9-17.

26. Chovatiya, R., and Medzhitov, R. (2014). Stress, inflammation, and defense of homeostasis. Molecular cell 54, 281-288.

27. Wynn, T.A., Chawla, A., and Pollard, J.W. (2013). Macrophage biology in development, homeostasis and disease. Nature 496, 445-455.

28. Mosser, D.M., and Edwards, J.P. (2008). Exploring the full spectrum of macrophage activation. Nature reviews 8, 958-969.

29. Kawai, T., and Akira, S. (2010). The role of pattern-recognition receptors in innate immunity: update on Toll-like receptors. Nature immunology 11, 373-384.

30. Wynn, T.A., and Vannella, K.M. (2016). Macrophages in Tissue Repair, Regeneration, and Fibrosis. Immunity 44, 450-462.

31. Batista, F.D., and Harwood, N.E. (2009). The who, how and where of antigen presentation to B cells. Nature reviews 9, 15-27.

32. Hume, D.A. (2008). Macrophages as APC and the dendritic cell myth. J Immunol 181, 5829-5835.

33. Jantsch, J., Binger, K.J., Muller, D.N., and Titze, J. (2014). Macrophages in homeostatic immune function. Front Physiol 5, 146.

34. Pyonteck, S.M., Akkari, L., Schuhmacher, A.J., Bowman, R.L., Sevenich, L., Quail, D.F., Olson, O.C., Quick, M.L., Huse, J.T., Teijeiro, V., et al. (2013). CSF-1R inhibition alters macrophage polarization and blocks glioma progression. Nature medicine 19, 1264-1272.

35. Kim, J., Modlin, R.L., Moy, R.L., Dubinett, S.M., McHugh, T., Nickoloff, B.J., and Uyemura, K. (1995). IL-10 production in cutaneous basal and squamous cell carcinomas. A mechanism for evading the local T cell immune response. J Immunol 155, 2240-2247.

36. Mantovani, A., Sozzani, S., Locati, M., Allavena, P., and Sica, A. (2002). Macrophage polarization: tumor-associated macrophages as a paradigm for polarized M2 mononuclear phagocytes. Trends in immunology 23, 549-555.

37. Qian, B.Z., and Pollard, J.W. (2010). Macrophage diversity enhances tumor progression and metastasis. Cell 141, 39-51.

38. Dominguez-Soto, A., Sierra-Filardi, E., Puig-Kroger, A., Perez-Maceda, B., Gomez-Aguado, F., Corcuera, M.T., Sanchez-Mateos, P., and Corbi, A.L. (2011). Dendritic cell-specific ICAM-3-grabbing nonintegrin expression on M2-polarized and tumor-associated macrophages is macrophage-CSF dependent and enhanced by tumor-derived IL-6 and IL-10. J Immunol 186, 2192-2200.

39. Lin, E.Y., Nguyen, A.V., Russell, R.G., and Pollard, J.W. (2001). Colony-stimulating factor 1 promotes progression of mammary tumors to malignancy. The Journal of experimental medicine 193, 727-740.

40. Goswami, S., Sahai, E., Wyckoff, J.B., Cammer, M., Cox, D., Pixley, F.J., Stanley, E.R., Segall, J.E., and Condeelis, J.S. (2005). Macrophages promote the invasion of breast carcinoma cells via a colony-stimulating factor-1/epidermal growth factor paracrine loop. Cancer research 65, 5278-5283.

41. Gazzaniga, S., Bravo, A.I., Guglielmotti, A., van Rooijen, N., Maschi, F., Vecchi, A., Mantovani, A., Mordoh, J., and Wainstok, R. (2007). Targeting tumor-associated macrophages and inhibition of MCP-1 reduce angiogenesis and tumor growth in a human melanoma xenograft. The Journal of investigative dermatology 127, 2031-2041.

42. Zeisberger, S.M., Odermatt, B., Marty, C., Zehnder-Fjallman, A.H., Ballmer-Hofer, K., and Schwendener, R.A. (2006). Clodronate-liposome-mediated depletion of tumour-associated macrophages: a new and highly effective antiangiogenic therapy approach. British journal of cancer 95, 272-281.

43. Priceman, S.J., Sung, J.L., Shaposhnik, Z., Burton, J.B., Torres-Collado, A.X., Moughon, D.L., Johnson, M., Lusis, A.J., Cohen, D.A., Iruela-Arispe, M.L., et al. (2010). Targeting distinct tumor-infiltrating myeloid cells by inhibiting CSF-1 receptor: combating tumor evasion of antiangiogenic therapy. Blood 115, 1461-1471.

44. Zhang, C.C., Yan, Z., Zhang, Q., Kuszpit, K., Zasadny, K., Qiu, M., Painter, C.L., Wong, A., Kraynov, E., Arango, M.E., et al. (2010). PF-03732010: a fully human monoclonal antibody against P-cadherin with antitumor and antimetastatic activity. Clinical cancer research : an official journal of the American Association for Cancer Research 16, 5177-5188.

45. Steinbach, E.C., and Plevy, S.E. (2014). The role of macrophages and dendritic cells in the initiation of inflammation in IBD. Inflammatory bowel diseases 20, 166-175.

46. Udalova, I.A., Mantovani, A., and Feldmann, M. (2016). Macrophage heterogeneity in the context of rheumatoid arthritis. Nat Rev Rheumatol 12, 472-485.

47. Heppner, F.L., Ransohoff, R.M., and Becher, B. (2015). Immune attack: the role of inflammation in Alzheimer disease. Nature reviews Neuroscience 16, 358-372.

48. Tacke, F., and Zimmermann, H.W. (2014). Macrophage heterogeneity in liver injury and fibrosis. Journal of hepatology 60, 1090-1096.

49. Gosselin, D., Link, V.M., Romanoski, C.E., Fonseca, G.J., Eichenfield, D.Z., Spann, N.J., Stender, J.D., Chun, H.B., Garner, H., Geissmann, F., et al. (2014). Environment drives selection and function of enhancers controlling tissue-specific macrophage identities. Cell 159, 1327-1340.

50. Amit, I., Winter, D.R., and Jung, S. (2016). The role of the local environment and epigenetics in shaping macrophage identity and their effect on tissue homeostasis. Nature immunology 17, 18-25.

51. Ushach, I., and Zlotnik, A. (2016). Biological role of granulocyte macrophage colony-stimulating factor (GM-CSF) and macrophage colony-stimulating factor (M-CSF) on cells of the myeloid lineage. J Leukoc Biol.

52. Wang, Y., Szretter, K.J., Vermi, W., Gilfillan, S., Rossini, C., Cella, M., Barrow, A.D., Diamond, M.S., and Colonna, M. (2012). IL-34 is a tissue-restricted ligand of CSF1R required for the development of Langerhans cells and microglia. Nature immunology 13, 753-760.

53. Greter, M., Lelios, I., Pelczar, P., Hoeffel, G., Price, J., Leboeuf, M., Kundig, T.M., Frei, K., Ginhoux, F., Merad, M., et al. (2012). Stroma-derived interleukin-34 controls the development and maintenance of langerhans cells and the maintenance of microglia. Immunity 37, 1050-1060.

54. Cecchini, M.G., Dominguez, M.G., Mocci, S., Wetterwald, A., Felix, R., Fleisch, H., Chisholm, O., Hofstetter, W., Pollard, J.W., and Stanley, E.R. (1994). Role of colony stimulating factor-1 in the establishment and regulation of tissue macrophages during postnatal development of the mouse. Development (Cambridge, England) 120, 1357-1372.

55. Hamilton, J.A. (2008). Colony-stimulating factors in inflammation and autoimmunity. Nature reviews 8, 533-544.

56. Verreck, F.A., de Boer, T., Langenberg, D.M., Hoeve, M.A., Kramer, M., Vaisberg, E., Kastelein, R., Kolk, A., de Waal-Malefyt, R., and Ottenhoff, T.H. (2004). Human IL-23-producing type 1 macrophages promote but IL-10-producing type 2 macrophages subvert immunity to (myco)bacteria. Proceedings of the National Academy of Sciences of the United States of America 101, 4560-4565.

57. Fleetwood, A.J., Lawrence, T., Hamilton, J.A., and Cook, A.D. (2007). Granulocyte-macrophage colony-stimulating factor (CSF) and macrophage CSF-dependent macrophage phenotypes display differences in cytokine profiles and transcription factor activities: implications for CSF blockade in inflammation. J Immunol 178, 5245-5252.

58. Lacey, D.C., Achuthan, A., Fleetwood, A.J., Dinh, H., Roiniotis, J., Scholz, G.M., Chang, M.W., Beckman, S.K., Cook, A.D., and Hamilton, J.A. (2012). Defining GM-CSF- and Macrophage-CSF-Dependent Macrophage Responses by In Vitro Models. J Immunol 188, 5752-5765.

59. Kong, Y.Y., Yoshida, H., Sarosi, I., Tan, H.L., Timms, E., Capparelli, C., Morony, S., Oliveira-dos-Santos, A.J., Van, G., Itie, A., et al. (1999). OPGL is a key regulator of osteoclastogenesis, lymphocyte development and lymph-node organogenesis. Nature 397, 315-323.

60. Kim, J.H., and Kim, N. (2014). Regulation of NFATc1 in Osteoclast Differentiation. Journal of bone metabolism 21, 233-241.

61. Shibata, Y., Berclaz, P.Y., Chroneos, Z.C., Yoshida, M., Whitsett, J.A., and Trapnell, B.C. (2001). GM-CSF regulates alveolar macrophage differentiation and innate immunity in the lung through PU.1. Immunity 15, 557-567.

62. Schneider, C., Nobs, S.P., Kurrer, M., Rehrauer, H., Thiele, C., and Kopf, M. (2014). Induction of the nuclear receptor PPAR-gamma by the cytokine GM-CSF is critical for the differentiation of fetal monocytes into alveolar macrophages. Nature immunology 15, 1026-1037.

63. Okabe, Y., and Medzhitov, R. (2014). Tissue-specific signals control reversible program of localization and functional polarization of macrophages. Cell 157, 832-844.

64. N, A.G., Guillen, J.A., Gallardo, G., Diaz, M., de la Rosa, J.V., Hernandez, I.H., Casanova-Acebes, M., Lopez, F., Tabraue, C., Beceiro, S., et al. (2013). The nuclear receptor LXRαlpha controls the functional specialization of splenic macrophages. Nature immunology 14, 831-839.

65. Haldar, M., Kohyama, M., So, A.Y., Kc, W., Wu, X., Briseno, C.G., Satpathy, A.T., Kretzer, N.M., Arase, H., Rajasekaran, N.S., et al. (2014). Heme-mediated SPI-C induction promotes monocyte differentiation into iron-recycling macrophages. Cell 156, 1223-1234.

66. Muller, P.A., Koscso, B., Rajani, G.M., Stevanovic, K., Berres, M.L., Hashimoto, D., Mortha, A., Leboeuf, M., Li, X.M., Mucida, D., et al. (2014). Crosstalk between muscularis macrophages and enteric neurons regulates gastrointestinal motility. Cell 158, 300-313.

67. Kohyama, M., Ise, W., Edelson, B.T., Wilker, P.R., Hildner, K., Mejia, C., Frazier, W.A., Murphy, T.L., and Murphy, K.M. (2009). Role for Spi-C in the development of red pulp macrophages and splenic iron homeostasis. Nature 457, 318-321.

68. Lumeng, C.N., Bodzin, J.L., and Saltiel, A.R. (2007). Obesity induces a phenotypic switch in adipose tissue macrophage polarization. The Journal of clinical investigation 117, 175-184.

69. Thomassen, M.J., Barna, B.P., Malur, A.G., Bonfield, T.L., Farver, C.F., Malur, A., Dalrymple, H., Kavuru, M.S., and Febbraio, M. (2007). ABCG1 is deficient in alveolar macrophages of GM-CSF knockout mice and patients with pulmonary alveolar proteinosis. Journal of lipid research 48, 2762-2768.

70. Cappariello, A., Maurizi, A., Veeriah, V., and Teti, A. (2014). The Great Beauty of the osteoclast. Arch Biochem Biophys 558, 70-78.

71. Nilsson, S.K., and Bertoncello, I. (1994). The development and establishment of hemopoiesis in fetal and newborn osteopetrotic (op/op) mice. Developmental biology 164, 456-462.

72. Xue, J., Schmidt, S.V., Sander, J., Draffehn, A., Krebs, W., Quester, I., De Nardo, D., Gohel, T.D., Emde, M., Schmidleithner, L., et al. (2014). Transcriptome-based network analysis reveals a spectrum model of human macrophage activation. Immunity 40, 274-288.

73. Ginhoux, F., Schultze, J.L., Murray, P.J., Ochando, J., and Biswas, S.K. (2016). New insights into the multidimensional concept of macrophage ontogeny, activation and function. Nature immunology 17, 34-40.

74. Schultze, J.L., Freeman, T., Hume, D.A., and Latz, E. (2015). A transcriptional perspective on human macrophage biology. Seminars in immunology 27, 44-50.

75. Murray, P.J., Allen, J.E., Biswas, S.K., Fisher, E.A., Gilroy, D.W., Goerdt, S., Gordon, S., Hamilton, J.A., Ivashkiv, L.B., Lawrence, T., et al. (2014). Macrophage activation and polarization: nomenclature and experimental guidelines. Immunity 41, 14-20.

76. Martinez, F.O., and Gordon, S. (2014). The M1 and M2 paradigm of macrophage activation: time for reassessment. F1000prime reports 6, 13.

77. Sica, A., and Mantovani, A. (2012). Macrophage plasticity and polarization: in vivo veritas. J Clin Invest 122, 787-795.

78. Soler Palacios, B., Estrada-Capetillo, L., Izquierdo, E., Criado, G., Nieto, C., Municio, C., Gonzalez-Alvaro, I., Sanchez-Mateos, P., Pablos, J.L., Corbi, A.L., et al. (2015). Macrophages from the synovium of active rheumatoid arthritis exhibit an activin A-dependent pro-inflammatory profile. The Journal of pathology 235, 515-526.

79. Gonzalez-Dominguez, E., Samaniego, R., Flores-Sevilla, J.L., Campos-Campos, S.F., Gomez-Campos, G., Salas, A., Campos-Pena, V., Corbi, A.L., Sanchez-Mateos, P., and Sanchez-Torres, C. (2015). CD163L1 and CLEC5A discriminate subsets of human resident and inflammatory macrophages in vivo. Journal of leukocyte biology 98, 453-466.

80. Denning, T.L., Wang, Y.C., Patel, S.R., Williams, I.R., and Pulendran, B. (2007). Lamina propria macrophages and dendritic cells differentially induce regulatory and interleukin 17-producing T cell responses. Nature immunology 8, 1086-1094.

81. Biswas, S.K., Gangi, L., Paul, S., Schioppa, T., Saccani, A., Sironi, M., Bottazzi, B., Doni, A., Vincenzo, B., Pasqualini, F., et al. (2006). A distinct and unique transcriptional program expressed by tumor-associated macrophages (defective NF-kappaB and enhanced IRF-3/STAT1 activation). Blood 107, 2112-2122.

82. Shay, T., Jojic, V., Zuk, O., Rothamel, K., Puyraimond-Zemmour, D., Feng, T., Wakamatsu, E., Benoist, C., Koller, D., and Regev, A. (2013). Conservation and divergence in the transcriptional programs of the human and mouse immune systems. Proceedings of the National Academy of Sciences of the United States of America 110, 2946-2951.

83. Martinez, F.O., Helming, L., Milde, R., Varin, A., Melgert, B.N., Draijer, C., Thomas, B., Fabbri, M., Crawshaw, A., Ho, L.P., et al. (2013). Genetic programs expressed in resting and IL-4 alternatively activated mouse and human macrophages: similarities and differences. Blood 121, e57-69.

84. Schroder, K., Irvine, K.M., Taylor, M.S., Bokil, N.J., Le Cao, K.A., Masterman, K.A., Labzin, L.I., Semple, C.A., Kapetanovic, R., Fairbairn, L., et al. (2012). Conservation and divergence in Toll-like receptor 4-regulated gene expression in primary human versus mouse macrophages. Proceedings of the National Academy of Sciences of the United States of America 109, E944-953.

85. Mestas, J., and Hughes, C.C. (2004). Of mice and not men: differences between mouse and human immunology. J Immunol 172, 2731-2738.

86. Seok, J., Warren, H.S., Cuenca, A.G., Mindrinos, M.N., Baker, H.V., Xu, W., Richards, D.R., McDonald-Smith, G.P., Gao, H., Hennessy, L., et al. (2013). Genomic responses in mouse models poorly mimic human inflammatory diseases. Proceedings of the National Academy of Sciences of the United States of America 110, 3507-3512.

87. Ullah, M.O., Sweet, M.J., Mansell, A., Kellie, S., and Kobe, B. (2016). TRIF-dependent TLR signaling, its functions in host defense and inflammation, and its potential as a therapeutic target. Journal of leukocyte biology 100, 27-45.

88. Janeway, C.A., Jr., and Medzhitov, R. (2002). Innate immune recognition. Annual review of immunology 20, 197-216.

89. Bryant, C.E., Gay, N.J., Heymans, S., Sacre, S., Schaefer, L., and Midwood, K.S. (2015). Advances in Toll-like receptor biology: Modes of activation by diverse stimuli. Critical reviews in biochemistry and molecular biology 50, 359-379.

90. Akira, S., and Takeda, K. (2004). Toll-like receptor signalling. Nature reviews 4, 499-511.

91. Colegio, O.R., and Medzhitov, R. (2012). TLR Signaling and Tumour-Associated Macrophages. In Tumour-Associated Macrophages, T. Lawrence and T. Hagemann, eds. (New York, NY, Springer New York), pp 119-133.

92. Takeda, K., and Akira, S. (2004). TLR signaling pathways. Seminars in immunology 16, 3-9.

93. Agrawal, A., Dillon, S., Denning, T.L., and Pulendran, B. (2006). ERK1-/- mice exhibit Th1 cell polarization and increased susceptibility to experimental autoimmune encephalomyelitis. J Immunol 176, 5788-5796.

94. Ma, W., Lim, W., Gee, K., Aucoin, S., Nandan, D., Kozlowski, M., Diaz-Mitoma, F., and Kumar, A. (2001). The p38 mitogen-activated kinase pathway regulates the human interleukin-10 promoter via the activation of Sp1 transcription factor in lipopolysaccharide-stimulated human macrophages. The Journal of biological chemistry 276, 13664-13674.

95. Fleetwood, A.J., Dinh, H., Cook, A.D., Hertzog, P.J., and Hamilton, J.A. (2009). GM-CSF- and M-CSF-dependent macrophage phenotypes display differential dependence on type I interferon signaling. Journal of leukocyte biology 86, 411-421.

96. Eychene, A., Rocques, N., and Pouponnot, C. (2008). A new MAFia in cancer. Nature reviews 8, 683-693.

97. Kataoka, K., Fujiwara, K.T., Noda, M., and Nishizawa, M. (1994). MafB, a new Maf family transcription activator that can associate with Maf and Fos but not with Jun. Molecular and cellular biology 14, 7581-7591.

98. Tillmanns, S., Otto, C., Jaffray, E., Du Roure, C., Bakri, Y., Vanhille, L., Sarrazin, S., Hay, R.T., and Sieweke, M.H. (2007). SUMO modification regulates MafB-driven macrophage differentiation by enabling Myb-dependent transcriptional repression. Molecular and cellular biology 27, 5554-5564.

99. Kim, K., Kim, J.H., Lee, J., Jin, H.M., Kook, H., Kim, K.K., Lee, S.Y., and Kim, N. (2007). MafB negatively regulates RANKL-mediated osteoclast differentiation. Blood 109, 3253-3259.

100. Zhang, Y., Chen, Q., and Ross, A.C. (2012). Retinoic acid and tumor necrosis factor-alpha induced monocytic cell gene expression is regulated in part by induction of transcription factor MafB. Exp Cell Res 318, 2407-2416.

101. Dieterich, L.C., Klein, S., Mathelier, A., Sliwa-Primorac, A., Ma, Q., Hong, Y.K., Shin, J.W., Hamada, M., Lizio, M., Itoh, M., et al. (2015). DeepCAGE Transcriptomics Reveal an Important Role of the Transcription Factor MAFB in the Lymphatic Endothelium. Cell Rep 13, 1493-1504.

102. Gemelli, C., Zanocco Marani, T., Bicciato, S., Mazza, E.M., Boraschi, D., Salsi, V., Zappavigna, V., Parenti, S., Selmi, T., Tagliafico, E., et al. (2014). MafB is a downstream target of the IL-10/STAT3 signaling pathway, involved in the regulation of macrophage de-activation. Biochim Biophys Acta 1843, 955-964.

103. Gemelli, C., Orlandi, C., Zanocco Marani, T., Martello, A., Vignudelli, T., Ferrari, F., Montanari, M., Parenti, S., Testa, A., Grande, A., et al. (2008). The vitamin D3/Hox-A10 pathway supports MafB function during the monocyte differentiation of human CD34+ hemopoietic progenitors. J Immunol 181, 5660-5672.

104. Niceta, M., Stellacci, E., Gripp, K.W., Zampino, G., Kousi, M., Anselmi, M., Traversa, A., Ciolfi, A., Stabley, D., Bruselles, A., et al. (2015). Mutations Impairing GSK3-Mediated MAF Phosphorylation Cause Cataract, Deafness, Intellectual Disability, Seizures, and a Down Syndrome-like Facies. Am J Hum Genet 96, 816-825.

105. Rocques, N., Abou Zeid, N., Sii-Felice, K., Lecoin, L., Felder-Schmittbuhl, M.P., Eychene, A., and Pouponnot, C. (2007). GSK-3-mediated phosphorylation enhances Maf-transforming activity. Molecular cell 28, 584-597.

106. Tanahashi, H., Kito, K., Ito, T., and Yoshioka, K. (2010). MafB protein stability is regulated by the JNK and ubiquitin-proteasome pathways. Arch Biochem Biophys 494, 94-100.

107. Sii-Felice, K., Pouponnot, C., Gillet, S., Lecoin, L., Girault, J.A., Eychene, A., and Felder-Schmittbuhl, M.P. (2005). MafA transcription factor is phosphorylated by p38 MAP kinase. FEBS letters 579, 3547-3554.

108. Cordes, S.P., and Barsh, G.S. (1994). The mouse segmentation gene kr encodes a novel basic domain-leucine zipper transcription factor. Cell 79, 1025-1034.

109. Conrad, E., Dai, C., Spaeth, J., Guo, M., Cyphert, H.A., Scoville, D., Carroll, J., Yu, W.M., Goodrich, L.V., Harlan, D.M., et al. (2016). The MAFB transcription factor impacts islet alpha-cell function in rodents and represents a unique signature of primate islet beta-cells. Am J Physiol Endocrinol Metab 310, E91-E102.

110. Hang, Y., and Stein, R. (2011). MafA and MafB activity in pancreatic beta cells. Trends Endocrinol Metab 22, 364-373.

111. Lopez-Pajares, V., Qu, K., Zhang, J., Webster, D.E., Barajas, B.C., Siprashvili, Z., Zarnegar, B.J., Boxer, L.D., Rios, E.J., Tao, S., et al. (2015). A LncRNA-MAF:MAFB transcription factor network regulates epidermal differentiation. Dev Cell 32, 693-706.

112. Zhang, Y., and Ross, A.C. (2013). Retinoic acid and the transcription factor MafB act together and differentially to regulate aggrecan and matrix metalloproteinase gene expression in neonatal chondrocytes. Journal of cellular biochemistry 114, 471-479.

113. Moriguchi, T., Hamada, M., Morito, N., Terunuma, T., Hasegawa, K., Zhang, C., Yokomizo, T., Esaki, R., Kuroda, E., Yoh, K., et al. (2006). MafB is essential for renal development and F4/80 expression in macrophages. Molecular and cellular biology 26, 5715-5727.

114. Morito, N., Yoh, K., Ojima, M., Okamura, M., Nakamura, M., Hamada, M., Shimohata, H., Moriguchi, T., Yamagata, K., and Takahashi, S. (2014). Overexpression of Mafb in podocytes protects against diabetic nephropathy. J Am Soc Nephrol 25, 2546-2557.

115. Kann, M., Ettou, S., Jung, Y.L., Lenz, M.O., Taglienti, M.E., Park, P.J., Schermer, B., Benzing, T., and Kreidberg, J.A. (2015). Genome-Wide Analysis of Wilms' Tumor 1-Controlled Gene Expression in Podocytes Reveals Key Regulatory Mechanisms. J Am Soc Nephrol 26, 2097-2104.

116. Dong, L., Pietsch, S., and Englert, C. (2015). Towards an understanding of kidney diseases associated with WT1 mutations. Kidney Int 88, 684-690.

117. Kim, H., and Seed, B. (2010). The transcription factor MafB antagonizes antiviral responses by blocking recruitment of coactivators to the transcription factor IRF3. Nature immunology 11, 743-750.

118. Sieweke, M.H., Tekotte, H., Frampton, J., and Graf, T. (1996). MafB is an interaction partner and repressor of Ets-1 that inhibits erythroid differentiation. Cell 85, 49-60.

119. Kelly, L.M., Englmeier, U., Lafon, I., Sieweke, M.H., and Graf, T. (2000). MafB is an inducer of monocytic differentiation. The EMBO journal 19, 1987-1997.

120. Gemelli, C., Montanari, M., Tenedini, E., Zanocco Marani, T., Vignudelli, T., Siena, M., Zini, R., Salati, S., Tagliafico, E., Manfredini, R., et al. (2006). Virally mediated MafB transduction induces the monocyte commitment of human CD34+ hematopoietic stem/progenitor cells. Cell Death Differ 13, 1686-1696.

121. Sarrazin, S., Mossadegh-Keller, N., Fukao, T., Aziz, A., Mourcin, F., Vanhille, L., Kelly Modis, L., Kastner, P., Chan, S., Duprez, E., et al. (2009). MafB restricts M-CSF-dependent myeloid commitment divisions of hematopoietic stem cells. Cell 138, 300-313.

122. Bakri, Y., Sarrazin, S., Mayer, U.P., Tillmanns, S., Nerlov, C., Boned, A., and Sieweke, M.H. (2005). Balance of MafB and PU.1 specifies alternative macrophage or dendritic cell fate. Blood 105, 2707-2716.

123. Blanchi, B., Kelly, L.M., Viemari, J.C., Lafon, I., Burnet, H., Bevengut, M., Tillmanns, S., Daniel, L., Graf, T., Hilaire, G., et al. (2003). MafB deficiency causes defective respiratory rhythmogenesis and fatal central apnea at birth. Nat Neurosci 6, 1091-1100.

124. Aziz, A., Vanhille, L., Mohideen, P., Kelly, L.M., Otto, C., Bakri, Y., Mossadegh, N., Sarrazin, S., and Sieweke, M.H. (2006). Development of macrophages with altered actin organization in the absence of MafB. Molecular and cellular biology 26, 6808-6818.

125. Aziz, A., Soucie, E., Sarrazin, S., and Sieweke, M.H. (2009). MafB/c-Maf deficiency enables self-renewal of differentiated functional macrophages. Science (New York, NY 326, 867-871.

126. Park, J.G., Tischfield, M.A., Nugent, A.A., Cheng, L., Di Gioia, S.A., Chan, W.M., Maconachie, G., Bosley, T.M., Summers, C.G., Hunter, D.G., et al. (2016). Loss of MAFB Function in Humans and Mice Causes Duane Syndrome, Aberrant Extraocular Muscle Innervation, and Inner-Ear Defects. Am J Hum Genet 98, 1220-1227.

127. Stralen, E., Leguit, R.J., Begthel, H., Michaux, L., Buijs, A., Lemmens, H., Scheiff, J.M., Doyen, C., Pierre, P., Forget, F., et al. (2009). MafB oncoprotein detected by immunohistochemistry as a highly sensitive and specific marker for the prognostic unfavorable t(14;20) (q32;q12) in multiple myeloma patients. Leukemia 23, 801-803.

128. Lee, L.C., Zhang, A.Y., Chong, A.K., Pham, H., Longaker, M.T., and Chang, J. (2006). Expression of a novel gene, MafB, in Dupuytren's disease. J Hand Surg Am 31, 211-218.

129. Hamada, M., Nakamura, M., Tran, M.T., Moriguchi, T., Hong, C., Ohsumi, T., Dinh, T.T., Kusakabe, M., Hattori, M., Katsumata, T., et al. (2014). MafB promotes atherosclerosis by inhibiting foam-cell apoptosis. Nat Commun 5, 3147.

130. Sadl, V., Jin, F., Yu, J., Cui, S., Holmyard, D., Quaggin, S., Barsh, G., and Cordes, S. (2002). The mouse Kreisler (Krml1/MafB) segmentation gene is required for differentiation of glomerular visceral epithelial cells. Developmental biology 249, 16-29.

131. Aida, Y., Shibata, Y., Abe, S., Inoue, S., Kimura, T., Igarashi, A., Yamauchi, K., Nunomiya, K., Kishi, H., Nemoto, T., et al. (2014). Inhibition of elastase-pulmonary emphysema in dominant-negative MafB transgenic mice. Int J Biol Sci 10, 882-894.

132. Pettersson, A.M., Acosta, J.R., Bjork, C., Kratzel, J., Stenson, B., Blomqvist, L., Viguerie, N., Langin, D., Arner, P., and Laurencikiene, J. (2015). MAFB as a novel regulator of human adipose tissue inflammation. Diabetologia 58, 2115-2123.

133. Zankl, A., Duncan, E.L., Leo, P.J., Clark, G.R., Glazov, E.A., Addor, M.C., Herlin, T., Kim, C.A., Leheup, B.P., McGill, J., et al. (2012). Multicentric carpotarsal osteolysis is caused by mutations clustering in the amino-terminal transcriptional activation domain of MAFB. Am J Hum Genet 90, 494-501.

134. Mehawej, C., Courcet, J.B., Baujat, G., Mouy, R., Gerard, M., Landru, I., Gosselin, M., Koehrer, P., Mousson, C., Breton, S., et al. (2013). The identification of MAFB mutations in eight patients with multicentric carpo-tarsal osteolysis supports genetic homogeneity but clinical variability. Am J Med Genet A 161A, 3023-3029.

135. Mumm, S., Huskey, M., Duan, S., Wenkert, D., Madson, K.L., Gottesman, G.S., Nenninger, A.R., Laxer, R.M., McAlister, W.H., and Whyte, M.P. (2014). Multicentric carpotarsal osteolysis syndrome is caused by only a few domain-specific mutations in MAFB, a negative regulator of RANKL-induced osteoclastogenesis. Am J Med Genet A 164A, 2287-2293.

136. Urlus, M., Roosen, P., Lammens, J., Victor, J., De Smet, L., Molenaers, G., and Fabry, G. (1993). Carpo-tarsal osteolysis. Case report and review of the literature. Genetic counseling (Geneva, Switzerland) 4, 25-36.

137. Dworschak, G.C., Draaken, M., Hilger, A., Born, M., Reutter, H., and Ludwig, M. (2013). An incompletely penetrant novel MAFB (p.Ser56Phe) variant in autosomal dominant multicentric carpotarsal osteolysis syndrome. Int J Mol Med 32, 174-178.

138. Sierra-Filardi, E., Puig-Kroger, A., Blanco, F.J., Nieto, C., Bragado, R., Palomero, M.I., Bernabeu, C., Vega, M.A., and Corbi, A.L. (2011). Activin A skews macrophage polarization by promoting a proinflammatory phenotype and inhibiting the acquisition of anti-inflammatory macrophage markers. Blood 117, 5092-5101.

139. Kawai, T., and Akira, S. (2011). Toll-like receptors and their crosstalk with other innate receptors in infection and immunity. Immunity 34, 637-650.

140. Joosten, L.A., Abdollahi-Roodsaz, S., Dinarello, C.A., O'Neill, L., and Netea, M.G. (2016). Toll-like receptors and chronic inflammation in rheumatic diseases: new developments. Nat Rev Rheumatol 12, 344-357.

141. Favata, M.F., Horiuchi, K.Y., Manos, E.J., Daulerio, A.J., Stradley, D.A., Feeser, W.S., Van Dyk, D.E., Pitts, W.J., Earl, R.A., Hobbs, F., et al. (1998). Identification of a novel inhibitor of mitogen-activated protein kinase kinase. The Journal of biological chemistry 273, 18623-18632.

142. Bennett, B.L., Sasaki, D.T., Murray, B.W., O'Leary, E.C., Sakata, S.T., Xu, W., Leisten, J.C., Motiwala, A., Pierce, S., Satoh, Y., et al. (2001). SP600125, an anthrapyrazolone inhibitor of Jun N-terminal kinase. Proceedings of the National Academy of Sciences of the United States of America 98, 13681-13686.

143. Kuma, Y., Sabio, G., Bain, J., Shpiro, N., Marquez, R., and Cuenda, A. (2005). BIRB796 inhibits all p38 MAPK isoforms in vitro and in vivo. The Journal of biological chemistry 280, 19472-19479.

144. Heldin, C.H., and Westermark, B. (1999). Mechanism of action and in vivo role of platelet-derived growth factor. Physiol Rev 79, 1283-1316.

145. Rothhammer, V., Mascanfroni, I.D., Bunse, L., Takenaka, M.C., Kenison, J.E., Mayo, L., Chao, C.C., Patel, B., Yan, R., Blain, M., et al. (2016). Type I interferons and microbial metabolites of tryptophan modulate astrocyte activity and central nervous system inflammation via the aryl hydrocarbon receptor. Nature medicine 22, 586-597.

146. Zadjali, F., Santana-Farre, R., Vesterlund, M., Carow, B., Mirecki-Garrido, M., Hernandez-Hernandez, I., Flodstrom-Tullberg, M., Parini, P., Rottenberg, M., Norstedt, G., et al. (2012). SOCS2 deletion protects against hepatic steatosis but worsens insulin resistance in high-fat-diet-fed mice. FASEB J 26, 3282-3291.

147. Posselt, G., Schwarz, H., Duschl, A., and Horejs-Hoeck, J. (2011). Suppressor of cytokine signaling 2 is a feedback inhibitor of TLR-induced activation in human monocyte-derived dendritic cells. J Immunol 187, 2875-2884.

148. Vukicevic, S., and Grgurevic, L. (2009). BMP-6 and mesenchymal stem cell differentiation. Cytokine & growth factor reviews 20, 441-448.

149. Jenkins, S.J., and Hume, D.A. (2014). Homeostasis in the mononuclear phagocyte system. Trends in immunology 35, 358-367.

150. de las Casas-Engel, M., Dominguez-Soto, A., Sierra-Filardi, E., Bragado, R., Nieto, C., Puig-Kroger, A., Samaniego, R., Loza, M., Corcuera, M.T., Gomez-Aguado, F., et al. (2013). Serotonin skews human macrophage polarization through HTR2B and HTR7. J Immunol 190, 2301-2310.

151. Gonzalez-Dominguez, E., Dominguez-Soto, A., Nieto, C., Flores-Sevilla, J.L., Pacheco-Blanco, M., Campos-Pena, V., Meraz-Rios, M.A., Vega, M.A., Corbi, A.L., and Sanchez-Torres, C. (2016). Atypical Activin A and IL-10 Production Impairs Human CD16+ Monocyte Differentiation into Anti-Inflammatory Macrophages. J Immunol 196, 1327-1337.

152. Sierra-Filardi, E., Nieto, C., Dominguez-Soto, A., Barroso, R., Sanchez-Mateos, P., Puig-Kroger, A., Lopez-Bravo, M., Joven, J., Ardavin, C., Rodriguez-Fernandez, J.L., et al. (2014). CCL2 shapes macrophage polarization by GM-CSF and M-CSF: identification of CCL2/CCR2-dependent gene expression profile. J Immunol 192, 3858-3867.

153. Kzhyshkowska, J., Workman, G., Cardo-Vila, M., Arap, W., Pasqualini, R., Gratchev, A., Krusell, L., Goerdt, S., and Sage, E.H. (2006). Novel function of alternatively activated macrophages: stabilin-1-mediated clearance of SPARC. J Immunol 176, 5825-5832.

154. Chen, E.Y., Tan, C.M., Kou, Y., Duan, Q., Wang, Z., Meirelles, G.V., Clark, N.R., and Ma'ayan, A. (2013). Enrichr: interactive and collaborative HTML5 gene list enrichment analysis tool. BMC Bioinformatics 14, 128.

155. Kuleshov, M.V., Jones, M.R., Rouillard, A.D., Fernandez, N.F., Duan, Q., Wang, Z., Koplev, S., Jenkins, S.L., Jagodnik, K.M., Lachmann, A., et al. (2016). Enrichr: a comprehensive gene set enrichment analysis web server 2016 update. Nucleic acids research 44, W90-W97.

156. Henning, P., Conaway, H.H., and Lerner, U.H. (2015). Retinoid receptors in bone and their role in bone remodeling. Front Endocrinol (Lausanne) 6, 31.

157. Soucie, E.L., Weng, Z., Geirsdottir, L., Molawi, K., Maurizio, J., Fenouil, R., Mossadegh-Keller, N., Gimenez, G., VanHille, L., Beniazza, M., et al. (2016). Lineage-specific enhancers activate self-renewal genes in macrophages and embryonic stem cells. Science (New York, NY 351, aad5510.

158. Anta Martínez, L.V.R., A.; Pombo Expósito, S.; Sines Castro, F. (2011). Osteolisis Carpo-Tarsal Multicéntrica. XX Congreso Hispano Luso de Cirugía de la mano.

159. Faber, M.R., Verlaak, R., Fiselier, T.J., Hamel, B.C., Franssen, M.J., and Gerrits, G.P. (2004). Inherited multicentric osteolysis with carpal-tarsal localisation mimicking juvenile idiopathic arthritis. Eur J Pediatr 163, 612-618.

160. Escribese, M.M., Sierra-Filardi, E., Nieto, C., Samaniego, R., Sanchez-Torres, C., Matsuyama, T., Calderon-Gomez, E., Vega, M.A., Salas, A., Sanchez-Mateos, P., et al. (2012). The prolyl hydroxylase PHD3 identifies proinflammatory macrophages and its expression is regulated by activin A. J Immunol 189, 1946-1954.

161. Ruffell, B., and Coussens, L.M. (2015). Macrophages and therapeutic resistance in cancer. Cancer Cell 27, 462-472.

162. Rivollier, A., He, J., Kole, A., Valatas, V., and Kelsall, B.L. (2012). Inflammation switches the differentiation program of Ly6Chi monocytes from antiinflammatory macrophages to inflammatory dendritic cells in the colon. The Journal of experimental medicine 209, 139-155.

163. Bulger, M., and Palis, J. (2015). Environmentally-defined enhancer populations regulate diversity of tissue-resident macrophages. Trends in immunology 36, 61-62.

164. Schultze, J.L. (2016). Reprogramming of macrophages--new opportunities for therapeutic targeting. Current opinion in pharmacology 26, 10-15.

165. Martinez, F.O., Gordon, S., Locati, M., and Mantovani, A. (2006). Transcriptional profiling of the human monocyte-to-macrophage differentiation and polarization: new molecules and patterns of gene expression. J Immunol 177, 7303-7311.

166. Elder, D.E. (2006). Precursors to melanoma and their mimics: nevi of special sites. Modern pathology : an official journal of the United States and Canadian Academy of Pathology, Inc 19 Suppl 2, S4-20.

167. Goldstein, A.M., and Tucker, M.A. (2013). Dysplastic nevi and melanoma. Cancer epidemiology, biomarkers & prevention : a publication of the American Association for Cancer Research, cosponsored by the American Society of Preventive Oncology 22, 528-532.

168. Scope, A., Marchetti, M.A., Marghoob, A.A., Dusza, S.W., Geller, A.C., Satagopan, J.M., Weinstock, M.A., Berwick, M., and Halpern, A.C. (2016). The study of nevi in children: Principles learned and implications for melanoma diagnosis. Journal of the American Academy of Dermatology 75, 813-823.

169. Zigmond, E., and Jung, S. (2013). Intestinal macrophages: well educated exceptions from the rule. Trends in immunology 34, 162-168.

170. Mantovani, A., and Allavena, P. (2015). The interaction of anticancer therapies with tumor-associated macrophages. The Journal of experimental medicine 212, 435-445.

171. Mooi, W.J., and Peeper, D.S. (2006). Oncogene-induced cell senescence--halting on the road to cancer. The New England journal of medicine 355, 1037-1046.

172. Munoz-Espin, D., Canamero, M., Maraver, A., Gomez-Lopez, G., Contreras, J., Murillo-Cuesta, S., Rodriguez-Baeza, A., Varela-Nieto, I., Ruberte, J., Collado, M., et al. (2013). Programmed cell senescence during mammalian embryonic development. Cell 155, 1104-1118.

173. Storer, M., Mas, A., Robert-Moreno, A., Pecoraro, M., Ortells, M.C., Di Giacomo, V., Yosef, R., Pilpel, N., Krizhanovsky, V., Sharpe, J., et al. (2013). Senescence is a developmental mechanism that contributes to embryonic growth and patterning. Cell 155, 1119-1130.

174. Kang, T.W., Yevsa, T., Woller, N., Hoenicke, L., Wuestefeld, T., Dauch, D., Hohmeyer, A., Gereke, M., Rudalska, R., Potapova, A., et al. (2011). Senescence surveillance of pre-malignant hepatocytes limits liver cancer development. Nature 479, 547-551.

175. Xue, W., Zender, L., Miething, C., Dickins, R.A., Hernando, E., Krizhanovsky, V., Cordon-Cardo, C., and Lowe, S.W. (2007). Senescence and tumour clearance is triggered by p53 restoration in murine liver carcinomas. Nature 445, 656-660.

176. Davalos, A.R., Kawahara, M., Malhotra, G.K., Schaum, N., Huang, J., Ved, U., Beausejour, C.M., Coppe, J.P., Rodier, F., and Campisi, J. (2013). p53-dependent release of Alarmin HMGB1 is a central mediator of senescent phenotypes. The Journal of cell biology 201, 613-629.

177. Ivanov, S., Dragoi, A.M., Wang, X., Dallacosta, C., Louten, J., Musco, G., Sitia, G., Yap, G.S., Wan, Y., Biron, C.A., et al. (2007). A novel role for HMGB1 in TLR9-mediated inflammatory responses to CpG-DNA. Blood 110, 1970-1981.

178. Park, J.S., Svetkauskaite, D., He, Q., Kim, J.Y., Strassheim, D., Ishizaka, A., and Abraham, E. (2004). Involvement of toll-like receptors 2 and 4 in cellular activation by high mobility group box 1 protein. The Journal of biological chemistry 279, 7370-7377.

179. Huber, R., Meier, B., Otsuka, A., Fenini, G., Satoh, T., Gehrke, S., Widmer, D., Levesque, M.P., Mangana, J., Kerl, K., et al. (2016). Tumour hypoxia promotes melanoma growth and metastasis via High Mobility Group Box-1 and M2-like macrophages. Sci Rep 6, 29914.

180. Hauser, M.A., and Legler, D.F. (2016). Common and biased signaling pathways of the chemokine receptor CCR7 elicited by its ligands CCL19 and CCL21 in leukocytes. Journal of leukocyte biology 99, 869-882.

181. Comerford, I., Harata-Lee, Y., Bunting, M.D., Gregor, C., Kara, E.E., and McColl, S.R. (2013). A myriad of functions and complex regulation of the CCR7/CCL19/CCL21 chemokine axis in the adaptive immune system. Cytokine & growth factor reviews 24, 269-283.

182. Noor, S., and Wilson, E.H. (2012). Role of C-C chemokine receptor type 7 and its ligands during neuroinflammation. J Neuroinflammation 9, 77.

183. Otero, C., Groettrup, M., and Legler, D.F. (2006). Opposite fate of endocytosed CCR7 and its ligands: recycling versus degradation. J Immunol 177, 2314-2323.

184. Bardi, G., Lipp, M., Baggiolini, M., and Loetscher, P. (2001). The T cell chemokine receptor CCR7 is internalized on stimulation with ELC, but not with SLC. European journal of immunology 31, 3291-3297.

185. Kohout, T.A., Nicholas, S.L., Perry, S.J., Reinhart, G., Junger, S., and Struthers, R.S. (2004). Differential desensitization, receptor phosphorylation, beta-arrestin recruitment, and ERK1/2 activation by the two endogenous ligands for the CC chemokine receptor 7. The Journal of biological chemistry 279, 23214-23222.

186. Letellier, E., and Haan, S. (2016). SOCS2: physiological and pathological functions. Front Biosci (Elite Ed) 8, 189-204.

187. McBerry, C., Gonzalez, R.M., Shryock, N., Dias, A., and Aliberti, J. (2012). SOCS2-induced proteasome-dependent TRAF6 degradation: a common anti-inflammatory pathway for control of innate immune responses. PloS one 7, e38384.

188. Machado, F.S., Esper, L., Dias, A., Madan, R., Gu, Y., Hildeman, D., Serhan, C.N., Karp, C.L., and Aliberti, J. (2008). Native and aspirin-triggered lipoxins control innate immunity by inducing proteasomal degradation of TRAF6. The Journal of experimental medicine 205, 1077-1086.

189. Machado, F.S., Johndrow, J.E., Esper, L., Dias, A., Bafica, A., Serhan, C.N., and Aliberti, J. (2006). Anti-inflammatory actions of lipoxin A4 and aspirin-triggered lipoxin are SOCS-2 dependent. Nature medicine 12, 330-334.

190. de Andres, M.C., Imagawa, K., Hashimoto, K., Gonzalez, A., Goldring, M.B., Roach, H.I., and Oreffo, R.O. (2011). Suppressors of cytokine signalling (SOCS) are reduced in osteoarthritis. Biochemical and biophysical research communications 407, 54-59.

191. Pollard, J.W. (2009). Trophic macrophages in development and disease. Nature reviews 9, 259-270.

192. Farooqi, A.A., Waseem, S., Riaz, A.M., Dilawar, B.A., Mukhtar, S., Minhaj, S., Waseem, M.S., Daniel, S., Malik, B.A., Nawaz, A., et al. (2011). PDGF: the nuts and bolts of signalling toolbox. Tumour biology : the journal of the International Society for Oncodevelopmental Biology and Medicine 32, 1057-1070.

193. Heldin, C.H. (2013). Targeting the PDGF signaling pathway in tumor treatment. Cell communication and signaling : CCS 11, 97.

194. Buchbinder, E.I., Sosman, J.A., Lawrence, D.P., McDermott, D.F., Ramaiya, N.H., Van den Abbeele, A.D., Linette, G.P., Giobbie-Hurder, A., and Hodi, F.S. (2015). Phase 2 study of sunitinib in patients with metastatic mucosal or acral melanoma. Cancer 121, 4007-4015.

195. Pasonen-Seppanen, S., Takabe, P., Edward, M., Rauhala, L., Rilla, K., Tammi, M., and Tammi, R. (2012). Melanoma cell-derived factors stimulate hyaluronan synthesis in dermal fibroblasts by upregulating HAS2 through PDGFR-PI3K-AKT and p38 signaling. Histochemistry and cell biology 138, 895-911.

196. Willenberg, A., Saalbach, A., Simon, J.C., and Anderegg, U. (2012). Melanoma cells control HA synthesis in peritumoral fibroblasts via PDGF-AA and PDGF-CC: impact on melanoma cell proliferation. The Journal of investigative dermatology 132, 385-393.

197. Meynard, D., Kautz, L., Darnaud, V., Canonne-Hergaux, F., Coppin, H., and Roth, M.P. (2009). Lack of the bone morphogenetic protein BMP6 induces massive iron overload. Nat Genet 41, 478-481.

198. Hentze, M.W., Muckenthaler, M.U., Galy, B., and Camaschella, C. (2010). Two to tango: regulation of Mammalian iron metabolism. Cell 142, 24-38.

199. Soares, M.P., and Hamza, I. (2016). Macrophages and Iron Metabolism. Immunity 44, 492-504.

200. Le, N.T., and Richardson, D.R. (2002). The role of iron in cell cycle progression and the proliferation of neoplastic cells. Biochim Biophys Acta 1603, 31-46.

201. Otterbein, L.E., Soares, M.P., Yamashita, K., and Bach, F.H. (2003). Heme oxygenase-1: unleashing the protective properties of heme. Trends in immunology 24, 449-455.

202. Torti, S.V., and Torti, F.M. (2013). Iron and cancer: more ore to be mined. Nature reviews 13, 342-355.

203. Zhang, S., Chen, Y., Guo, W., Yuan, L., Zhang, D., Xu, Y., Nemeth, E., Ganz, T., and Liu, S. (2014). Disordered hepcidin-ferroportin signaling promotes breast cancer growth. Cellular signalling 26, 2539-2550.

204. Sierra-Filardi, E., Vega, M.A., Sanchez-Mateos, P., Corbi, A.L., and Puig-Kroger, A. (2010). Heme Oxygenase-1 expression in M-CSF-polarized M2 macrophages contributes to LPS-induced IL-10 release. Immunobiology 215, 788-795.

205. Bersten, D.C., Sullivan, A.E., Peet, D.J., and Whitelaw, M.L. (2013). bHLH-PAS proteins in cancer. Nature reviews 13, 827-841.

206. Keith, B., Adelman, D.M., and Simon, M.C. (2001). Targeted mutation of the murine arylhydrocarbon receptor nuclear translocator 2 (Arnt2) gene reveals partial redundancy with Arnt. Proceedings of the National Academy of Sciences of the United States of America 98, 6692-6697.

207. Hao, N., Bhakti, V.L., Peet, D.J., and Whitelaw, M.L. (2013). Reciprocal regulation of the basic helix-loop-helix/Per-Arnt-Sim partner proteins, Arnt and Arnt2, during neuronal differentiation. Nucleic acids research 41, 5626-5638.

208. Sekine, H., Mimura, J., Yamamoto, M., and Fujii-Kuriyama, Y. (2006). Unique and overlapping transcriptional roles of arylhydrocarbon receptor nuclear translocator (Arnt) and Arnt2 in xenobiotic and hypoxic responses. The Journal of biological chemistry 281, 37507-37516.

209. Dougherty, E.J., and Pollenz, R.S. (2008). Analysis of Ah receptor-ARNT and Ah receptor-ARNT2 complexes in vitro and in cell culture. Toxicological sciences : an official journal of the Society of Toxicology 103, 191-206.

210. Hankinson, O. (2008). Why does ARNT2 behave differently from ARNT? Toxicological sciences : an official journal of the Society of Toxicology 103, 1-3.

211. Izquierdo, E., Cuevas, V.D., Fernandez-Arroyo, S., Riera-Borrull, M., Orta-Zavalza, E., Joven, J., Rial, E., Corbi, A.L., and Escribese, M.M. (2015). Reshaping of Human Macrophage Polarization through Modulation of Glucose Catabolic Pathways. J Immunol 195, 2442-2451.

212. Vicente-Duenas, C., Romero-Camarero, I., Gonzalez-Herrero, I., Alonso-Escudero, E., Abollo-Jimenez, F., Jiang, X., Gutierrez, N.C., Orfao, A., Marin, N., Villar, L.M., et al. (2012). A novel molecular mechanism involved in multiple myeloma development revealed by targeting MafB to haematopoietic progenitors. The EMBO journal 31, 3704-3717.

213. Boersma-Vreugdenhil, G.R., Kuipers, J., Van Stralen, E., Peeters, T., Michaux, L., Hagemeijer, A., Pearson, P.L., Clevers, H.C., and Bast, B.J. (2004). The recurrent translocation t(14;20)(q32;q12) in multiple myeloma results in aberrant expression of MAFB: a molecular and genetic analysis of the chromosomal breakpoint. Br J Haematol 126, 355-363.

214. van Stralen, E., van de Wetering, M., Agnelli, L., Neri, A., Clevers, H.C., and Bast, B.J. (2009). Identification of primary MAFB target genes in multiple myeloma. Experimental hematology 37, 78-86.

215. Gabrysova, L., Howes, A., Saraiva, M., and O'Garra, A. (2014). The regulation of IL-10 expression. Curr Top Microbiol Immunol 380, 157-190.

216. Suzuki, H.I., Arase, M., Matsuyama, H., Choi, Y.L., Ueno, T., Mano, H., Sugimoto, K., and Miyazono, K. (2011). MCPIP1 ribonuclease antagonizes dicer and terminates microRNA biogenesis through precursor microRNA degradation. Molecular cell 44, 424-436.

217. Matsushita, K., Takeuchi, O., Standley, D.M., Kumagai, Y., Kawagoe, T., Miyake, T., Satoh, T., Kato, H., Tsujimura, T., Nakamura, H., et al. (2009). Zc3h12a is an RNase essential for controlling immune responses by regulating mRNA decay. Nature 458, 1185-1190.

218. Lin, H.H., Faunce, D.E., Stacey, M., Terajewicz, A., Nakamura, T., Zhang-Hoover, J., Kerley, M., Mucenski, M.L., Gordon, S., and Stein-Streilein, J. (2005). The macrophage F4/80 receptor is required for the induction of antigen-specific efferent regulatory T cells in peripheral tolerance. The Journal of experimental medicine 201, 1615-1625.

219. Nakamura, M., Hamada, M., Hasegawa, K., Kusakabe, M., Suzuki, H., Greaves, D.R., Moriguchi, T., Kudo, T., and Takahashi, S. (2009). c-Maf is essential for the F4/80 expression in macrophages in vivo. Gene 445, 66-72.

220. DeAngelis, M.M., Grimsby, J.L., Sandberg, M.A., Berson, E.L., and Dryja, T.P. (2002). Novel mutations in the NRL gene and associated clinical findings in patients with dominant retinitis pigmentosa. Archives of ophthalmology (Chicago, Ill : 1960) 120, 369-375.

221. Ramsey, J.E., and Fontes, J.D. (2013). The zinc finger transcription factor ZXDC activates CCL2 gene expression by opposing BCL6-mediated repression. Molecular immunology 56, 768-780.

222. Nagamura-Inoue, T., Tamura, T., and Ozato, K. (2001). Transcription factors that regulate growth and differentiation of myeloid cells. Int Rev Immunol 20, 83-105.

223. Nie, J., and Pei, D. (2003). Direct activation of pro-matrix metalloproteinase-2 by leukolysin/membrane-type 6 matrix metalloproteinase/matrix metalloproteinase 25 at the asn(109)-Tyr bond. Cancer research 63, 6758-6762.

224. Evans, B.R., Mosig, R.A., Lobl, M., Martignetti, C.R., Camacho, C., Grum-Tokars, V., Glucksman, M.J., and Martignetti, J.A. (2012). Mutation of membrane type-1 metalloproteinase, MT1-MMP, causes the multicentric osteolysis and arthritis disease Winchester syndrome. Am J Hum Genet 91, 572-576.

225. Superti-Furga, A., and Unger, S. (2007). Nosology and classification of genetic skeletal disorders: 2006 revision. Am J Med Genet A 143A, 1-18.

226. Sato, H., Kinoshita, T., Takino, T., Nakayama, K., and Seiki, M. (1996). Activation of a recombinant membrane type 1-matrix metalloproteinase (MT1-MMP) by furin and its interaction with tissue inhibitor of metalloproteinases (TIMP)-2. FEBS letters 393, 101-104.

227. Lehti, K., Lohi, J., Valtanen, H., and Keski-Oja, J. (1998). Proteolytic processing of membrane-type-1 matrix metalloproteinase is associated with gelatinase A activation at the cell surface. The Biochemical journal 334 (Pt 2), 345-353.

228. Han, K.Y., Dugas-Ford, J., Seiki, M., Chang, J.H., and Azar, D.T. (2015). Evidence for the Involvement of MMP14 in MMP2 Processing and Recruitment in Exosomes of Corneal Fibroblasts. Invest Ophthalmol Vis Sci 56, 5323-5329.

229. Wilkinson, J.M., Davidson, R.K., Swingler, T.E., Jones, E.R., Corps, A.N., Johnston, P., Riley, G.P., Chojnowski, A.J., and Clark, I.M. (2012). MMP-14 and MMP-2 are key metalloproteases in Dupuytren's disease fibroblast-mediated contraction. Biochim Biophys Acta 1822, 897-905.

230. Dellinger, M.T., Garg, N., and Olsen, B.R. (2014). Viewpoints on vessels and vanishing bones in Gorham-Stout disease. Bone 63, 47-52.

231. Koshida, R., Oishi, H., Hamada, M., and Takahashi, S. (2015). MafB antagonizes phenotypic alteration induced by GM-CSF in microglia. Biochemical and biophysical research communications 463, 109-115.

232. Hochberg, Y., and Benjamini, Y. (1990). More powerful procedures for multiple significance testing. Stat Med 9, 811-818.

233. Subramanian, A., Tamayo, P., Mootha, V.K., Mukherjee, S., Ebert, B.L., Gillette, M.A., Paulovich, A., Pomeroy, S.L., Golub, T.R., Lander, E.S., et al. (2005). Gene wide expression profiles. Proceedings of the National Academy of Sciences of the United States of America 102, 15545-15550.